Host Diet and Pathogen Diversity: How Soil Nutrients Affect Plant Virus Interactions

A DISSERTATION
SUBMITTED TO THE FACULTY OF THE GRADUATE SCHOOL
OF THE UNIVERSITY OF MINNESOTA
BY

Amy Elizabeth Kendig

IN PARTIAL FULFILLMENT OF THE REQUIREMENTS
FOR THE DEGREE OF
DOCTOR OF PHILOSOPHY

Drs. Eric Seabloom and Elizabeth Borer

December 2017

Acknowledgements

I would like to thank my advisors, Eric Seabloom and Elizabeth Borer, for providing kind and thoughtful guidance throughout my graduate education. Thank you for continually demonstrating how to be great scientists, from carefully dissecting a problem to fostering a supportive community.

I am grateful for the time and helpful feedback that my committee members, including Meggan Craft, Allison Shaw, Linda Kinkel, and Clarence Lehman, contributed to this dissertation. Thank you for being enthusiastic, inclusive, and attentive mentors throughout this process.

I received excellent mentoring and assistance in the lab from Christelle Lacroix, Missy Rudeen, and Anita Krause. Thank you for creating such a warm and welcoming environment. Undergraduate researchers, including Tashina Picard, Emily Boak, Nicholas Cupery, Casey Easterday, Alexis Rogers, Kurra Renner, and Jessica Lettelleir, contributed enormously to this research and made my time in the lab much more fun.

The Borer-Seabloom lab members provided me with constructive feedback throughout my dissertation and great examples of how to do exciting and rigorous science. I also received abundant support and camaraderie from my IGERT cohort, my EEB 2011 cohort, and many members of the EEB community.

I am so grateful to my friends and loved ones that gave me all the encouragement and inspiration in the world. I would especially like to thank Anika Bratt, Clare Kazanski, Marta Lyons, María Rebolleda Gómez, Melanie Bowman,

Danielle Drabeck, Meredith Steck, Jake Grossman, Amanda Gorton, Anna Baker, Gabriela Huelgas Morales, Jessica Meyer, Isabelle Bouchard, and Zach Moore for all of the laughter and thoughtful conversations that made the last several years so incredible.

I am thankful to my family members, and their continuous support and love. I would especially like to thank Mom, Dad, Robert, Gail, Josh, Bob, and Annabelle for cheering me on for as long as I can remember.

Dedication

In loving memory of Ben Brunell

Abstract

Human activities and management choices can impact the spread and intensity of diseases in plant and animal populations. For example, high nutrient inputs to terrestrial and aquatic systems may enhance pathogen success or aid hosts in resisting and tolerating disease. Because nutrient supply rates and ratios mediate interactions among free-living species, they may also influence interactions between hosts and pathogens. Further, it is increasingly clear that infections involve multiple different kinds of pathogens, and their interactions may also be mediated by environmental nutrients. The goal of my dissertation research was to understand how soil nutrients affect interactions among plant viruses and the consequences of these interactions for disease dynamics. We used field-collected data to determine how nutrients, among other factors, affected spatial patterns of viruses in grasslands. We found that virus pairs frequently co-occurred, and phosphorus (P) addition promoted the aggregation of one pair. Then, we performed growth chamber experiments to evaluate how nitrogen (N) and P mediated within-host interactions between two viruses, disease severity, and transmission to new hosts. We found that pathogens coexisted within hosts and occasionally benefitted from increased N. Disease severity was not strongly influenced by soil nutrients, but modeling results indicated that this outcome depended on the mechanism behind virulence. Finally, we found that the viruses were likely to coexist at the host population scale, despite inhibition that occurred during transmission. These results indicate that soil N and P influence some aspects of the system, but are not the main drivers behind

virus diversity. This research contributes to a growing body of knowledge about the mechanisms linking environmental nutrients to disease across systems.

Table of Contents

List of Tables

List of Figures

Introduction

Human impacts on the environment can alter the prevalence, severity, and distribution of infectious diseases (Walsh et al. 1993, Harvell et al. 2002, Johnson et al. 2010). One of the largest changes driven by human activities is the addition of nutrients to the environment (Steffen et al. 2015). Fertilizers and emissions from vehicles and industry increase the amount of nitrogen and phosphorus in aquatic and terrestrial systems (Vitousek et al. 1997, Cordell et al. 2009). These nutrients can enhance the prevalence and severity of plant and animal diseases when they are taken up or consumed by hosts (Smith 2007, Dordas 2009). It has long been known that nutrition is an important factor regulating health (Hagan 1943, Gaumann 1950). It can mediate infectious diseases by aiding pathogens in reproduction (Clasen and Elser 2007, Whitaker et al. 2015, Mancio-Silva et al. 2017), enhancing host defenses (Zeier et al. 2004, Jin et al. 2014), or altering the rate of transmission (Voss and Richardson 2006, Civitello et al. 2013).

The amounts and ratios of environmental nutrients mediate ecological interactions among free-living species (Miller et al. 2005, Borer et al. 2014a, Harpole et al. 2016). When species overlap in their resource requirements, the rate and ratio of limiting nutrients can lead to competitive exclusion or coexistence (Tilman 1982). Species can also facilitate one another in obtaining limiting nutrients (Maestre et al. 2009, Harcombe 2010). Infectious disease is the result of multiple ecological interactions: between the host and the pathogen, the pathogen and other microbes within

the host, and the host and its predators, competitors, and mutualists. In fact, it is common for a host to be infected by multiple pathogens in some systems (i.e. coinfection, Petney and Andrews 1998, Balmer and Tanner 2011, Roossinck 2012). Coinfection can alter the virulence of a disease as well as its transmission to new hosts (Graham et al. 2007, Rigaud et al. 2010, Griffiths et al. 2011). Therefore, the effects of nutrients on interactions between coinfecting pathogens may have important consequences for the prevalence and severity of disease. Few studies have evaluated the effects of nutrients on pathogen interactions (but see Lacroix et al. 2014, Lange et al. 2014, Wale et al. 2017) or resulting changes in transmission and symptoms (but see Lacroix et al. 2017).

The goal of this dissertation was to investigate how nutrients mediate pathogen interactions and what the broader effects are for host health and pathogen diversity. Here, I present three chapters that contribute to this goal. The study system I used for all three chapters is a group of viruses known as the barley and cereal yellow dwarf viruses (B/CYDVs). These virus species can infect over 150 plant species in the family *Poaceae*, including wild grasses and cultivated grasses, such as barley, wheat, and rye (Griesbach et al. 1990, D'Arcy and Burnett 1995). They are obligately vectored by grain aphids, which feed on the plant phloem, where the viruses are found (Gray and Gildow 2003). They cause stunted growth, discoloration of leaves, and reduced fecundity. They have been well-studied in the applied literature due to the economic impact they can have on agriculture (D'Arcy and Burnett 1995, Miller and Rasochova 1997, Nega 2014, Choudhury et al. 2017). The viruses are globally distributed (D'Arcy

and Burnett 1995), can mediate plant species interactions (Malmstrom et al. 2005b, Borer et al. 2007), and are affected by environmental factors such as fertilization and climate (Seabloom et al. 2010, Borer et al. 2010b, Rúa et al. 2013, Nancarrow et al. 2014). Therefore, they have also been used as a model system for basic disease ecology (Power et al. 2011). They are frequently found coinfecting plants and they have nutrient-mediated interactions (Seabloom et al. 2009, Lacroix et al. 2014), making them an ideal system for understanding how nutrients can affect host health and pathogen diversity through pathogen interactions.

In the first chapter, I collaborated with my advisors, Drs. Elizabeth Borer and Eric Seabloom, as well as Drs. Charles Mitchell and Alison Power. My four collaborators performed field experiments in 2007 and 2008 to identify the roles of biotic and abiotic factors in regulating B/CYDV prevalence in U.S. west coast grasslands. They found that perennial grass cover and phosphorus (P) fertilization increased virus prevalence, and that laboratory tests of aphid preference for different grass species predicted infection rates for those species in the field (Borer et al. 2010b, Seabloom et al. 2013). Using the same dataset, I built off these studies to determine how biotic and abiotic factors affected the spatial patterns of viruses in the field. I characterized spatial patterns of single viruses, the overlap between pairs of virus species, and the distribution of virus communities (i.e. the composition of viruses present) using spatial correlograms. I then determined how sharing a vector species, fertilization treatments, perennial grass cover, spatial variation in plant size, and spatial variation in plant appeal to vectors affected virus spatial patterns. Among other results,

we found that spatial overlap between virus pairs occurred frequently and was enhanced with P fertilization for one virus pair (Kendig et al. 2017). These results motivated a more in-depth investigation of coinfection between these two viruses, PAV and RPV, for my second and third chapters.

In the second chapter, I performed a growth chamber experiment with oats, PAV, and RPV to determine how nutrients modify pathogen interactions and what the consequences are for host symptoms. I manipulated the supply rates of nitrogen (N) and P to the oat plants, inoculated them with one or both viruses, and measured virus concentration and plant traits that serve as indicators for disease severity. I completed this laboratory experiment with the help of undergraduate researchers, including one of my co-authors, Tashina Picard, who performed analyses of plant tissue nutrient concentration for an independent undergraduate project. I also collaborated with Drs. Bruce Pell and Yang Kuang to develop a mathematical model to accompany this experiment. We used the model to understand how the mechanism behind disease symptoms influences the relationship between the resource supply rate and the proportion of mass lost from a plant host.

In the third chapter, I combined the experiment performed for the second chapter and a new experiment to determine how nutrients mediate coexistence between plant viruses, one of the components contributing to pathogen diversity. In addition to the measurements I made for the second chapter, I also performed transmission trials. This involved allowing aphids to feed on the plants and transferring them to new plants grown in the N and P treatments, and then testing those plants for the presence or

absence of viruses. I used this experiment to determine if the viruses affected one another's transmission to a new plant, and if this depended on nutrient supply rates. I paired this experiment with a simple analysis of a mathematical model to predict whether coinfection effects on transmission were likely to influence virus coexistence at the host population scale. The second experiment was a test of the mutual invasibility principle, which is an indicator of niche differences between species. I performed a growth chamber experiment with oats grown in the same nutrient treatments as the first experiment. I established infections with each of the viruses and then inoculated the plants with the second virus. I measured virus concentration to determine if the viruses could invade one another, how their growth rates changed when they were the "invader" or the "resident", and whether competitive exclusion occurred. Again, this experiment was completed with the assistance of multiple undergraduate researchers, including one of my co-authors, Emily Boak, who participated in data interpretation and writing.

Chapter 1

Characteristics and drivers of plant virus community spatial patterns in U.S. West Coast grasslands

Amy E. Kendig, Elizabeth T. Borer, Charles E. Mitchell, Alison G. Power, and Eric W. Seabloom

Summary

The spatial distribution of disease risk caused by multi-pathogen infections is not frequently characterized, limiting understanding of the drivers of infection and thwarting prediction of future risk in a changing environment. Further complicating this predictive understanding is that interactions among multiple pathogens within a host commonly alter transmission success, infection risk, and disease dynamics. By characterizing spatial patterns of Barley and Cereal Yellow Dwarf Virus (B/CYDV) infections that range from the scale of an individual plant to thousands of neighboring plants, we examined the contributions of spatial processes to the distribution of disease risk. In a two-year field experiment, we planted grass hosts of B/CYDVs into fertilized plots of U.S. west coast grasslands. We determined how vector-sharing, environmental conditions, and spatial variation in host quality affected spatial patterns of single viruses, pairs of viruses, and the whole virus community across out-planted grass hosts. We found that single viruses and virus communities were spatially random, indicating that infection does not solely spread through the community in a wave-like manner. On the other hand, we found that pairs of viruses, especially those that share a vector species, were aggregated spatially. This suggests that if within-host competition exists, it is not strong. Aggregation in one pair of viruses was more frequent due to environmental conditions and spatial variation in out-planted host quality, measured as vector preference. These results highlight the importance of insect vectors for predicting the spatial distribution of coinfection risk by B/CYDVs.

Key words: barley and cereal yellow dwarf viruses, disease ecology, insect-vectored plant pathogens

Introduction

Multi-pathogen infections can increase virulence and alter disease dynamics relative to single infections (Graham et al. 2007, Griffiths et al. 2011). While spatial patterns of disease risk are used to infer valuable information about disease spread, such as the mode of transmission, the distance between transmission events, and spatial variation in hosts or environmental conditions (Caraco et al. 2001, Jolles et al. 2002, Kikuti et al. 2015, Nessa et al. 2015), they are not well characterized for multi-pathogen infections (but see Raybould et al. 1999, Turechek and Madden 2000, Muller and van Woesik 2012). However, spatial patterns of communities of free-living organisms have been well studied and are influenced by dispersal, biotic interactions, and environmental heterogeneity (Bolker and Pacala 1999, Hanson et al. 2012, Benot et al. 2013). Recent applications of community ecology theory to multi-pathogen communities demonstrate that analogous processes (transmission, pathogen interactions, and variation in the host community) mediate the diversity of co-infecting pathogens within a host individual or population (Seabloom et al. 2015, Johnson et al. 2016, Mordecai et al. 2016). Therefore, it is likely that transmission, pathogen interactions, and spatial variation in hosts also contribute to the spatial patterns of pathogen communities, but the roles and strengths of these processes are unclear.

The distance and mode of transmission between hosts likely influence the spatial patterns of multi-pathogen communities. If transmission of a single pathogen is localized, infection tends to be aggregated across hosts (i.e. infected hosts tend to be geographically close to other infected hosts, leading to spatially clustered occurrences of infection). However, if transmission is coming from a distant source, infection tends to be spatially random (Gibson 1997, Filipe and Maule 2004). Building on this, areas with higher initial prevalence have more local sources of infection, so they are more likely to have aggregations of infection (Jolles et al. 2002, Rappussi et al. 2012). If multiple species in a community have localized dispersal, communities that are geographically close to one another tend to have more similar species composition (i.e. the distance-decay relationship, Nekola and White 1999). Transmission mode also may affect the spatial patterns of pathogen communities. For example, the spatial patterns of pathogens vectored by insects are influenced by foraging behavior (McElhany et al. 1995, Ferrari et al. 2006). Different pathogens can share the same mode of transmission, such as insects or needles, which may lead to aggregation between these pathogens (Ridzon et al. 1997, Manguin et al. 2010, Hersh et al. 2014).

Interactions among pathogens also can determine whether different pathogens are aggregated relative to one another, or regularly spaced (i.e. segregated from one another, like a checkerboard pattern). While facilitation between different free-living species causes aggregation, and competition leads to regular spatial patterns (Callaway 1995, Seabloom et al. 2005), the spatially continuous nature of these interactions does not easily extend to obligate pathogens. Pathogens can have facilitative or competitive

interactions, but these are typically mediated through host resources or the immune system (Pedersen and Fenton 2007). In addition, the extent that pathogens overlap in their host specificity determines the frequency with which they will interact (Brisson and Dykhuizen 2004, Malpica et al. 2006, Johnson et al. 2016). Therefore, pathogens that successfully infect the same hosts and have positive or neutral interactions are expected to aggregate while those with different host "preferences" or negative interactions are expected to segregate. However, these patterns are restricted to the scale of a host individual or smaller, as the presence of a pathogen in one host is unlikely to affect the presence of a different pathogen in a different host.

Multiple factors, including genetics, nutrition, healthcare, and environmental conditions, affect host susceptibility and competence, measures of host quality. Overlap in host quality requirements among pathogens can contribute to the distance-decay relationship of pathogen communities if there is a spatial gradient in host quality (Bell 2010, King et al. 2010, Astorga et al. 2012). For single pathogens, spatial variation in genetic resistance has been linked to aggregation of infection (Laine 2006, Paull et al. 2012b). Disease risk caused by single infections and coinfections also can be affected by spatially variable environmental conditions that alter host susceptibility or pathogen fitness (Jarosz and Burdon 1988, Raso et al. 2006, Kikuti et al. 2015). Localized transmission and low competitive exclusion among pathogens must work in tandem with spatial variation in host quality for pathogen communities to be aggregated (Leibold et al. 2004, Seabloom et al. 2005, Hanson et al. 2012).

Here, we use a grassland experiment, repeated over two years, to evaluate the role of spatial processes in structuring an aphid-vectored plant virus community. We planted six grass species into plots with full-factorial nitrogen (N) and phosphorus (P) fertilization for a growing season (Borer et al. 2010b, Seabloom et al. 2013). We quantified spatial variation in the host quality of out-planted grasses through plant size and aphid feeding preference. Using the infection status of out-planted grasses for four viruses, we characterized the spatial patterns of single virus species, pairs of virus species, and the whole virus community within experimental plots. We tested if these spatial patterns could be explained by spatial variation in host quality and two environmental conditions that drive plot-scale infection prevalence (fertilization and perennial grass cover, Borer et al. 2010b). We did not observe aggregation of single infections or the virus community, which would have indicated strictly localized transmission. However, we did find close associations among virus pairs, suggesting the importance of shared aphid vectors in determining the spatial patterns of this plant virus community.

Methods

Experimental system

A group of plant viruses known as the Barley and Cereal Yellow Dwarf viruses (B/CYDVs) are an ideal study system for investigating spatial patterns of pathogen communities. Their stationary hosts make the characterization of spatial patterns straightforward, and the ecology of these pathogens has been well studied (Power et al.

2011). They can infect over 150 species of perennial and annual grasses, including crops and wild grasses (D'Arcy and Burnett 1995). The virus species included in this study are BYDV-MAV, BYDV-PAV, CYDV-RPV, and BYDV-RMV (henceforth MAV, PAV, RPV, and RMV, respectively). Each virus is obligately vectored by a different aphid species, except PAV, which shares one vector species with RPV (*Rhopalosiphum padi*) and two with MAV (*Sitobian avenae* and *Metopolophium dirhodum*) (Power et al. 2011). However, facilitation during coinfection allows viruses to be vectored by aphids that they are typically incompatible with (Wen and Lister 1991). Within-host pathogen interactions can also be competitive (Wen et al. 1991), and they may depend on soil nutrient content (Lacroix et al. 2014). Hosts that are fast-growing tend to have high susceptibility and competence (Cronin et al. 2010), which is why the mass of out-planted grasses are approximations for host quality. Aphids typically walk between plants or make flights of a few meters, but they have the ability to fly tens of kilometers with wind assistance (Parry 2013).

Field experiment

The experiment was repeated in two years (2007 and 2008). In the first year, sites included the Hopland Research and Extension Center (39°N, 123°W), the McLaughlin Natural Reserve (38.8°N, 122.3°W), and the Sierra Foothill Research and Extension Centers (38.7°N, 121.1°W) in California, USA. In the second year, two more sites in Oregon were added: Baskett Slough National Wildlife Refuge (44.9°N, 122.7°W) and William L. Finley National Wildlife Refuge (44.4°N, 122.6°W). Two experimental blocks were established at each site with four 40 m x 40 m plots within

each block (Fig. S1). The plots in each block received a factorial combination of nitrogen (N, 10 g m^{-2} $year^{-1}$ added quarterly as calcium nitrate) and phosphorus (P, 4.3 g m^{-2} $year^{-1}$ added quarterly as triple super phosphate) addition (plot-level treatments: control, +N, +P, or +N and P). Fertilizers were first applied to plots in December 2006, one month prior to the first planting. We estimated aerial cover of naturally-occurring plant species in two 0.5 m x 1 m quadrats within each plot. Cover of each species was estimated separately such that the combined cover could exceed 100%.

Within each plot, 10 transects were established with 20 subplots each. Transects were spaced 4 m apart and the centers of subplots were 2 m apart along each transect (Fig. S1). Each year, 2-3 transects per plot were randomly selected to be used in the experiment. In January 2007 and 2008, after approximately one month of growth in a greenhouse, we planted six individual plants of different species in the subplots of these selected transects. All subplots received the same six species. The plants were spaced 0.25 m apart parallel to the transect and 0.2 m apart perpendicular to the transect (Fig. S1). Three phylogenetic groups are represented by the six species, which are common to West Coast grasslands. For each phylogenetic group, one species is an exotic annual and one is a native perennial, respectively: Brome (*Bromus hordeaceus/Bromus carinatus*), Oat (*Avena fatua/Koeleria macrantha*), and Rye (*Taeniatherum caput-medusae/Elymus glaucus*). The plants were randomly assigned to a position within each subplot (i.e. A through E in Fig. S1). The out-planted grasses were in the field prior to seasonal aphid flight and harvested before the onset of senescence, in late May and early June. Post-harvest, we shipped all green tissue overnight to labs at Cornell

University and the University of North Carolina to test them for the presence of MAV, PAV, and RPV in 2007, and MAV, PAV, RPV, and RMV in 2008 with double antibody sandwich enzyme-linked immunosorbent assay (DAS-ELISA). Plants tested for viruses were individually weighed in 2008. These analyses resulted in a dataset of over 3000 plants from the first experimental year and over 5000 plants from the second year. Data are available from the Dryad Digital Repository: http://dx.doi.org/10.5061/dryad.22dt8 (Borer et al. 2010a).

General approach for characterizing spatial patterns

Spatial correlograms are nonparametric statistical tools used to quantify associations among individual units (i.e. autocorrelation) across geographical distances (Bjørnstad and Falck 2001). Similarly, spatial cross-correlograms estimate distance-based cross-correlations between units representing two different groups, and multivariate correlograms estimate compositional similarity or dissimilarity across space (e.g. the Mantel correlogram) (Bjørnstad and Falck 2001). We used spatial correlograms to characterize spatial variation in host quality and spatial patterns of viruses within out-planted grasses. Based on the planting layout described above, we assigned spatial coordinates to all out-planted grasses. Coordinates accurately represented the space between plants within each plot, but were set such that spatial associations between plants from different plots would not be evaluated. We used the spline.correlog function in the ncf package in R to build spatial correlograms (Bjørnstad 2016). For all correlograms, we used df = 15, a maximum lag distance of 30 m (to include 85% of the pairwise comparisons), and 1000 permutations to calculate 95%

confidence intervals (CI) through bootstrapping. We chose to use df=15 because this roughly corresponds to 15 distance classes (Bjørnstad et al. 1999), which is appropriate for our experimental set-up. However, variation in the df can modify the outcome of our analyses (Methods S1).

After we fit spatial correlograms to host quality data and virus infection data, we used the output of these correlograms as predictor variables and response variables, respectively, in linear regressions. The spline.correlog function provides estimates for the y-intercept (i.e. correlation at the scale of a single plant) and the x-intercept (i.e. the geographic distance at which the correlation is no longer significantly different from zero) of each correlogram. When the 95% CI included the origin, we categorized the correlogram as "random". When the y-intercept was significantly positive, we categorized the correlogram as "aggregated", and when the y-intercept was significantly negative, we categorized it as "regular". To reduce the carryover of error in estimating spatial correlograms to analyses with linear regressions, we used 0 or 1 to represent whether the spatial correlogram was random or significantly different from random rather than the x- or y-intercepts.

In U.S. west coast grasslands, most, if not all, grasses are potential hosts to B/CYDVs. We present some of our results in units of individual plants to estimate the number of hosts that are affected by the disease. To convert geographic distances from meters to number of individual plants, we used measurements from common annual and perennial grass species in a restored grassland at the Sedgwick Natural Reserve in California, USA, which is ecologically similar to the grasslands in our study (Seabloom

et al. 2005). The basal radius, averaged across plant species from Sedgwick, is 1.52 cm and the average maximum radius is 11.69 cm. To estimate the number of plants included in an aggregate, the x-intercept of the correlogram was assumed to be the diameter of a circle. Based on the values from Sedgwick, experimental plots encompass approximately one million to ten million individual plants, depending on the sizes of plants.

Characterizing spatial patterns of host quality

Spatial variation in host quality was characterized by creating correlograms of two metrics for each experimental plot: host mass and aphid preference. We created correlograms of host mass using the wet mass of each out-planted grass following harvest in the second experimental year (data were not collected the first year). While these data may show a spatial pattern, we acknowledge that non-experimental host plants may not adhere to this pattern due to variation in age and species. We used laboratory experiments of aphid preference with the species *R. padi* to assign each out-planted grass an aphid preference value based on its species (Experiment III in Borer et al. 2009). These values and the corresponding plant positions in the field were used to build correlograms of aphid preference. Because one of each plant species is in each subplot, these correlograms are affected by experimental design. However, they may also be influenced by less predictable factors, such as the random placement of species within a subplot and individual survival over the growing season.

Characterizing spatial patterns of viruses

We used correlograms to characterize the spatial pattern of each virus species based on presence or absence in each out-planted grass. We used cross-correlograms to characterize the relative spatial patterns between virus species pairs and multivariate correlograms to analyze community-wide spatial patterns, both relying on presence/absence data. We reduced the df to 7 and removed permutations that caused errors in the multivariate correlogram due to low infection prevalence, which did not affect the overall results.

Evaluating drivers of virus spatial patterns

Coinfection may drive aggregation between virus pairs when local transmission from coinfected plants occurs, particularly in the presence of mutualistic interactions. In addition, positive y-intercepts of cross-correlograms may result from coinfection, although they can be interpolated from positive associations between adjacent plants as well. Conversely, spatial aggregation of virus pairs can increase coinfection rates by making transmission of virus pairs to the same plant individual more likely. Because we cannot disentangle cause and effect when examining coinfection and cross-correlograms, we compared these metrics using Pearson's correlation coefficient. We examined the relationship between x-intercepts of significantly aggregated cross-correlograms and the relative coinfection rate for each pair of viruses in each plot . Relative coinfection rate measures the rate of coinfection relative to what is expected due to chance encounters between viruses. It was calculated by the plot-scale coinfection rate minus the product of each virus's plot-scale prevalence (modification of Malpica et al. 2006). We chose the relative coinfection rate rather than the raw

coinfection rate because cross-correlograms indicate whether pairs of viruses co-occur more often than expected by chance.

Next, we evaluated the effects of a shared transmission route (i.e. the same vector species) on whether or not aggregation occurred between each virus pair in each experimental plot, with aggregation determined by a cross-correlogram having a significantly positive y-intercept. We fit a generalized linear mixed-effects model to the relationship between whether or not aggregation occurred and whether or not the virus pair share the same vector (R package lme4, Bates et al. 2015). The initial random effects were the identity of the viruses nested within plot nested within block nested within site nested within state, which reduced down to virus identities nested within site based on backwards stepwise model selection with likelihood ratio tests (Crawley 2007).

Then, we assessed the effects of N addition, P addition, the interaction between N and P addition, perennial grass percent cover, spatial variation in plant mass, and spatial variation in aphid preference on whether or not aggregation between virus pairs occurred with generalized linear regressions. We built separate models for each virus pair in each year. Models for the first year did not include spatial variation in plant mass or perennial cover (most CA plots had no perennial grasses). Each host quality variation metric (aphid preference and plant mass) was represented by a 1 or 0 for each experimental plot, indicating the presence or absence, respectively, of a significant correlogram y-intercept (i.e. significant aggregation or segregation). We began by building mixed-effects models with block nested within site nested within state (for the

second experimental year) as the random effects. We used backwards stepwise selection with likelihood ratio tests for model simplification of random effects, then fixed effects (Crawley 2007). The fixed-effects models were significantly better than the mixed-effects models for the first experimental year and we had issues with model convergence for mixed-effects models from the second experimental year, so only the fixed-effects models were used. All statistical analyses were performed in R version 3.3.1 (R Core Team 2016).

Results

Spatial patterns of host quality: random patterns of grass mass and regular patterns of aphid preference

Spatial correlograms of out-planted host mass revealed random spatial patterns in more than 80% of plots, with local aggregation occurring in six out of 35 plots (Table 1). On the other hand, plants with similar aphid preference scores had regular spatial patterns in most plots and random patterns in a minority of plots (Table 1). The average distance of segregation between plants with similar aphid preference scores was about the distance between subplots along a transect (2.0 m), indicating that aphid preference segregation was driven by experimental design and likely represents plant species differences. These differences are not strictly constrained to be aphid preference because, as we measured it, this is a species-specific trait.

Table 1. Summary of correlograms by experimental plot for metrics of spatial variation in host quality, which were used as predictor variables in analyses that follow. Prop. sig. is the proportion of experimental plots with significant y-intercepts.

Host heterogeneity metric	Expt. year	Prop. sig.	Mean ± std. error of sig. x-int. (m)	Mean ± std. error of sig. y-int. (m)
Individual plant mass	2	6/35	8.1 ± 2.0	0.381 ± 0.062
Aphid preference	1	22/24	2.03 ± 0.20	-0.2217 ± 0.0050
Aphid preference	2	27/35	1.839 ± 0.068	-0.2119 ± 0.0054

Single virus spatial patterns were predominantly random

Spatial patterns of single pathogens provide insights about the scale of transmission (i.e. more localized transmission leads to aggregation) and spatial variation in host quality. Contrary to expectations, most virus spatial correlograms depicted random patterns (Fig. S2). There were three exceptions to this trend, all from the first experimental year: RPV had two negative correlograms and PAV had one (Fig. S3). The x- and y-intercepts of these correlograms are close to those found for aphid preference (Table 1), indicating that the patterns were likely to be driven by differences among plant species, potentially due to characteristics such as aphid preference or susceptibility to infection.

Aggregated spatial patterns of virus pairs were related to coinfection and vector-sharing, but only one pair was affected by environmental conditions and spatial variation in host quality

Cross-correlograms between pathogens are influenced by transmission, interactions between pathogens, and overlapping host quality requirements. The cross-correlograms between pairs of B/CYDV species indicated either random or aggregated spatial patterns, but none were regular (Table 2, Fig. S2). Across both experimental years, aggregation between virus pairs occurred out to 3.93 ± 0.46 m on average, which encompasses approximately 10,000 to 80,000 plants. Significantly positive y-intercepts occurred at least once for every virus pair, but the average of these intercepts was somewhat low (correlation of 0.1671 ± 0.0070). This indicates that the net interactions between virus pairs are either positive or neutral with aggregation driven by shared transmission routes or overlapping host quality preferences between virus species.

Table 2. Summary of cross-correlograms by experimental plot for virus pairs. Prop. sig. is the proportion of experimental plots with significant cross-correlations.

Virus Pair	Expt. year	Prop. sig.	Mean ± std. error of sig. x-int. (m)	Mean ± std. error of sig. y-int. (m)
MAV-PAV	1	7/24	4.2 ± 1.2	0.140 ± 0.015
MAV-PAV	2	17/34	3.6 ± 1.1	0.194 ± 0.019
MAV-RPV	1	14/24	4.4 ± 1.2	0.162 ± 0.012
MAV-RPV	2	13/34	4.3 ± 1.2	0.167 ± 0.016
MAV-RMV	2	1/34	1.4	0.146
PAV-RPV	1	6/24	6.1 ± 2.0	0.1107 ± 0.0062

PAV-RPV	2	15/35	3.2 ± 0.88	0.188 ± 0.017
PAV-RMV	2	2/35	2.3 ± 0.28	0.154 ± 0.037
RPV-RMV	2	2/35	1.8 ± 0.49	0.1072 ± 0.0066

We compared the cross-correlogram length to the relative coinfection rate to evaluate how much aggregation between virus pairs relates to coinfection and, potentially, transmission from coinfected plants. We expected a positive relationship between these metrics due to overlapping biological processes. We found that in both years, aggregation between virus pairs only occurred above a threshold relative coinfection rate, but without a clear linear relationship beyond this threshold (Pearson's $r = -0.11$, $p=0.59$; Pearson's $r = 0.02$, $p=0.92$ for years one and two, respectively; Fig. 1). Therefore, it is likely that some minimum rate of coinfection is required for aggregation between viruses to occur, consistent with the concept that the y-intercept of cross-correlograms represents coinfection. However, spatial relationships between viruses beyond a single host are independent of coinfection rate.

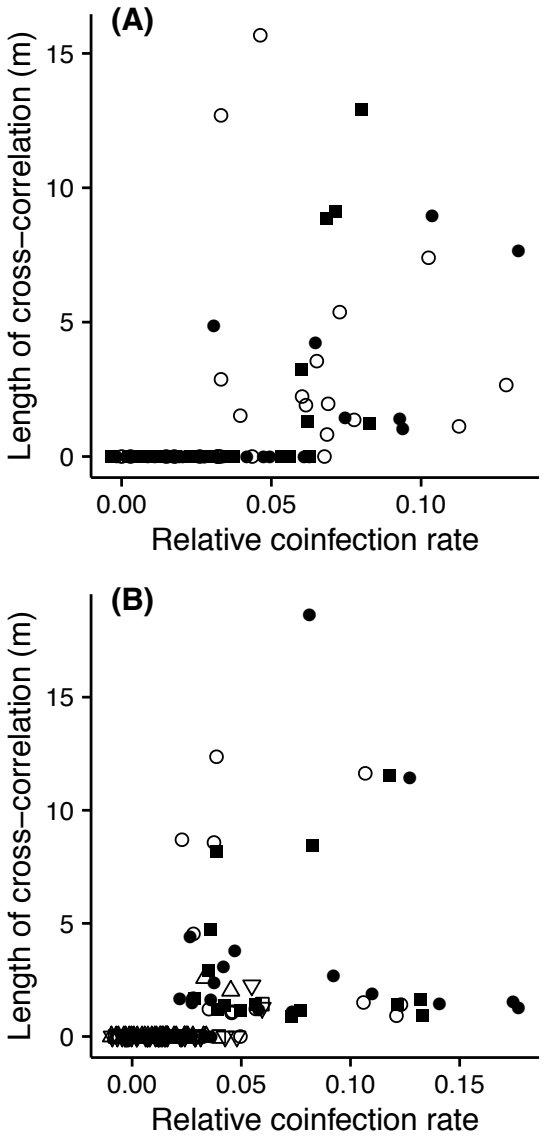

Figure 1. The length of the cross-correlation for each virus pair in each plot against their relative coinfection rate (see main text for details) (A) for the first experimental year (Pearson's r = -0.11, p=0.59) and (B) the second (Pearson's r = 0.02, p=0.92). Each virus pair is represented by a different symbol: ● MAV-PAV, ○ MAV-RPV, ■ PAV-RPV, □ MAV-RMV, △ PAV-RMV, and ▽ RPV-RMV.

There were only enough virus pairs to statistically evaluate the effect of a shared transmission route (i.e. the same vector species) on aggregation between viruses in the second experimental year. As expected, virus pairs that share a vector species aggregated more frequently than those that do not ($p=0.003$, Fig. 2b, Table S2). This result arose despite high frequency of aggregation between one pair of viruses that do not share a vector, RPV and MAV (Fig. 2).

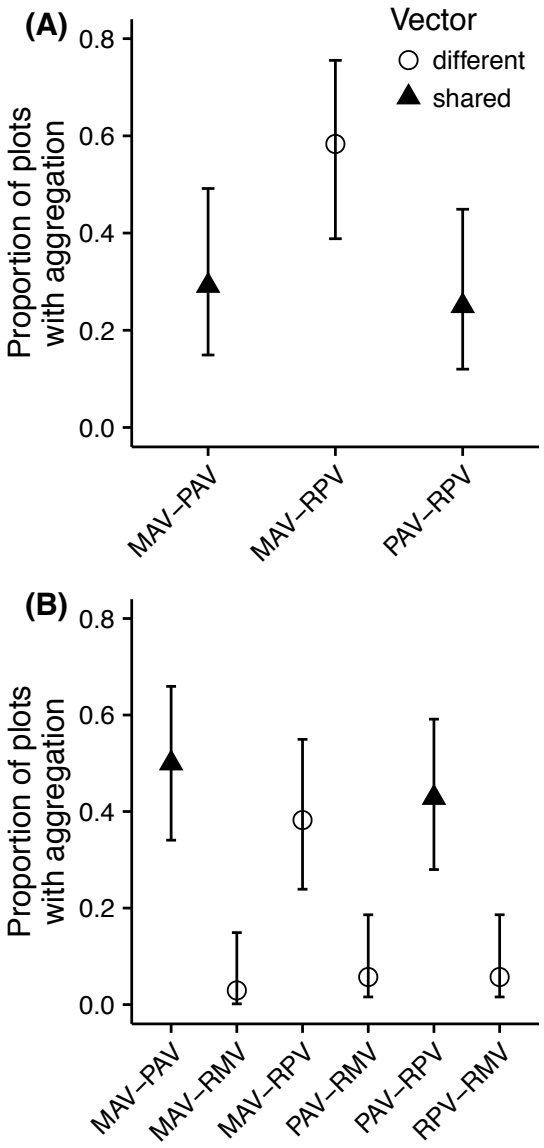

Figure 2. The mean proportion of experimental plots with positive y-intercepts (with 95% CI) for each virus pair, coded by whether or not they share a vector (A) for the first experimental year and (B) the second. Vector-sharing increased the rate of aggregation in the second experimental year (p=0.003).

We also investigated the effects of two environmental conditions that increase prevalence (plot-scale nutrient addition and perennial grass percent cover) and two metrics of spatial variation in out-planted host quality (aphid preference and plant mass) on the aggregation of virus pairs. For all pairs involving RMV, aggregation only occurred in one to two plots, preventing model convergence. During the second experimental year, the frequency of aggregation between PAV and RPV increased when there was significant segregation between out-planted grasses based on aphid preference ($p=0.02$; Fig. 3a, Table S3). Also in the second experimental year, perennial grass percent cover ($p=0.005$, Fig 3b, Table S3) and P addition ($p=0.007$, Fig. 3c, Table S3) increased aggregation of PAV and RPV. We found no significant effects of these environmental conditions or spatial variation in host quality on the aggregation of other virus pairs in the second experimental year or any virus pairs in the first year.

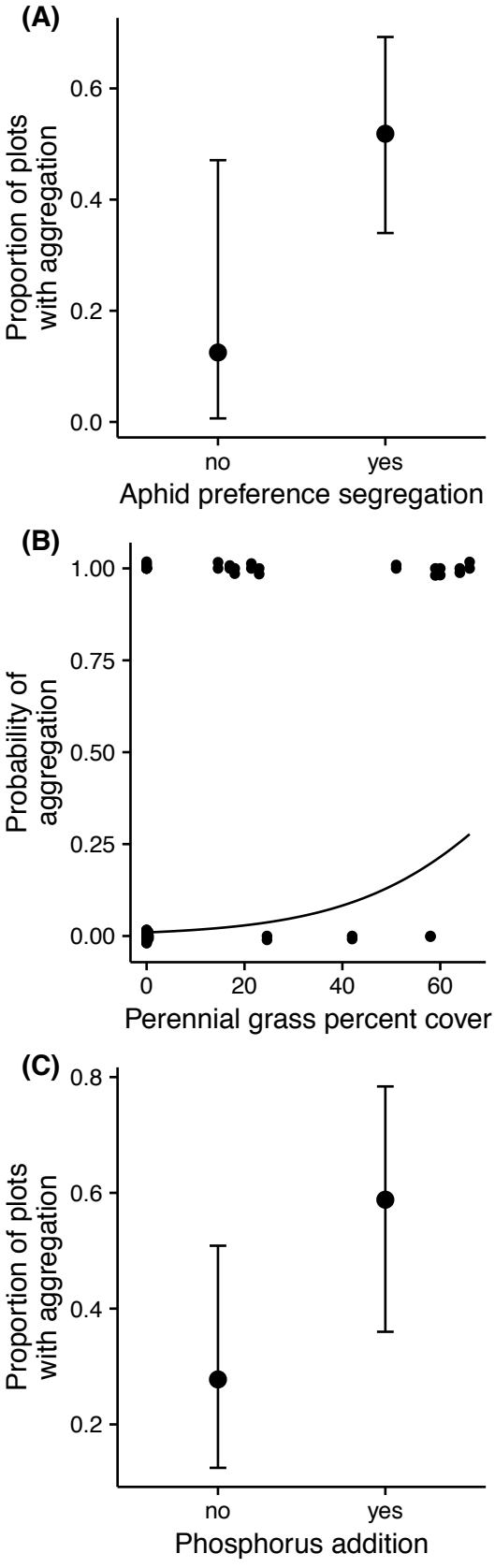
(A)
Proportion of plots with aggregation
0.0
0.2
0.4
0.6
no
yes
Aphid preference segregation
(B)
Probability of aggregation
0.00
0.25
0.50
0.75
1.00
0
20
40
60
Perennial grass percent cover
(C)
Proportion of plots with aggregation
0.2
0.4
0.6
0.8
no
yes
Phosphorus addition

Figure 3. The effect of (A) whether or not there is segregation among out-planted hosts based on their aphid preference values (p=0.02), (B) perennial grass cover (p=0.006), and (C) P addition (p=0.007) on aggregation between PAV and RPV in the second experimental year. In (B), points are data, jittered along the y-axis by 0.05, and the line represents predicted probabilities based on the simplest generalized linear model. (A) and (C) are the mean proportion of experimental plots with positive y-intercepts (with 95% CI), determined from the data.

Virus community spatial patterns were random

Multivariate correlograms indicate whether within-host pathogen communities are more similar in geographically closer plants, and how this relationship decays with distance. They can be influenced by transmission, pathogen interactions, and spatial variation in host quality. The spatial pattern of the B/CYDV community was random for every experimental plot in both experimental years, indicating that geographically closer plants do not have more similar virus communities. Because MAV and RPV frequently aggregated despite not sharing a vector (Fig. 2), we suspected that the aggregation of MAV and RPV may have been caused by shared aggregation with PAV, but the multivariate correlograms of these three viruses when RMV was removed from the dataset were still random.

Discussion

Here we presented a unique spatial analysis of multiple pathogens vectored by multiple aphid species in a diverse host environment. Our results complement growing knowledge about drivers of pathogen community diversity (Seabloom et al. 2015). While the out-planted grass hosts were species commonly found in U.S. West Coast grasslands, they may differ from the background plant community in characteristics relevant to B/CYDV spread, so we refrain from extrapolating our results to this background community or naturally-occurring grasslands in general. Spatial patterns of single virus species and the virus community were random among out-planted grasses, which suggests that infection did not solely spread in a wave-like manner from a small set of initial points. Rather, at least some transmission events occurred between non-neighboring plants (Filipe and Maule 2004). In addition, virus pairs were frequently aggregated relative to each other, and this rate was even higher for those that share a vector species. Finally, spatial variation among out-planted hosts, quantified here by aphid preference, and environmental factors that increase prevalence contributed to aggregation between one pair of viruses, but did not influence the others. Forms of spatial heterogeneity that we did not measure may contribute to aggregation between these other pairs. Nonetheless, frequent aggregation between virus pairs at the scale of an individual host indicates that within-host competition, if it exists, is not strong. Together, these results suggest that aphid-vectored transmission and a lack of intense competition contributed to aggregation of virus pairs, but, despite expectations, strictly local transmission, measures of spatial variation in host quality, and environmental conditions that increase prevalence often did not affect virus spatial patterns.

We expected that aggregation of infection would arise from aphids walking between plants (Power 1991, Parry 2013) and environmental conditions that increase disease prevalence and local inoculum (Jolles et al. 2002, Rappussi et al. 2012). However, we found almost all spatial patterns of single viruses were random. Spatial patterns of virus pairs also provided evidence that transmission is not likely to be strictly localized. We expected coinfection to increase aggregation between virus pairs in geographically close plants due to localized transmission, particularly when facilitative interactions, such as heterologous encapsidation (i.e. when the RNA from one virus is encased in the protein coat of another), occurred (Wen and Lister 1991). A minimum rate of coinfection was necessary for aggregation to occur, but more coinfected plants did not lead to extended aggregation between viruses. While there is evidence for local dispersal of B/CYDVs from "spillover" hosts (Power and Mitchell 2004), this and other studies showing plant disease aggregation often occur in assemblages of low plant diversity (Sone et al. 2012, Nessa et al. 2015). Natural grasslands and other highly diverse ecological environments are likely to obscure aggregation caused by localized dispersal through mechanisms such as variation in host quality, vector foraging preferences, and the initial spatial distribution of disease inoculum (Caraco et al. 2001, Medel et al. 2004, Ferrari et al. 2006, Gosme and Lucas 2011). Regardless of diversity, longer-lived plants can accumulate infections over time, resulting in random spatial patterns of disease (Raybould et al. 1999). Our experiment controlled the age of out-planted grasses, but not that of plants in the surrounding community.

While sources of local inoculum did not lead to aggregation of single viruses in the out-planted grasses, they may have increased aggregation between PAV and RPV. Previous analyses on these data demonstrated that P addition increases the prevalence of PAV and perennial grass cover increases the prevalences of both PAV and RPV (Seabloom et al. 2013). Presumably, these factors increase viral prevalence in out-planted grass hosts through increased prevalence in the background grass community. P addition may increase the maintenance of infection, as some viruses require an environment with high P concentrations for replication (Clasen and Elser 2007). Perennial grasses are expected to serve as refuges for B/CYDVs between growing seasons (Mckirdy and Jones 1993, Power et al. 2011). Given the generality of these mechanisms, it is surprising that only one pair of viruses was affected by environmental conditions. This may be due to variation across virus species in response to P addition or their ability to maintain long-term infection in perennial hosts (Mckirdy and Jones 1993, Lacroix et al. 2014). The effect of local inoculum on pathogen spatial patterns has primarily been evaluated for single pathogen species (Jolles et al. 2002, Rappussi et al. 2012). We expect that higher inoculum levels can increase the co-occurrence of pathogens with positive interactions or aggregating forces, particularly when disease prevalence is low. However, spatially explicit models of multi-pathogen communities are necessary to solidify this hypothesis.

The high frequency of aggregation between viruses that share a vector suggests that viruses are either co-transmitted by the same vector individual, or individuals within the same vector species have similar foraging behavior and are spatially

aggregated. In addition, the finding that PAV and RPV tend to be more aggregated when grasses preferred by their aphid vector are regularly spaced suggests that *R. padi* transmitted both viruses to highly preferred plants, which is consistent with a previous analysis of this dataset (Seabloom et al. 2013). The relative influence of co-transmission and sequential transmission depends on pathogen interactions with one another and their vector. For example, *Babesia microti* and *Borrelia burgdorferi* have facilitative interactions and are frequently found together in their shared tick vector, *Ixodes scapularis* (Dunn et al. 2014, Hersh et al. 2014). On the other hand, *Anopheles* spp. mosquitoes can transmit *Plasmodium* spp. and *Wuchereria bancrofti*, but co-transmission of these pathogens leads to decreased transmission and mosquito survival, suggesting that sequential transmission is more likely to occur than co-transmission (Manguin et al. 2010). The latter example is relevant for PAV, which has decreased transmission when a vector has previously acquired MAV (Gildow and Rochow 1980). On the other hand, facilitation through heterologous encapsidation may contribute to the high rate of aggregation between MAV and RPV, which do not share a vector (Wen and Lister 1991). Interestingly, the strong effect of shared dispersal mechanisms on community spatial patterns has also been demonstrated for plants with animal-dispersed seeds (Mellado and Zamora 2016, Wright et al. 2016).

Many communities of free-living microbes show patterns consistent with the distance-decay relationship (Hanson et al. 2012). Often, spatial heterogeneity in the environment has a stronger influence on the distance-decay relationship in these communities than dispersal limitation (Bell 2010, King et al. 2010, Astorga et al. 2012).

However, B/CYDV communities were spatially random, suggesting that neither dispersal limitation nor environmental gradients are strong in this system at the scales we measured. In many systems, variation among hosts is assumed to affect disease spread through processes such as the dilution effect (Ostfeld and Keesing 2012). Therefore, it is striking that, with the exception of PAV and RPV, we did not find evidence for the influence of spatial variation in host quality on B/CYDV spatial patterns. Heterogeneity in host quality may be structuring B/CYDV communities at different scales than those we examined. For example, transmission events between neighboring plants and small aggregates of plants favorable to aphids or infection may not have been detected by our analyses. In addition, the scale of environmental heterogeneity likely to drive the distance-decay relationship for B/CYDVs may be larger than an experimental plot. For instance, perennial grass cover increases prevalence for three B/CYDV species, and there is more variation in this factor across regions than there is across meters (Borer et al. 2010b, Seabloom et al. 2013). Experimental manipulation of host quality at varying scales would help clarify the extent to which host heterogeneity influences the spatial structure of pathogen communities.

Given that some processes that generate spatial co-occurrence of virus pairs also are likely to cause aggregation of single viruses and virus communities, it is surprising that we saw aggregation in the former, but not the latter two. For example, overlapping preference for a spatially aggregated host characteristic would be expected to increase aggregation of all three (Seabloom et al. 2005, King et al. 2010). However, cross-

correlograms assess the relative spatial patterns of two entities while correlograms and multivariate correlograms measure the autocorrelation of a single entity (either one virus species or a particular composition of viruses) over space (Bjørnstad and Falck 2001). Therefore, co-occurrence of virus pairs in the same plant, same subplot, or neighboring subplots can lead to significant cross-correlograms, but will not necessarily affect the other two forms of virus spatial patterns. A similar result was found for viruses in *Brassica*, with random spatial patterns of each of the four viruses, but positive associations between most of the virus pairs at the scale of a single plant (Raybould et al. 1999). On the other hand, two fungal diseases were found to each have aggregated spatial patterns in strawberry fields while they had low spatial associations with one another (Turechek and Madden 2000). These limited examples suggest that the pathogen type and mode of transmission may be important for understanding the differences among single and multiple plant pathogen spatial patterns.

Due to the complexity of our system, the experimental results incorporate various ecological interactions, providing a meaningful contribution to the rising understanding of pathogen community spatial patterns. The strong signal of co-transmission in pathogen spatial patterns highlights vector control as a coinfection management strategy. While the effects of co-transmission are analogous to effects of co-dispersal observed for free-living organisms (Mellado and Zamora 2016, Wright et al. 2016), pathogen-specific factors can shape pathogen community spatial patterns as well. Importantly, pathogen spatial patterns are intrinsically linked with other living organisms – their hosts. In fact, virulence-induced mortality and behavioral changes due

to infection can affect disease patterns (Vasconcelos et al. 1996, Muller and van Woesik 2012). Additionally, ecological interactions between hosts and other organisms can modify spatial patterns of disease (Byers et al. 2008). As we have demonstrated here, the study of pathogen community spatial patterns provides important insights for disease management and a platform to draw comparisons between the ecology of pathogens and free-living organisms.

Acknowledgments

The work presented here would not have been possible without the support of many people and organizations. Marty Dekkers, Burl Martin, Emily Orling, Jasmine Peters, Vincent Adams, the 2006-2008 field crews, and many students were responsible for the data collection. Staff of the University of California Reserve System, University of California Research and Extension Centers, and the U.S. Fish and Wildlife Service provided generous support. Support was provided, in part, by NSF/NIH EID grants EF-0525666 and DEB-1015805 to ETB and EWS, EF-0525641 and DEB-1015909 to CEM, and EF-0525669 and DEB-1015903 to AGP. AEK was supported by an NSF IGERT graduate fellowship at the University of Minnesota (DGE-0653827) and an NSF Graduate Research Fellowship (base award number 0006595).

Chapter 2

Soil nutrients and coinfection mediate the virulence of plant virus infections

Amy E. Kendig, Eric W. Seabloom, Bruce E. Pell, Tashina C. Picard, Yang Kuang, and Elizabeth T. Borer

Summary

Pathogens induce harmful effects on their hosts (i.e. virulence) that can vary over space and time. This variation is due in part to ecological interactions and abiotic conditions that affect host or pathogen fitness. We experimentally manipulated nitrogen (N) and phosphorus (P) soil concentrations and induced single- and co-infections of viruses in oat plants to test the hypothesis that resource availability and coinfection would interact to mediate virulence. Augmented N partially offset infection-induced losses in shoot mass and reduced virulence quantified with chlorophyll content. Facilitation between viruses may have enhanced virulence, but there was a weak connection between within-host virus density and plant growth. We then developed and parameterized a within-host model to evaluate how the mechanism leading to virulence and host and pathogen resource use affected the relationship between nutrient addition and virulence. Nutrient addition had the largest influence on virulence when it was due to pathogen resource use. Nutrients that aided pathogen growth generally increased virulence while nutrients that enhanced host growth could reduce virulence. Our empirical results and model identified multiple pathways through which ecological factors can modify virulence that are relevant for plant virus systems and have the potential to extend to other multi-pathogen disease systems.

Keywords: Barley and cereal yellow dwarf viruses, nitrogen, phosphorus, pathogen concentration, plant mass, oats

Introduction

Virulence, or decreased host fitness due to disease, is a key parameter in models that simulate the spread of disease through a population (S-I-R or compartmental models, Anderson and May 1979). These models are the basis for methods used to predict whether or not an epidemic can occur (Heffernan et al. 2005), the number of individuals that will become infected or die from disease (Hethcote 2000), and the proportion of the population that needs to be vaccinated for herd immunity to take effect (Fine et al. 2011). Given the underlying importance of virulence to these many characteristics of disease, it is crucial to understand what drives variation in virulence over space and time, as well as across different pathogens and hosts. While the evolution of virulence has received much attention to address this question (Anderson and May 1982, Read 1994, Ewald 2004, Alizon et al. 2009), ecology can play an important role in shaping virulence as well (Barrett et al. 2009).

Environmental context and ecological interactions may affect a host's tolerance or resistance to disease, or a pathogen's fitness within the host. For example, climate and resource availability can affect virulence by moderating pathogen growth (Hall et al. 2009, Thompson et al. 2010), host resistance (Zeier et al. 2004, Jin et al. 2014), or host sensitivity (Lafferty and Kuris 1999, Jokela et al. 2005). Ecological interactions between the host and its competitors, mutualists, and predators can mediate the host's response to infection (Duffy et al. 2011, Wiewiora et al. 2015), as well as pathogen fitness if these species are alternate hosts or coinfecting organisms (Power and Mitchell

2004, Seabloom et al. 2015). It is unclear how these ecological factors will ultimately affect host fitness when they have the same directional effect on both the host and the pathogen (i.e. favorable or unfavorable for both, Lafferty and Holt 2003, Paull et al. 2012a).

When pathogen fitness depends on resources that are consumed by the host, opportunities for resource competition arise (Fig. 4, Smith and Holt 1996, Frost et al. 2008, Cressler et al. 2014). Competitive interactions between the pathogen and the host's cells or microbial community are mediated by the supply rate and ratio of limiting resources (Smith and Holt 1996). A host's diet can also bolster its defense mechanisms or provide it with the resources to tolerate infection (Dietrich et al. 2004, Cornet et al. 2014, Howick and Lazzaro 2014, Zeller and Koella 2017). In addition, the pathogen may down-regulate its own reproduction when the host is stressed by nutrient restriction (Mancio-Silva et al. 2017). Therefore, resources consumed by the host that fuel pathogen growth, host growth, the host microbiome, or host defenses can potentially mediate virulence.

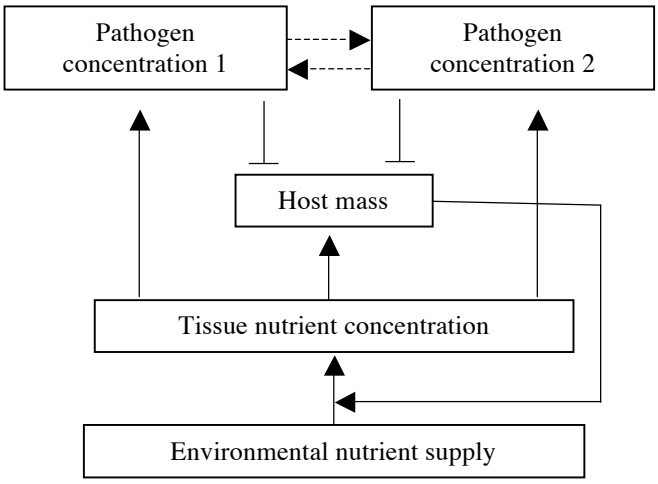

Figure 4. Conceptual diagram of how environmental nutrients, coinfection, and their interaction can affect virulence through reducing host mass (a proxy for fitness metrics such as survival or reproduction). Solid arrows represent positive flows, "T-lines" represent negative impacts, and dashed arrows represent potentially positive or negative interactions.

The impact of resource availability on virulence may depend on other ecological factors, such as the diversity of pathogens in an infection. Coinfection of a single host by multiple pathogens is common in various systems and can have consequences for pathogen and host fitness (Johnson and Hoverman 2012, Alizon et al. 2013, Tollenaere et al. 2016). Coinfecting pathogens may interact through resource or spatial competition, chemical interference, the production of "public goods", or the immune system (Pedersen and Fenton 2007, Bashey 2015). There is both empirical (Hodgson et al. 2004, Lacroix et al. 2014, Lange et al. 2014) and theoretical (Bertness and Callaway 1994, Smith and Holt 1996, Maestre et al. 2009) support that resource availability can mediate these interactions (Fig. 4). When pathogens coexist or have facilitative interactions, they are likely to have higher within-host concentrations than if competition is intense (Loreau 2004). Virulence mechanism that are related to pathogen concentration, such as resource use or toxin production (Culver and Padmanabhan 2007, Mengiste 2012), may then be more intense with positive pathogen interactions. Pathogens that exclude one another from a host or are obligate mutualists determine whether the host experiences symptoms from coinfection.

Ecological factors mediate virulence across a variety of systems (Dordas 2009, Johnson et al. 2010, Griffiths et al. 2011, Seabloom et al. 2015), but resource availability is particularly relevant for agricultural plant systems that are impacted by nutrient deposition and fertilization (Stevens et al. 2015, Ladha et al. 2016). We experimentally manipulated two essential plant nutrients and induced coinfection of two frequently co-occurring grass viruses in a full-factorial design to assess how virulence is affected by each of these ecological factors and their interaction. We altered nitrogen (N) and phosphorus (P) concentrations in soil, expecting that enhanced plant growth or defenses would reduce mass lost due to infection (Dietrich et al. 2004, Dordas 2009, Bellin et al. 2013). However, because viruses require N- and P-containing resources from the host (e.g. ribosomes and nucleic acids, Sterner and Elser 2002, Clasen and Elser 2007, Jover et al. 2014), nutrient addition was expected to increase virus growth and, at least temporarily, alleviate competitive interactions between viruses (Seabloom et al. 2013, Lacroix et al. 2014, Borer et al. 2014b). Therefore, nutrient addition could enhance or reduce virulence depending on the relative responses of hosts and pathogens. We then analyzed how the mechanism causing virulence and nutrient limitation of the host and pathogen contribute to nutrient-mediated virulence using a mathematical model.

Experiment Methods

Study system

The barley and cereal yellow dwarf virus (B/CYDV) group of the family *Luteoviridae* contains several virus species. They infect over 150 grass species, including crops (e.g. barley, wheat, rye, and oats) and wild grasses. The virions are isometric particles composed of a protein capsid and positive single-stranded RNA and their transmission depends on grass-feeding aphids (D'Arcy and Burnett 1995). The virus species used in this experiment were Barley yellow dwarf virus PAV (genus *Luteovirus*, PAV hereafter) and Cereal yellow dwarf virus RPV (genus *Polerovirus*, RPV hereafter). Both virus species are efficiently transmitted by the aphid species *Rhopalosiphum padi* (D'Arcy and Burnett 1995), which we used for experimental inoculations. B/CYDV's affect the fitness of their hosts by reducing fecundity, but other plant traits, such as aboveground biomass, can be proxies for reduced fitness (Malmstrom et al. 2005a). B/CYDV's also cause leaf discoloration, stunt growth, and reduce the root-to-shoot ratio (D'Arcy and Burnett 1995, Erion and Riedell 2012).

Experimental set-up

We maintained colonies of PAV, RPV, and *R. padi*, on *Avena sativa* L. cv. Coast Black Oat (i.e. cultivated oats) in laboratory growth chambers (see Lacroix et al. 2014 for details). To alter nutrient supply rates, we manipulated the concentrations of potassium phosphate and ammonium nitrate in a modified Hoagland solution to create two levels of P and N, respectively, for four nutrient treatments: low levels of both ("Low"), increased P ("P"), increased N ("N"), and increased N and P ("N+P", Table S4, Hoagland and Arnon 1938, Seabloom et al. 2011, Lacroix et al. 2014). The N to P concentration ratio (N:P) for each treatment was 0.15 (P), 7.5 (Low and N+P), and 375

(N). We grew individual *A. sativa* plants in nutrient-deficient soil (70% Sunshine medium vermiculite, Sun Gro Horticulture, Agawam, MA, USA, and 30% Turface MVP, Turface Athletics, Buffalo Grove, IL, USA) and watered them with 30 ml of their assigned solution twice per week prior to the virus inoculations and once per week following the inoculations.

For each nutrient treatment, we applied four inoculation treatments to our experimental plants (mock-inoculation, RPV, PAV, or coinfection) using a two-step process. *1) Aphid acquisition of viruses:* Eight to nine days after the experimental plants were planted, *R. padi* aphids were starved for up to four hours, then allowed to feed on 39.0 mg ± 10.3 mg of healthy, PAV-infected, or RPV-infected leaves for 44-48 hours. *2) Aphid inoculation of plants:* We secured one 2.5 x 8.5 cm, 118 μm polyester mesh cage (Sefar America Inc., Kansas City, MO, USA) to the larger (older) leaf of each experimental plant and pooled the aphids into plastic containers according to the type of leaves they had fed on. We then transferred ten aphids to one cage per plant based on the inoculation treatment (in parentheses): ten aphids that fed on healthy leaves (mock-inoculation), five aphids that fed on RPV-infected and five that fed on healthy leaves (RPV), five aphids that fed on PAV-infected and five that fed on healthy leaves (PAV), or five aphids that fed on PAV-infected and five that fed on RPV-infected (co-inoculation). We secured the cages on both ends with Parafilm® (Bemis Company, Inc., Neenah, WI, USA) and bobby pins to ensure that aphids remained inside for 95-123 hours, at which time we manually crushed them, removed the cages, and gently wiped the leaves with a gloved hand.

The experiment was performed in five temporal blocks from February to August 2014 (blocks one to four) and August to September 2015 (block five). Experimental treatments consisted of all unique combinations of the nutrient treatments (low, N, P, N+P), inoculation treatments (mock, PAV, RPV, co-inoculated), and harvesting days (5, 8, 12, 16, 19, 22, 26, and 29 days post inoculation (dpi)), leading to 128 treatments. Block one contained two replicates per treatment, blocks two through four contained one replicate each, and the fifth block had one to three replicates for treatments that needed additional replication due to losses that occurred in the first four temporal blocks.

Data collection

At each harvesting day, we measured chlorophyll three times along the largest leaf on each plant using a SPAD-502 (Konica Minolta, Tokyo, Japan). Then, we split the plants into shoots (stem and leaves) and roots by dividing them at the highest roots. We weighed the aboveground tissue immediately, and the belowground tissue after rinsing with tap water and drying on paper towels. We stored plant tissue at -80^{o}C until it was analyzed for virus concentrations. We extracted the total plant RNA and quantified virus densities using one-step reverse-transcription quantitative polymerase chain reaction (RT-qPCR, for more details, see Methods S2). This method has a lower limit to reliable quantification, which many of the PAV measurements did not exceed. We addressed this by presenting results with and without these values included.

Statistical analysis

To determine how the experimental treatments affected virus densities (viral copies per mg plant shoot), we took advantage of a natural break in the data and fit regression models to the first three harvesting days and last five harvesting days separately. We assumed the first three days were the exponential growth phase of logistic growth, and examined the effects of dpi, the nutrient treatments, and coinfection on log-transformed density values for each virus. Assuming the last five harvesting days represented fluctuations around a carrying capacity, we examined the effects of the nutrient treatments and coinfection on each virus's densities. To assess how the plants responded to the nutrient treatments and infection over time, we tested the effects of dpi, the nutrient treatments, PAV infection, RPV infection, and all interactions on shoot mass, root mass, and mean leaf chlorophyll per plant using regression models. Finally, we assessed the effects of virus density on the plant traits. We first fit linear mixed-effects models to the traits with all significant nutrient treatments and dpi (based on our first analysis of plant traits). We then fit the residuals of these models to the log-transformed density of each virus, with an interaction term with coinfection.

All regression models were analyzed using R, version 3.3.1 (R Core Team 2016) as follows: we compared the full models with and without random effects (experimental blocks; R package "lme4", Bates et al. 2015) using a likelihood ratio test and proceeded with the better fitting model. For the carrying capacity model, we crossed dpi with experimental block for the random effects. We then assessed the fixed effects by sequentially dropping terms and comparing nested models with Chi-squared tests for mixed-effects models and F-tests for linear models (Zuur et al. 2009). We repeated all

analyses twice: once with categorical N and P levels and once with N:P as a scaled continuous variable.

Experiment Results

Fifty-four percent and 92% of plants inoculated with PAV and RPV, respectively, tested positive for the target virus and had reliable quantities. There were no significant effects of the nutrient treatments or co-inoculation on PAV infection rates, and statistical tests could not be performed for RPV. Thirty-six percent of plants inoculated with PAV had quantities below the lower limit of reliable quantification. Because this percentage is so large, we present a second set of results with these values included, when relevant.

The levels and ratio of N and P mediated the intrinsic growth rate of RPV (i.e. the first three points in Fig. 5). N addition sharply increased RPV's growth rate (lmer: est. = 0.304), unless P was also added, which led to a reduction (lmer: est. = -0.329, χ^2 = 4.09, df = 1, p = 0.0432, Table S7, Fig. 5C-D). The strong deviation of the N treatment from the others caused a significant effect of N:P on RPV's intrinsic growth rates (Table S7). There were no significant effects of nutrient addition and coinfection on PAV's growth rate (Fig. 5A-B) unless samples with quantities below the quantification limit were included in the analysis. When that was the case, N and P interacted to affect PAV's growth rate with an increase due to N addition (lm: est. = 0.382), and a decrease with simultaneous N and P addition (lm: est. = -0.739, F = 5.69, df = 1, p = 0.0190, Table S8). These trends are evident in the more conservative

analysis of PAV's growth rate under coinfection (Fig. 5B). Coinfection increased RPV's carrying capacity (i.e. the last five points in Fig. 5, lm: est. = $6.89e^{4}$, F= 10.2, df = 1, p = $1.60e^{-3}$, Table S9), but there were no significant effects of treatments on PAV's carrying capacity in either analysis.

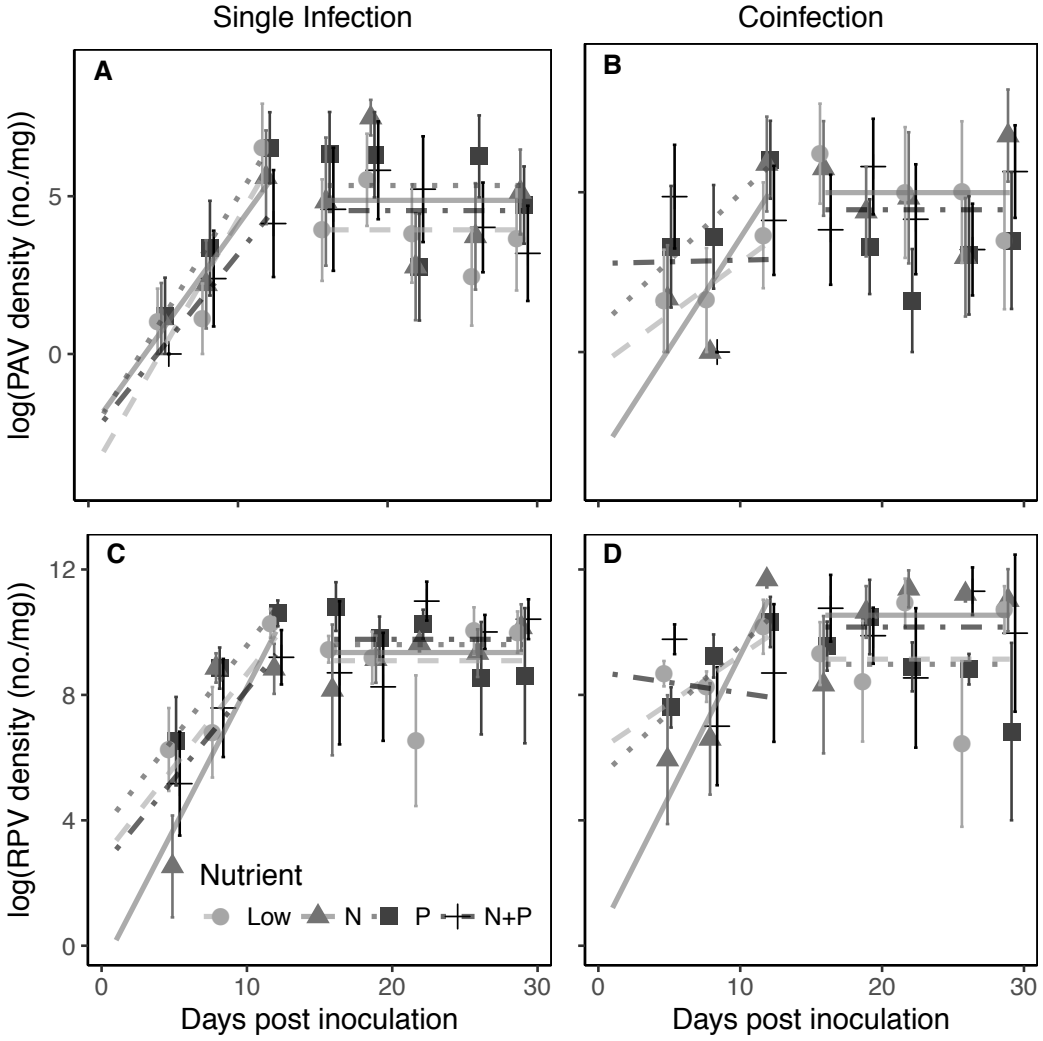

Figure 5. Log-transformed within-host virus densities over the course of infection from destructively sampled oats. The nutrient treatments and coinfection had no significant effect on PAV density (A-B), but N and P interacted to affect RPV's intrinsic growth

rate and coinfection increased RPV's carrying capacity (C-D, Table S7). The lines are predicted values from fitted linear models. Points and error bars represent data used to fit models (mean ± standard error).

We evaluated virulence by comparing the shoot mass, root mass, and leaf chlorophyll of infected plants to healthy plants over time for each of the nutrient treatments. N addition and higher N:P increased shoot mass over time, regardless of the infection status (Fig. 6A-B, Table S10). Infection by one or two viruses decreased shoot mass by about 0.011 g/day and 0.015 g/day, respectively (lmer: $\chi^2 = 6.30$, df = 1, p = 0.012, Table S10). The reduction in shoot mass caused by infection exceeded the positive effects of N addition (0.003 ± 0.003 g/day, lmer: $\chi^2 = 18.1$, df = 1, $p < 0.001$). Interestingly, infection by either virus increased the initial shoot mass, suggesting facilitative effects of early infection (Table S10). PAV, RPV, and coinfection reduced leaf chlorophyll content by 0.022 SPAD/day, 0.246 SPAD/day, and 0.189 SPAD/day, respectively (Fig. 6D-E, Table S11). Adding N reduced these infection-induced losses (lmer: $\chi^2 = 4.16$, df = 1, p = 0.041). When resources were analyzed as ratios, chlorophyll increased with N:P, but there was no interaction with infection (Table S11). There were no significant effects of nutrients or infection on root mass, and including sub-limit PAV quantities did not produce any additional significant findings.

After accounting for the effects of dpi and N addition on plant traits, we found that increasing RPV density reduced shoot mass (lm: F = 4.71, p = 0.01, Table S12, Fig. 6C), and the largest predicted decrease was 19% of the total mass lost due to infection.

There was no significant effect of RPV density on chlorophyll content (Fig. 6F) or PAV density on shoot mass or chlorophyll, regardless of if the sub-limit values were included (Fig. 6C, F).

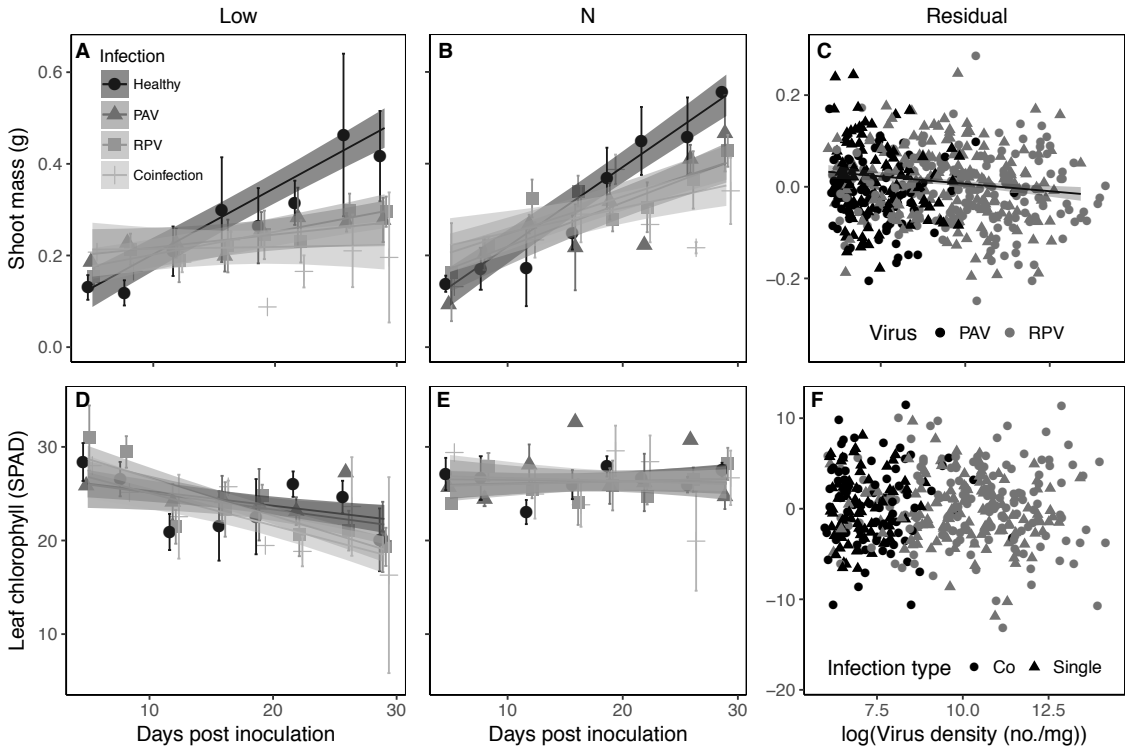

Figure 6. The effects of N addition and infection type on shoot mass (g, A-B) and leaf chlorophyll content (SPAD, D-E) over time and by log-transformed virus density, after accounting for dpi and N addition (no./mg, C, F). N addition had positive effects and infection had negative effects on shoot mass and leaf chlorophyll, but only RPV density affected shoot mass. The lines and shaded bands are the predicted means and standard errors from fitted linear mixed-effect models (Tables S10-S12), the points and error bars are the means and standard errors of the data used to fit the models (A-B, D-E), and the points alone are raw data (C, F).

Model Methods

In our experiment, nutrient addition affected virus density (Fig. 5), but this did not lead to enhanced virulence under high N:P (Fig. 6). This disconnect may have occurred because N addition also benefitted the host (Fig. 6) and virulence was primarily induced by the presence of viruses rather than virus concentration (Fig. 6). The relationship between nutrient supply and virulence appears to depend on (1) the mechanism that leads to virulence and (2) whether the manipulated nutrient affects host or virus growth. We developed a mathematical model to better understand how these two factors mediate virulence. Knowing that in our system, virulence is primarily linked to the presence of the viruses and the viruses sometimes benefit from nutrient addition that enhances host growth, we consider how this scenario fits into the larger realm of possible host-pathogen interactions.

Model description

The model includes equations describing the mass of nutrients in the environment (*E*), the concentration of nutrients (resources) within the plant (*R*), the total host plant mass (*H*), and the concentration of a single pathogen within the plant (*P*). The model can include *n* different nutrients, which are each represented by the subscript *i*. We focus our analyses on the cases of one or two nutrients. The general connections among the model compartments are depicted in Figure 1 with a single pathogen.

$$\frac{dE_i}{dt} = s_i - \frac{u_i E_i H}{E_i + c_i} \quad (1)$$

$$\frac{dR_i}{dt} = \frac{u_i E_i}{E_i + c_i} - \min_{i=1,n}\left(1 - \frac{y_i}{R_i}\right) r R_i - \min_{i=1,n}\left(1 - \frac{y_i + z_i}{R_i}\right) q_i k P \quad (2)$$

$$\frac{dH}{dt} = \min_{i=1,n}\left(1 - \frac{y_i}{R_i}\right) rH - bH - \frac{vPH}{P + w} \quad (3)$$

$$\frac{dP}{dt} = \min_{i=1,n}\left(1 - \frac{y_i + z_i}{R_i}\right) kP - mP. \quad (4)$$

In this model, which is derived from an established plant-resource model (Eq. 1-3, Grace and Tilman 2003), nutrient *i* is supplied at a constant rate (s_i), then taken up by the plant from the environment and enter the plant's tissues following a Monod function (Monod 1949) with a maximum uptake rate (u_i) and half-saturation constant (c_i, Eq. 1-2). The uptake function is multiplied by *H* because larger plants have a higher uptake rate, and u_i is in nutrient concentration units (Grace and Tilman 2003). Tissue nutrients are used to build plant biomass following a Droop function (Droop 1974), with a maximum intrinsic growth rate (*r*) and a minimum tissue nutrient concentration needed for growth (y_i, Eq. 2-3). The minimum functions incorporate the assumption that all of the nutrients are essential to host growth, and that the host will be limited by the nutrient that causes the smallest per unit increase in mass (von Liebig 1840, Leon and Tumpson 1975, Tilman 1981, Klausmeier et al. 2004). Plant mass is reduced at a constant rate (*b*) due to cell death.

We expanded this plant-resource model by adding an equation that describes pathogen growth (Eq. 4) and pathogen use of host resources (last term in Eq. 2). Building off previous models of nutrients, hosts, and pathogens (Fuhrman et al. 2011, Béchette et al. 2013, Gerla et al. 2013), we represented pathogen growth using a Droop function with a maximum intrinsic growth rate (*k*), a minimum function to select the

most limiting nutrient, and a constant loss rate (m, Eq. 4). The pathogen's minimum tissue nutrient concentration required for growth is defined relative to the hosts, with a term (z_i) quantifying how much they differ. For $z_i = 0$, the same tissue nutrient concentration that halts host growth also stops pathogen growth, consistent with virus replication that is limited by the host's molecular metabolites and protein synthesis machinery (Birch et al. 2012) and malaria parasites that sense caloric restrictions and reduce replication (Mancio-Silva et al. 2017). For $z_i > 0$, the host can grow at lower tissue nutrient concentration levels than the pathogen, which was demonstrated for a freshwater alga and its virus at low P:C (Clasen and Elser 2007). Finally, when $z_i < 0$, the pathogen can grow at tissue nutrient concentrations that are low enough to prevent host growth, which may be the mechanism behind trematode-induced death of starved clams (Jokela et al. 2005).

We represented the negative effects of the pathogen on the host through three mechanisms. The first is that the pathogen is drawing resources from the plant's tissue, which is represented by the same function used to describe pathogen growth, multiplied by the proportion of pathogen mass accounted for by the resource (q_i, Eq. 2). Second, as the pathogen grows, it may be able to cause more harm to the host through the production of molecules such as toxins, reactive oxygen species, and cell wall-degrading enzymes (Horbach et al. 2011). We represented this with a Monod function that includes a half-saturation constant (w) and maximum mass loss rate (v, Eq. 3). Finally, the presence of the pathogen alone may be the main factor that determines virulence through processes such as immune responses that are harmful to the host or

manipulated developmental pathways (Culver and Padmanabhan 2007, Pallas and García 2011). To represent these processes, we assume that w is very small, which leads to an essentially constant mass loss rate as long as the pathogen concentration is positive (Eq. 3).

Parameter estimation

Our experimental results indicated that plant growth was N-limited and that RPV growth was enhanced with higher N, particularly in coinfection. Therefore, we began by parameterizing the model with the assumption that the host and pathogen were limited by and consumed a single resource. We estimated values for the plant-resource parameters u, c, and y (note that subscript i was removed because the model deals with a single resource) using data from a single experiment in which barley was grown over a range of N concentrations (Mattsson et al. 1991, Table 3). We used values from the previously described experiment and additional small experiments to estimate the supply rate (s), the initial mass of N in the environment (E_0), the initial N concentration in plant tissue (R_0), the initial host mass (H_0), and the initial pathogen concentration (P_0). We fit the model without a pathogen (Eq. 1-3) to healthy plant mass data to estimate the remaining plant parameters (r, b). Because virulence was primarily caused by pathogen presence, we formatted the model to represent this mechanism and fit it to RPV concentrations and host mass from the high N coinfection treatment to estimate k, m, and v. Finally, we assumed each of the other two virulence mechanisms and fit the model to the host mass from the high N coinfection treatment to estimate z_1, and q. For more details on parameter estimation, see Methods S3.

Table 3. Model parameter and initial state variable values

Parameter	Value	Units	Explanation
s	$5.5e^{-5}$	g N day^{-1}	Supply rate of N
u	$4.9e^{-3}$	g N (g plant)$^{-1}$ day^{-1}	Maximum uptake rate of N
c	$4.3e^{-5}$	g N	Half-saturation constant (mass of E at half of u)
r	0.281	day^{-1}	Maximum intrinsic growth rate of plant mass
y_1	$7e^{-4}$	g N (g plant)$^{-1}$	Tissue N concentration required for plant growth
y_2	0	g resource (g plant)$^{-1}$	Tissue concentration of secondary resource required for plant growth
b	0.0949	day^{-1}	Host mortality rate
q	$8.70e^{-6}$	g N (pg virus)$^{-1}$	Pathogen resource use conversion coefficient
k	1.15	day^{-1}	Maximum intrinsic growth rate of pathogen
z_1	$5.08e^{-4}$	g N (g plant)$^{-1}$	Deviation of pathogen's minimum tissue N concentration from the host's
z_2	$y_1 + z_1$	g resource (g plant)$^{-1}$	Deviation of pathogen's minimum secondary resource tissue concentration

			from the host's
m	0.0882	day^{-1}	Pathogen mortality rate
v	0.0154	day^{-1}	Maximum mass loss due to pathogen presence
w	$1e^{-100}$ or 0.299	g virus (g plant)$^{-1}$	Half-saturation constant for presence virulence and concentration-dependent virulence
E_0	$1.94e^{-4}$	g N	Initial environmental mass of N
R_0	0.0188	g N (g plant)$^{-1}$	Initial plant N concentration
H_0	0.0292	g	Initial plant mass
P_0	0.001	pg virus (g plant)$^{-1}$	Initial pathogen concentration in the host

Note: Subscripts were removed from parameters and variables that apply to both N and the secondary resource (subscripts 1 and 2, respectively, Methods S3).

Simulations

We assessed the effects of resource supply rate on virulence for six model scenarios. Half of the model scenarios assumed that the same resource determined host and pathogen growth and the other half assumed that the pathogen was growth-limited by a secondary resource that had no effect on host growth. These situations are reflective of the impact coinfection had on the relationship between nutrient addition and virus growth in our experiment, where virus growth rates were more sensitive to N

addition in coinfection than single infection (Fig. 5). Within each of these two resource assumptions, we modified the model to represent the three different mechanisms behind virulence: presence ($q = 0$, small w, $v > 0$), concentration ($q = 0$, larger w, $v > 0$), and resource use ($q > 0$, $v = 0$). To determine a relevant range of values for the resource supply rate, we considered our experimental manipulations and values from the literature. The maximum global N deposition rate is approximately $1.12e^{-5}$ g N day^{-1} (Stevens et al. 2015) and the average global N fertilization rate for maize and rice in 2010 was approximately $3.73e^{-5}$ g N day^{-1} (Ladha et al. 2016). Therefore, we varied the value of s from $1e^{-7}$ to $1e^{-4}$ g N day^{-1} and calculated the proportion of total mass lost due to infection on the last day of the simulation (30 dpi). To constrain the model to realistic values, we log-transformed the pathogen concentration (Ramsay and Hooker 2017), which was becoming negative in some simulations. We also substituted zero for the minimum functions when they became negative.

Model Results

When we assumed N limited host and pathogen growth, the mechanism behind virulence altered the relationship between the resource supply rate and the proportion of mass lost (Fig. 7D). Except when the resource supply rate was very low, it had little effect on the proportion of mass lost when virulence was due to the presence of the pathogen, as we observed for PAV and RPV (Fig. 7D). This relationship results from a linear increase in healthy and infected host mass with increasing resource supply (Fig. 7A). Increasing the resource supply enhanced pathogen growth, leading to an increase

in the proportion of mass lost due to concentration-dependent virulence until it reached its maximum value (Fig. 7D, 7G). When resource supply rates were low and virulence was due to pathogen resource use, infected host mass did not deviate from healthy host mass (Fig. 7A). Eventually, pathogen competition with the host for resources increased the proportion of mass lost with increasing resource supply rate (Fig. 7D).

When the host and pathogen depended on different resources and the host's limiting resource was manipulated, the proportion of mass lost due to pathogen presence or concentration was similar because the pathogen concentration was high enough to draw down host mass at the maximum rate (Fig. 7E, 7H). Because the pathogen's resource was supplied at a constant rate, it suppressed host growth across low host resource supply rates (Fig. 7B) However, when the host's resource supply rate exceeded that of the pathogen (*s* in Table 3), the host drew down the pathogen's resources and recovered mass (Fig. 7B, 7E, 7H).

When the pathogen's limiting resource was manipulated, the plant's mass was consistently suppressed by the presence of the pathogen (Fig. 7C, 7F). Initial changes in pathogen concentration caused an increased in the proportion of host mass lost due to pathogen concentration (Fig. 7F, 7I). As the pathogen increased in concentration and consumed the resource limiting host growth, the host's mass decreased towards zero (Fig. 7C, 7I).

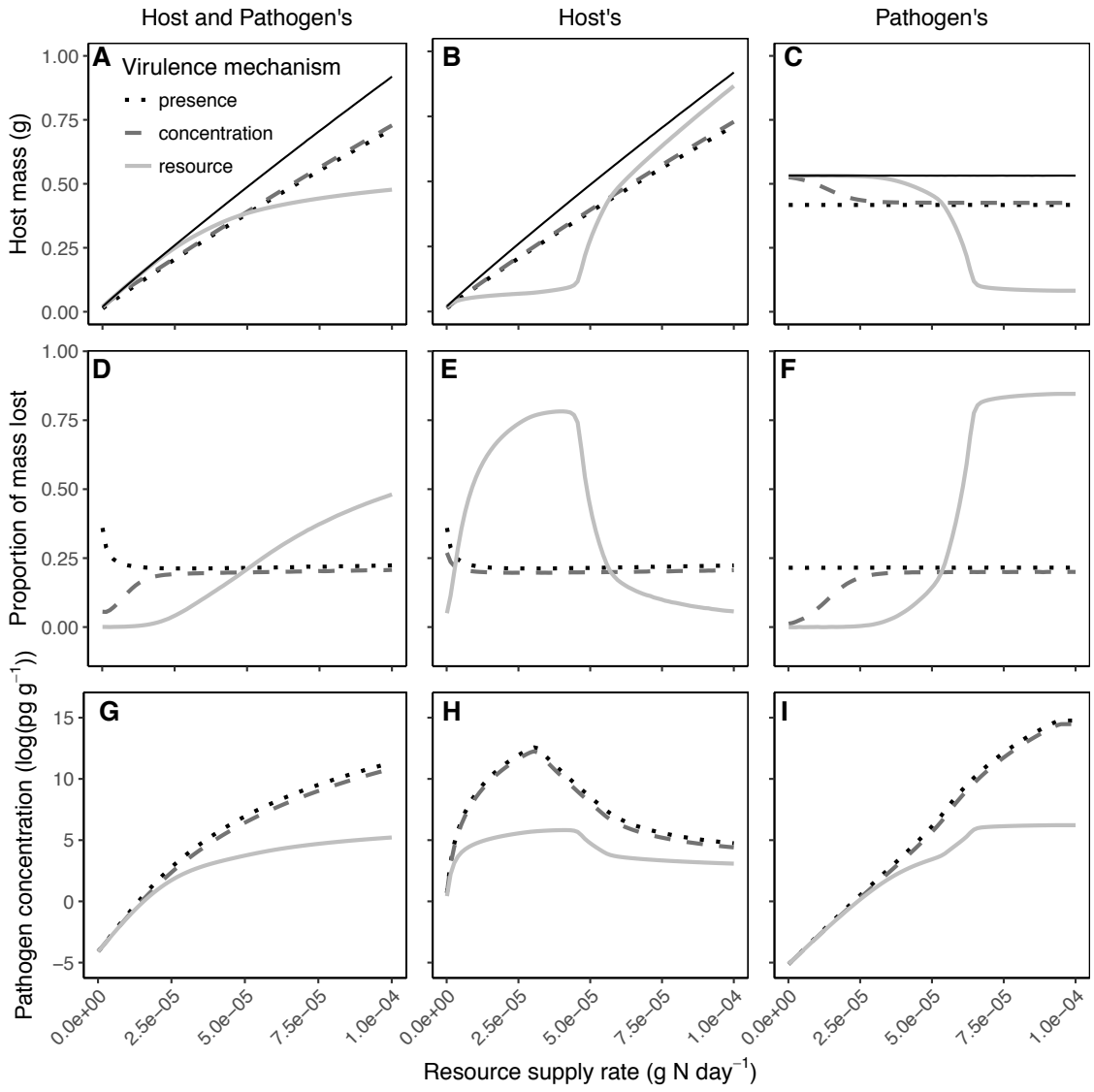

Figure 7. Model simulations showing the effects of the resource supply rate on host mass (A-C), the proportion of mass lost (D-F), and log-transformed pathogen concentration (G-I). The resource manipulated either limited both the host's and the pathogen's growth (A, D, G), the host's growth (B, E, H), or the pathogen's growth (C, F, I). Each line type represents a different mechanisms of virulence (legend) and the solid black lines in A-C represent healthy plants. Simulations were run for 30 dpi with the parameters in Table 3.

Discussion

Both resource availability and coinfection play prominent roles in a variety of disease systems (Dordas 2009, Johnson et al. 2010, Griffiths et al. 2011, Seabloom et al. 2015), but the potential for these ecological factors to alter both host and pathogen fitness makes predicting their effects on virulence challenging (Lafferty and Holt 2003, Paull et al. 2012a). For our empirical case study of two plant viruses in oats, nutrient addition that promoted plant growth partially offset infection-induced mass loss and counteracted the negative effects of infection on chlorophyll content. Facilitation between the viruses may have contributed to higher symptom intensity observed in coinfected plants. However, the effects of nutrients on virus growth rates did not appear to meaningfully affect virulence, likely due to a weak connection between virus density and host traits. Through analysis of a mathematical model, we determined that ecological factors are more likely to modify the proportion of host mass lost to infection when resource consumption is the primary mechanism behind virulence.

Our empirical results highlight two general ways in which resources that promote host growth can reduce virulence. First, adding N allowed the oat plants to recover shoot mass lost to infection in the low N treatments. In this scenario, the low N treatments represent an environmental stress. The compounding effects of environmental stress and infection on host fitness have been observed for a variety of systems and can have important consequences for disease dynamics (Walters and Plumb 1980, Harvell et al. 2002, Furlong and Groden 2003, Jokela et al. 2005). Second,

adding N reduced the proportion of chlorophyll lost due to infection, essentially removing the negative impacts of infection. This result suggests that nutrient allocation may be related to plant infection status, as has been shown for moth larvae (Cotter et al. 2011). Infection actually increased initial shoot mass, indicating that plants may allocate to growth early in infection or pathogens may induce early growth spurts, analogous to compensatory growth or reproduction observed in animals (Arnott et al. 2000, Chadwick and Little 2005). A third potential strategy would be for the plant to allocate resources to resistance, which would manifest as reduced symptoms and pathogen density with nutrient addition (Dietrich et al. 2004, Cornet et al. 2014).

Our model did not include alternate allocation strategies, but demonstrated additional mechanisms through which nutrient addition could reduce virulence. At very low resource supply rates, when the host mass was near zero, increasing host growth through resource availability decreased virulence caused by pathogen presence and concentration. When the pathogen caused virulence through resource use, increasing the nutrient that was limiting host growth, but not pathogen growth, allowed the host to draw down pathogen resources. While the second mechanism is consistent with resource competition theory (Smith and Holt 1996), the first is less well known, but perhaps relevant to plant virus systems, in which virulence tends to be caused by pathogen presence (Whitham and Wang 2004, Culver and Padmanabhan 2007, Pallas and García 2011). The potential for nutrient addition to decrease virulence through resource competition may be more applicable to animal hosts (Smith et al. 2005, Handel and Rohani 2015).

The other pathway through which resource availability mediates virulence is pathogen growth. When the pathogen caused virulence through resource use or concentration in the model, and when the supply rate of the resource limiting its growth increased, virulence also increased. Interestingly, this occurred when the host and pathogen were limited by the same resource, indicating that the pathogen could capture resources before the host, even with a higher minimum nutrient concentration requirement. This is consistent with bacterial pathogens that reduce iron availability in African violets (Neema et al. 1993) and fungal pathogens that alter tomato plant physiology to obtain N (Solomon and Oliver 2002). Expanding the model to more explicitly represent within-host nutrient allocation, including to immune functions (as in Cressler et al. 2014), would enhance host-pathogen resource competition theory.

While virulence was not altered, we did observe nutrient-mediated pathogen growth in our empirical case study: high N:P increased RPV and PAV's intrinsic growth rates. It is unclear what mechanisms drove this outcome, but increased host growth rate and production of C- or N-rich molecules have been linked to B/CYDV replication (Whitaker et al. 2015, Lacroix et al. 2017). In addition, the presence of PAV increased RPV's carrying capacity. RPV may have used excess coat proteins produced by PAV (Creamer and Falk 1990, Wen and Lister 1991), which are necessary for movement and further replication throughout the plant (Ali et al. 2014). Facilitation may have also been driven by immunosuppression (Syller 2012), because different B/CYDV species can produce different RNA silencing suppressors, which protect them against host defenses (Liu et al. 2012, Almasi et al. 2015). Regardless of the

mechanism, within-host facilitation may explain why B/CYDV coinfection rates are so high in the field (Seabloom et al. 2009). Expanding the model to explicitly include multiple pathogens may uncover additional mechanisms through which pathogen interactions can affect virulence.

Understanding the drivers of virulence is critical for managing disease emergence, herd immunity, and the overall impact of disease on a population (Hethcote 2000, Heffernan et al. 2005, Fine et al. 2011). The ecological interactions and abiotic conditions influencing host and pathogen fitness are numerous, but their realized effects on disease virulence depend on the underlying host-pathogen interaction (Zeier et al. 2004, Hall et al. 2009, Thompson et al. 2010, Jin et al. 2014). Our empirical case study demonstrated small to no effects of ecological factors on virulence, but we used our mathematical model to determine conditions under which nutrient supply rates can affect losses in host mass. We found that virulence is much more sensitive to variation in resource manipulation in systems where the pathogen consumes a large portion of host resources, which can be taken into consideration when evaluating potential impacts of human-mediated environmental nutrient supplies on disease.

Acknowledgements

We would like to thank Christelle Lacroix for help with developing virus quantification methods and performing the experiments. We are also grateful to Melissa Rudeen and many undergraduate researchers for assistance with the laboratory experiment, including Emily Boak, Alexis Rogers, Nicholas Cupery, Casey Easterday,

Luc Robichaud, Timothy Martin, and Kurra Renner. Linda Kinkel, Meggan Craft, and Allison Shaw provided thoughtful feedback on the manuscript. AEK was supported by an NSF IGERT graduate fellowship at the University of Minnesota (DGE-0653827) and an NSF Graduate Research Fellowship (base award number 0006595), YK was partially supported by NSF grants DMS-1518529 and DMS-1615879, and ETB and EWS received support from the NSF program in Ecology and Evolution of Infectious Diseases (grant DEB-1015805).

Chapter 3

Plant virus coexistence occurs at multiple scales regardless of environmental nutrient availability

Amy E. Kendig, Elizabeth T. Borer, Eric W. Seabloom, and Emily N. Boak

Summary

Individual plants and animals are frequently infected with multiple pathogens, motivating the question of how different pathogens coexist given overlapping resource requirements and immune reactions. Barley and Cereal Yellow Dwarf Viruses (B/CYDVs) are frequently found together in grasses, and soil nutrients mediate their prevalence and interactions. We examined the effects of soil nutrients on the coexistence of two B/CYDVs using the mutual invasibility criterion. In growth chambers, we inoculated oats grown in full factorial nitrogen and phosphorus addition treatments with "resident" and then "invader" viruses. The viruses could invade one another regardless of soil nutrient concentration, suggesting they can coexist within hosts. We also measured transmission from single- and co-infected plants to new plants. Coinfection decreased transmission of one virus while nitrogen addition to the receiving plant increased transmission for both viruses. Using a mathematical model, we demonstrated that reduced transmission from coinfected plants is unlikely to prevent coexistence at the host population scale.

Keywords: mutual invasion, Barley and cereal yellow dwarf viruses, nitrogen, phosphorus, within-host, among-host

Introduction

The mechanisms contributing to the coexistence of pathogens can have important implications for pathogen diversity (Ojosnegros et al. 2012, Cobey and Lipsitch 2013, Bashey 2015, Mordecai et al. 2016), the severity and prevalence of disease (de Roode et al. 2004, Vasco et al. 2007, Griffiths et al. 2011, Alizon et al. 2013), and the consequences of disease management (Colijn et al. 2010, Murall et al. 2012, Lloyd-Smith 2013). While theoretical and empirical studies have greatly contributed to our understanding of coexistence in communities of free-living organisms (Tilman 1982, Chesson 2000, Wright 2002, Silvertown 2004, Valladares et al. 2015), pathogen community ecology is a younger field (Holt and Dobson 2006, Pedersen and Fenton 2007, Johnson et al. 2015). For example, it is not widely known how frequently pathogens coexist, what mechanisms promote their coexistence, and at what spatial scale coexistence occurs. Ecological similarities between communities of free-living organisms and pathogen communities suggest that coexistence mechanisms found in the former are active in the latter (Seabloom et al. 2015).

Co-occurring species often overlap in their resource requirements or share natural enemies, which can lead to the competitive exclusion of species from a community (Gause 1934, Hardin 1960, Holt 1977). Therefore, coexistence mechanisms are needed to explain why many different species can co-occur over long periods of time despite the pressures of competition (Hutchinson 1959). Niche differences cause enough segregation between species' resource requirements that they can increase in abundance when they are rare, preventing exclusion (Chesson 2000). Mutual invasion

trials, in which each species is introduced to an environment where its competitors have established, test the nature of coexistence among species (Strobeck 1973, Turelli 1978). Successful mutual invasions by competing species indicate that they have niche differences and can coexist. If some invaders cannot grow while others can, then a competitive hierarchy exists, and if none can invade the others, then the first species to establish will exclude the rest (Siepielski and McPeek 2010, Vellend 2010). The growth rate of a species when it is invading relative to when it is common indicates the strength of niche differences (Adler et al. 2007).

Coexistence of pathogens can occur at two different scales: within host individuals and within the host community (Mihaljevic 2012, Borer et al. 2016). Within-host coexistence often leads to coexistence among hosts (Amarasekare 2003). Coexistence at the host community scale can occur regardless of within-host coexistence through mechanisms summarized by the "metacommunity framework" (Amarasekare 2003, Leibold et al. 2004). These include neutral dynamics (Hubbell 2001), a competition-colonization trade-off between species (Tilman 1994), source-sink dynamics (Pulliam 1988, Amarasekare and Nisbet 2001), or niche partitioning of patches with different characteristics (Tilman 1982, Chesson 2000, Cottenie et al. 2003). Some of these mechanisms apply to the coexistence of pathogen strains (Ojosnegros et al. 2010, Cobey and Lipsitch 2012). However, most studies do not employ the mutual invasibility criterion to rigorously evaluate pathogen coexistence (but see Mordecai et al. 2016).

The supply rates and ratios of resources may be an important factor mediating the coexistence of pathogens, as it is for some communities of free-living species (Tilman 1977, Miller et al. 2005, Borer et al. 2014a, Harpole et al. 2016). Coexistence arises when species have trade-offs in which resources are most limiting to their growth, and the supply rates and ratios are such that species consume more of the resource limiting their own growth (Tilman 1982). Competition for resources can also interact with facilitation or predation to create niche differences or reduce the impact of competition (Bertness and Callaway 1994, Gross 2008, Chesson and Kuang 2008, Maestre et al. 2009). There is some evidence that trade-offs in resource requirements among pathogens reduce competition (Fitt et al. 2006, Ramiro et al. 2016), and that host diet can mediate within-host pathogen interactions (Lacroix et al. 2014, Lange et al. 2014, Wale et al. 2017). Variation in resource availability among hosts may arise from habitat heterogeneity or diet choice (Coop and Kyriazakis 2001, Smith et al. 2005, Dordas 2009, Borer et al. 2010b, 2016), which can contribute to pathogen coexistence at the host community scale.

We tested the hypothesis that resources mediate pathogen coexistence by experimentally manipulating the supply rates and ratio of nitrogen (N) and phosphorus (P) in a plant-virus system. We examined the effects of this nutrient manipulation on the ability of each virus to invade a host individual or host population infected with the other. Invasion trials were performed at the within-host scale using experimental inoculations and at the host population scale by parameterizing a mathematical model with experimentally-estimated transmission rates. The viruses were able to coexist

within hosts regardless of the nutrient treatment, suggesting that another niche difference is important. On the other hand, transmission of one virus to new hosts was reduced by coinfection. Despite this transmission interference, the viruses are still likely to coexist at the host population scale.

Material and methods

Study system

The Barley and Cereal Yellow Dwarf Virus (B/CYDV) group is capable of infecting many grass species, including widespread crops such as barley, wheat, and oats. The single-stranded RNA viruses are persistently transmitted by grass-feeding aphids (D'Arcy and Burnett 1995). We used two B/CYDV species in this study: Barley yellow dwarf virus PAV (genus *Luteovirus*, PAV hereafter) and Cereal yellow dwarf virus RPV (genus *Polerovirus*, RPV hereafter), which are both vectored by the aphid species *Rhopalosiphum padi* (D'Arcy and Burnett 1995). PAV and RPV are frequently found together in natural grasslands, both within individual hosts and the same host community (Seabloom et al. 2009, Kendig et al. 2017). Laboratory experiments suggest that N may limit within-host pathogen growth and mediate the intensity of within-host competition (Lacroix et al. 2014, Whitaker et al. 2015). In the field, high P or high P:N fertilization treatments increased the infection prevalence of PAV, but not RPV (Seabloom et al. 2013, Borer et al. 2014b).

We maintained cultures of PAV and RPV in *A. sativa* L. cv. Coast Black Oat (National plant germplasm system, USDA; USA) by transferring *R. padi* aphids

between infected and healthy *A. sativa* every three weeks following the inoculation procedure described in the next section. We obtained the virus isolates from Dr. Stewart Gray at Cornell University (Ithaca, NY, USA), and the aphids from Dr. George Heimpel at the University of Minnesota (St. Paul, MN, USA), who each collected these organisms in their respective states. Healthy plants, infected plants, and *A. sativa* with *R. padi* were grown in Sunshine MVP potting soil (Sun Gro Horticulture, Agawam, MA, USA) and kept in separate growth chambers with a 16:8 h light:dark cycle.

Experimental set-up

We performed two experiments: one to test the effects of nutrients on within-host mutual invasibility ("invasion experiment"), which ran from September to December 2015, and one to test the effects of nutrients on B/CYDV transmission between plants ("transmission experiment"), which was carried out from February to August 2014. Both experiments followed the same methods, unless otherwise noted (see Table 4).

Table 4. Methodological details specific to the transmission experiment and invasion experiment

Experiment	Plant or virus stages	Inoculation trt. and aphids used	Inoculation times	No. of aphids/ plant and their inoculation trt.	Harvesting days	Rep./trt.	Rep./ block	No. temporal experiment blocks
Invasion	Resident and single viruses	PAV or RPV	11 DPP	5 with virus	5, 8, 12, 16, and 19 DPI invaders	4-5	1	4
	Invader viruses	Opposite virus (to residents) or mock (to singles)	23 DPP (same plants as above)	5 with virus or 5 mock				
Transmission	Source plants	PAV, RPV, or coinfection	10-11 DPP	Single virus: 5 with virus, 5 mock, Coinfection: 5 PAV and 5 RPV	5, 8, 12, 16, 19, 22, 26, 29 DPI	0-5	0-3	4
	Receiving plants	Same as source plant	Source plant harvesting days (9-11 DPP)	5 from source plants	14-15 DPI	0-5	0-3	

Note: DPP = days post planting, DPI = days post inoculation with "day 0" equal to the first day the aphids were introduced, Rep. = replicates, Trt. = treatments. For the transmission experiment, replicates are unique combinations of harvesting day, virus species, nutrient treatment, and coinfection for the source plants and virus species, source nutrient, receiving plant nutrient, and source coinfection status for the receiving plant. For the invasion experiment, replicates are unique combinations of virus species, nutrient treatment, harvesting day, and virus role.

A. sativa seeds were germinated in 164 mL conical pots filled with 70% Sunshine medium vermiculite (vermiculite and <1% crystalline silica; Sun Gro Horticulture, Agawam, MA, USA) and 30% Turface MVP (calcined clay containing up to 30% crystalline silica; Turface Athletics, Buffalo Grove, IL, USA) that had been saturated with tap water (approximately 5 L for every 20 L of soil mixture). Beginning two days after planting, we watered each plant with one of four modified Hoagland solutions: low N and P ("low"), low N and high P ("P"), high N and low P ("N"), or high N and P ("N+P") (Table S1, Hoagland and Arnon 1938, Seabloom et al. 2011, Lacroix et al. 2014, 2017). The low and N+P treatments had the same N:P of 7.5, and the other two were 0.15 and 375. Plants were watered twice per week with 30 mL of nutrient solution prior to inoculation and weekly following inoculation.

We performed the transmission experiment by inoculating "source plants" with viruses (PAV, RPV, or both), allowing the infections to progress for five to 29 days, and then using them to inoculate "receiving plants" (Table 4). We applied the described nutrient treatments to both the source plants and receiving plants. For more information about the source plants, see Ch. 2. The invasion experiment involved an initial infection to plants (PAV or RPV), which were then inoculated with an "invader" virus (into "residents") or a mock inoculation (into "singles", Table 4).

For the general inoculation procedure, *R. padi* were starved in sealed glass tubes in groups of twenty for up to four hours to help ensure feeding on target plants. Then, we added 39.0 mg ± 10.3 mg of healthy (mock-inoculation), PAV-infected, or RPV-

infected leaves from virus cultures to the tubes. After 44-48 hours, we pooled the aphids in large plastic containers according to their inoculation type, and added them to 2.5 x 8.5 cm, 118 µm polyester mesh cages (Sefar America Inc., Kansas City, MO, USA) affixed to the plants (aphid numbers in Table 4). The cages were secured to the plants with Parafilm® (Bemis Company, Inc., Neenah, WI, USA) and two bobby pins on either end. The aphids were allowed to feed for 95-123 hours, at which time they were manually crushed, the cages were removed, and the leaves were wiped with a gloved hand to remove any remaining aphids.

Data Collection

We destructively harvested the plants at multiple time points following inoculation (Table 4). Therefore, each treatment consists of a unique combination of nutrient treatment, inoculation treatment, and harvesting day. On each harvesting day, the plants were split into aboveground and belowground parts by separating them at the highest roots. For the transmission experiment, the plant material was weighed and either allocated to tubes for transmission trials or stored at -80°C for later molecular analysis. For the invasion experiment, we put the plant tissue in 15 mL plastic centrifuge tubes and submerged them in liquid nitrogen prior to storing them at -80°C. We weighed the plant material for the invasion experiment prior to molecular analysis.

The transmission trials occurred at each harvesting day of the transmission experiment and followed the general inoculation methods, with the following exceptions. For the aphids to acquire viruses from the experimental plants, we placed 25 aphids in sealed tubes with 40% of the aboveground source plant tissue. In the first

block of the experiment, there was a shortage of aphids for the second and third harvesting days. We used 13-25 aphids per tube and scaled down the plant tissue accordingly. We aimed to inoculate four receiving plants for each source plant, one grown in each nutrient treatment. They were later harvested and stored at -80°C.

Virus detection and quantification

Briefly, we extracted the total RNA from all aboveground plant tissue following the manufacturer's instructions for TRIzol™ Reagent (Invitrogen™, Thermo Fisher Scientific, Waltham, MA, USA). We quantified PAV and RPV density in the transmission experiment source plants and all plants from the invasion experiment using one-step reverse transcription-quantitative polymerase chain reaction (RT-qPCR). We prepared reactions using virus-specific primers and probes (Table S2), and the RNA-to-C_T™ 1-Step Kit (Applied Biosystems®, Thermo Fisher Scientific) for the transmission experiment and the Path-ID™ Multiplex One-Step RT-PCR Kit (Applied Biosystems®) for the invasion experiment. We switched kits between experiments because with the first kit, PAV detection was lower when we used primers and probes for both viruses in the same well, leading us to quantify each virus for the same sample in separate wells. We found that this problem was less severe for the second kit, so we chose to use it for the invasion experiment to reduce the number of times each sample was analyzed (for more details on the qPCR protocols, see Methods S1). We used reverse transcription PCR (RT-PCR) and gel electrophoresis (see Lacroix et al. 2014 for further details) to test the inoculation success of transmission receiving plants.

Statistical analysis

All analyses were performed in R version 3.3.3 (R Core Team 2016). We used the lme4 package to fit generalized linear mixed-effects models (glmer) with a logit link function to binary response variables and linear mixed-effects models (lmer) to continuous response variables (Bates et al. 2015). If glmer models did not converge, we used the "bobyqa" optimizer, allowing $2e^5$ function evaluations. We evaluated random effects using likelihood ratio tests and fixed effects using Chi-square tests and F-tests for models with and without random effects, respectively. We sequentially dropped terms by order and compared nested models (Zuur et al. 2009). We repeated all models twice: once with categorical N and P addition treatments (i.e. N x P where N and P can each be 0 or 1) and again with scaled values of N:P. We analyzed models for PAV and RPV separately.

To evaluate the factors affecting whether a virus was able to invade an established infection, we used presence/absence of the invader as the binary response variable, an interaction between nutrient treatments and days post inoculation of the invading viruses (DPI) as fixed effects, and experimental block as the random effect.

We compared the growth rates of invaders to singly-inoculated plants from the same experiment (i.e. high density) and the transmission experiment (i.e. low density) using log-transformed virus density over the first three harvesting days as the response variable (most treatments were increasing over this time period). Fixed effects included the full interaction set of nutrient treatment, DPI, and virus "role" (i.e. invader, high density, low density), and the random effect was the experimental block. The comparison between invaders and the high density singly-inoculated viruses indicates

whether viruses have a growth rate advantage when they are rare. The comparison with low density singly-inoculated viruses indicates whether a virus's low-density growth rate is altered when a resident is present. However, the latter result should be interpreted with caution given experimental differences (Table 4).

We evaluated whether invasion affected resident viruses by comparing their densities to those of singly-inoculated viruses. We used an interaction between nutrient treatment and "role" (i.e. resident vs. single) as the fixed effects and experimental block crossed with DPI as the random effects. We used the DPI as a random effect in this model and others rather than a temporal autocorrelation because the plants sampled at each harvesting day were independent from one another.

We analyzed the effects of nutrients on transmission rates using a binary response variable indicating whether the receiving plant tested positive for the virus of interest (i.e. PAV or RPV). To evaluate the effects of the source plant on transmission, the fixed effects included an interaction between the nutrient treatment of the source plant and the log-transformed virus density. This interaction term was added to a term representing attributes of the receiving plant, including an interaction between its nutrient treatment and whether the source plant was coinfected. We chose to put coinfection with the receiving plant nutrient treatment because viruses can interact within the vector (Gildow and Rochow 1980) or upon inoculation into the receiving plant (Wen et al. 1991). In addition, effects of coinfection on the focal virus in the source plant are included in the virus density measurement (Ch. 2). For the random effects, we nested the identity of the source plant (which were used to inoculate

multiple receiving plants) inside the experimental block. This term was crossed with DPI. We always kept the source plant identity in the random effects regardless of if it significantly affected the model fit.

Results

Within-host coexistence

PAV and RPV invaded each other regardless of the nutrient treatment. The detection rate of invading PAV infections increased over time (glmer: est. = 0.286, χ^2 = 43.4, df = 1, p = $4.40e^{-11}$, Fig. S5, Table S15) and RPV was detected in all plants it was inoculated with (Fig. S5). Invading viruses had higher growth rates than those that had established infections in singly-inoculated plants (high density), but lower growth rates than singly-inoculated viruses in the transmission experiment (low density) for both PAV (lmer: high density est. = -0.544, low density est. = 0.295, χ^2 = 21.5, df = 2, p = $2.12e^{-5}$, Fig. 8 Table S16) and RPV (lm: high density est. = -0.253, low density est. = 0.212, F = 8.56, df = 2, p = $2.85e^{-4}$, Fig. 8 Table S17). There were no significant effects of the nutrient treatments on the viruses' growth rates, except when the data from the transmission experiment were removed from the analysis. In this case, N addition significantly increased PAV's growth rate (lmer: est. = 0.113, χ^2 = 3.95, df = 1, p = 0.0469).

The proportion of plants successfully infected with residents or singly-inoculated viruses was at or near one across the experiment, indicating that invading viruses did not exclude residents (Fig. S5). Further, invasion did not significantly alter

the densities of residents relative to singly-inoculated viruses (Fig.8, Tables S18-S19). Singly-inoculated and resident PAV viruses increased in density with N addition (lmer: est. = 447, $\chi^2 = 4.24$, df = 1, p = 0.040, Table S18).

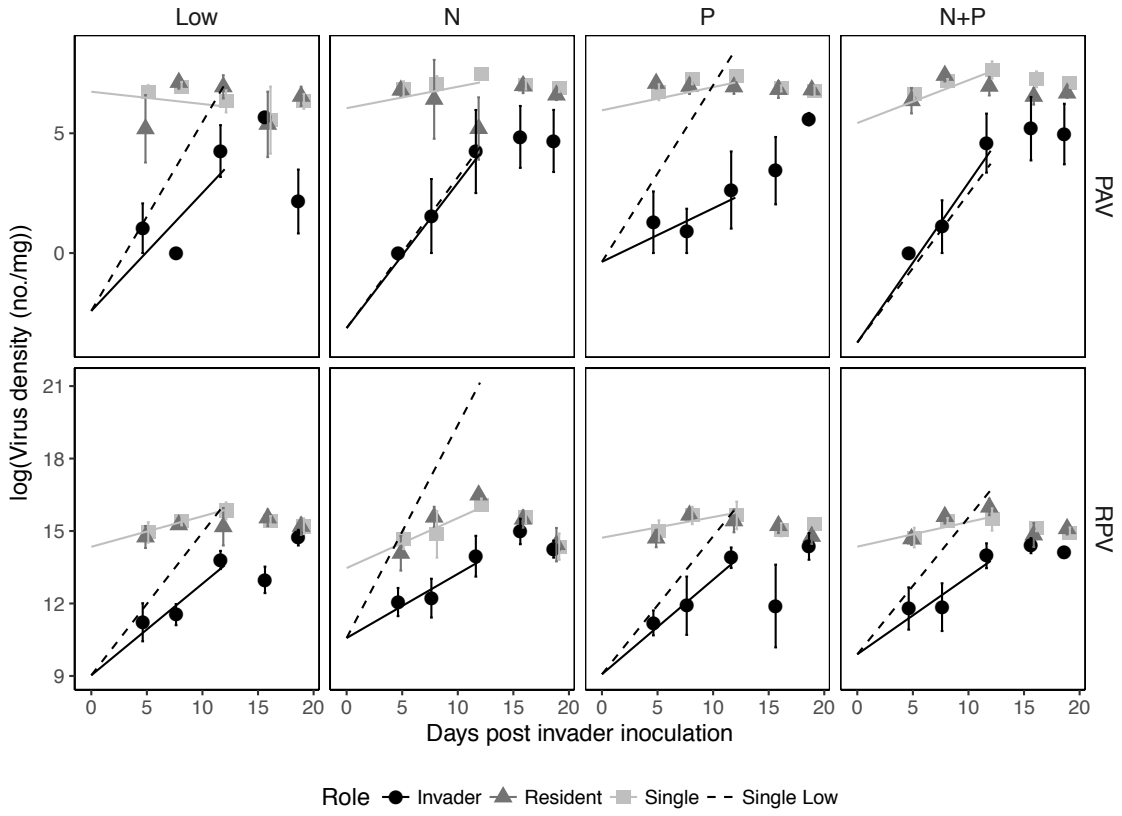

Figure 8. The log-transformed virus densities over time for each nutrient treatment. The points represent the mean ± SE (with jittered positions) for data collected from the invasion experiment. The slopes of the solid lines represent the growth rates for the invader and singly inoculated (high density) viruses. The dashed lines represent the growth rate for the singly-inoculated viruses from the transmission experiment (low

density), with the intercepts set to match the invader's. For both PAV and RPV, the invader's growth rate was higher than that of the high density viruses.

Coexistence at the host population scale

Coinfection and soil nutrients affected virus transmission between hosts (Fig. 9), but there was no effect of within-host virus density (Fig. 10). PAV transmission was affected by a three-way interaction among N addition to the receiving plant, P addition to the receiving plant, and coinfection of the source plant (glmer: $\chi^2 = 3.99$, df = 1, p = 0.046, Table S20). Coinfection reduced PAV transmission by 24% when the receiving plant had low nutrients, and this effect weakened with N addition and P addition (Fig. 9). P addition reduced PAV transmission by 25%, and this effect was lost with N addition (Fig. 9). Coinfection had no significant effect on RPV transmission (Table S21, Fig. 9). N addition to the receiving plant increased RPV transmission by 17% (glmer: $\chi^2 = 27.8$, df = 1, p = $8.16e^{-8}$, Table S21). This nutrient effect on RPV transmission was also driven by N:P (glmer: est. = 0.482, $\chi^2 = 12.2$, df = 1, p = $4.71e^{-4}$).

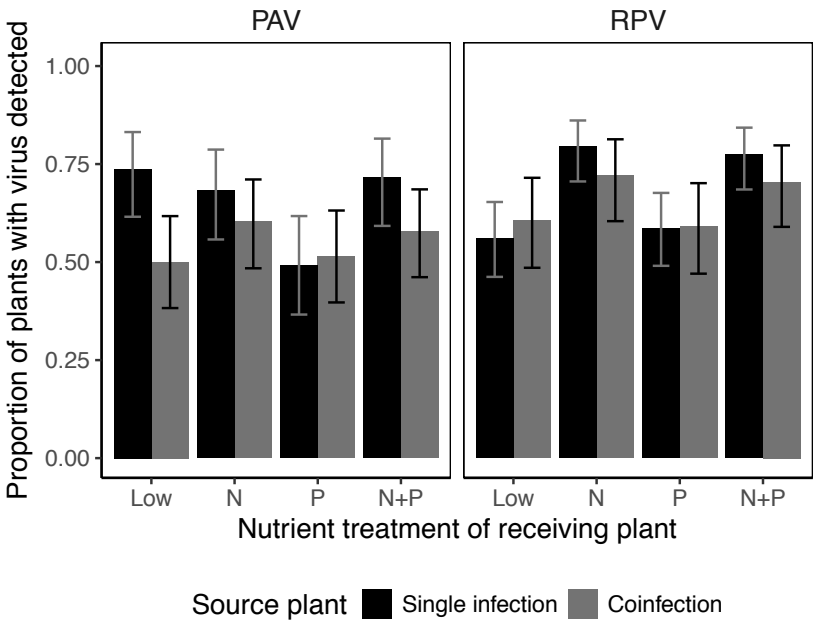

Figure 9. The proportion of receiving plants in the transmission experiment that were successfully inoculated (mean ± 95% CI). N addition and high N:P addition to the receiving plants significantly increased transmission for RPV. There was a three-way interaction among N addition, P addition, and coinfection for PAV transmission.

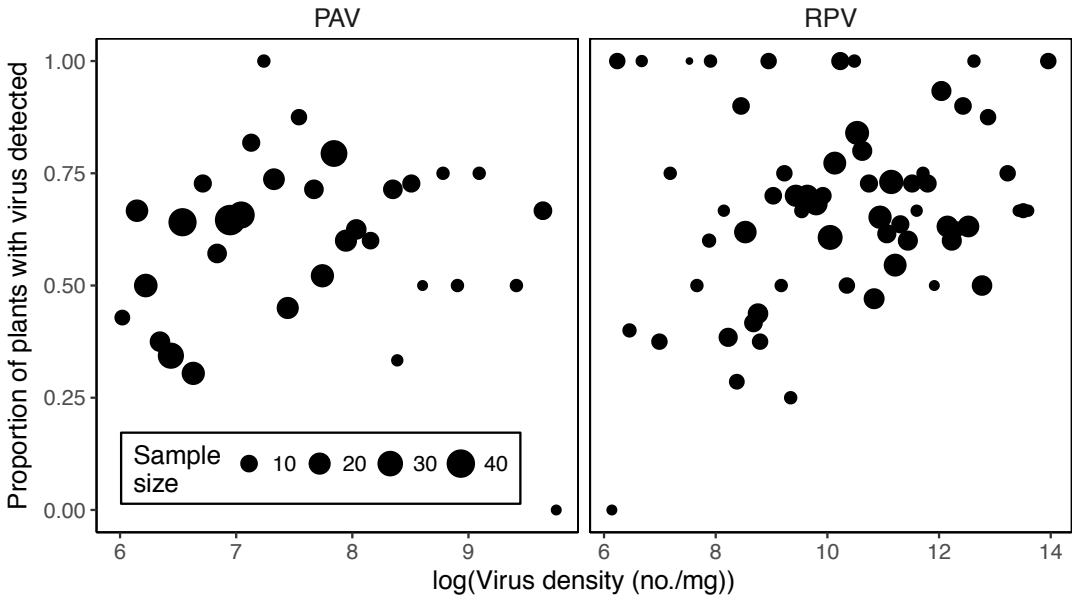

Figure 10. The proportion of receiving plants that were successfully inoculated with PAV or RPV in the transmission experiment was not related to the log-transformed virus densities in the source plants for either virus species. Samples were binned in increments of 0.1 to depict a proportion instead of binary response and "Sample size" indicates how many receiving plants are in each bin.

Given the reduction in PAV transmission with coinfection, it was unclear if PAV could invade a host population infected with RPV. Therefore, we used a mathematical model of a grass population with healthy individuals, singly infected individuals, and coinfected individuals to determine whether the viruses were likely to coexist at the host population scale (Box 1). We found that PAV could invade populations grown in each nutrient treatment and infected with RPV, despite the negative effect of RPV on PAV transmission (Fig. 11). By exploring a range of transmission interference rates and mortality rates, it became clear that the low

mortality rate of B/CYDV hosts contributes to their coexistence (Fig. 11). Further, even though there was low transmission interference with high P, PAV's low transmission rate with this nutrient treatment led to a reduced coexistence parameter space.

Box 1. Coinfection model to infer among-host coexistence

Within-season disease dynamics of PAV and RPV can be described by the following set of equations (Vasco et al. 2007, Seabloom et al. 2009, Mordecai et al. 2016).

$$\begin{aligned} S(t) &= 1 - I_R(t) - I_P(t) - I_{R,P}(t) \\ \dot{I_R} &= \beta_R\left(I_R + q_{R,P} I_{R,P}\right)S - \beta_P\left(I_P + q_{P,R} I_{R,P}\right)I_R - v_R I_R \\ \dot{I_P} &= \beta_P\left(I_P + q_{P,R} I_{R,P}\right)S - \beta_R\left(I_R + q_{R,P} I_{R,P}\right)I_P - v_P I_P \\ \dot{I_{R,P}} &= \beta_P\left(I_P + q_{P,R} I_{R,P}\right)I_R + \beta_R\left(I_R + q_{R,P} I_{R,P}\right)I_P - v_{R,P} I_{R,P} \end{aligned} \quad (5)$$

We assume that disease dynamics occur within a population that has a carrying capacity of one. Infection by RPV (I_R), PAV (I_P), or both ($I_{R,P}$) reduces the proportion of individuals within the susceptible (S) pool. Transmission of virus i occurs at a rate of β_i, which we estimate from the average proportion of plants infected during the transmission experiment (Fig. 9). Transmission of virus i from a coinfected plant relative to a singly-infected plant is scaled by $q_{i,j}$. Individuals infected with virus i are lost from the population at a rate of v_i.

To determine if PAV and RPV can coexist, we use the mutual invasibility criterion. For each virus i to invade a completely susceptible population on its own, the general expression for R_0 applies (Heesterbeek and Dietz 1996):

$$\beta_i / v_i > 1 \quad (6).$$

It is trivial to assess whether RPV can invade a population infected with PAV because PAV has no significant effect on RPV transmission. Thus, we assume a population is entirely infected with RPV ($I_R(t) = 1$, i.e. the most challenging scenario for PAV) and assess PAV's ability to invade. All new infections by PAV can then be described by $\dot{I_{R,P}}$. We assume that $q_{R,P} = 1$, $I_P(t) = 0$, and find that invasion occurs when

$$q_{P,R}\beta_P > v_{R,P} \quad (7),$$

which is similar to the coexistence criteria for two free-living species with fecundity competition (Klausmeier 2001).

Mortality of PAV-infected plants ranges from 0.2 year^{-1} (5.5e^{-4} day^{-1}) for wild perennials (Malmstrom et al. 2005a, Mordecai et al. 2016) to 0.0022 day^{-1} for cultivated barley (Leclercq-Le Quillec et al. 2000). We assumed that the observed transmission rates (Fig. 9) would remain equal with aphid feeding time restricted to a day (Gray et al. 1991, Power et al. 1991). Using PAV's transmission rates to plants grown in each nutrient treatment, we characterized the range of $q_{P,R}$ and $v_{R,P}$ values that would allow invasion, and plotted the values found in our experiment (Fig. 11). PAV's transmission rates were high enough for it to establish infection a healthy population (Eq. 6) and a population infected with RPV (Eq. 7, Fig. 11).

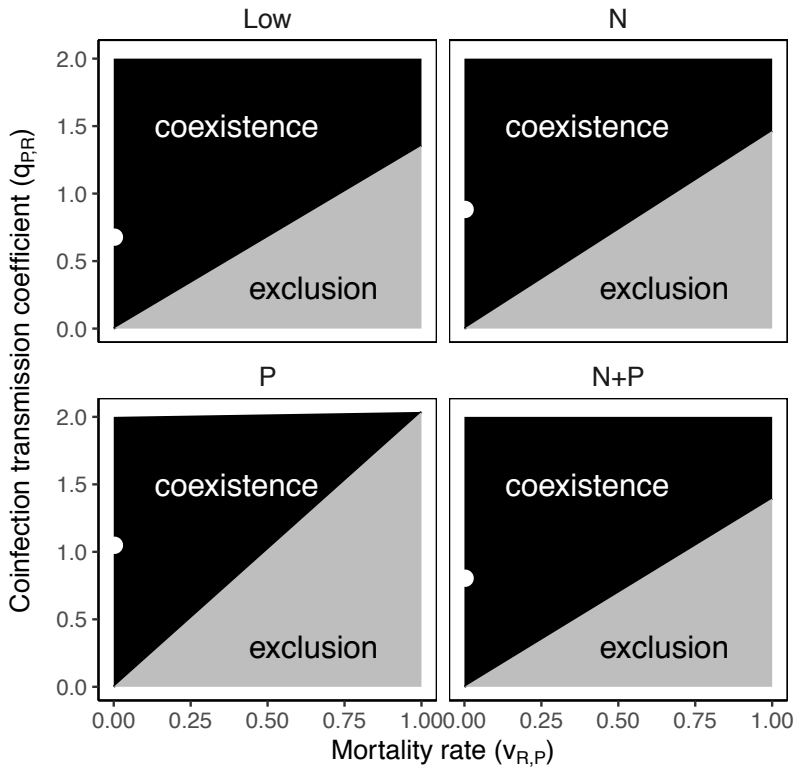

Figure 11. The combinations of coinfection transmission coefficients and mortality rates that lead to pathogen coexistence and exclusion given PAV's transmission rates to plants grown in each of the four nutrient treatments (see Box 1 for assumptions). The white points near the y-axis are the values estimated for PAV from the experiment and literature ($v_{R,P} = 0.0022$ day^{-1}).

Discussion

To our knowledge, this is the first study to use the mutual invasibility criterion to test the coexistence of pathogens under varying resource levels. Mutual invasibility provided strong evidence for coexistence of two grass viruses at two scales: within host

individuals and within host populations. However, the resource ratios and rates supplied to hosts did not affect this outcome. Therefore, within-host niche differences that do not depend on the tested supply rates of N and P promote coexistence of PAV and RPV within hosts, and outweigh competitive interference during transmission to uphold pathogen diversity at the host population scale.

Mutual invasibility experiments demonstrated that each virus could increase when rare inside of a host, regardless of soil nutrient levels. Therefore, niche differences between PAV and RPV exist, but are not dependent on N and P supply within the tested range. For resource-use overlap to prevent mutual invasion, it is assumed that the established species is at equilibrium and has drawn down resources to the minimum levels permitting growth (Turelli 1978, Tilman 1982, Adler et al. 2007). While viruses "consume" some N- and P-containing resources to build virions, including proteins and nucleic acids (Sterner and Elser 2002), host immune defenses (Zvereva and Pooggin 2012, Mandadi and Scholthof 2013) or incompatible interactions with host factors (Ahlquist et al. 2003, Whitham and Wang 2004, Pallas and García 2011) may prevent B/CYDVs from drawing down these resources to the point that another virus could not replicate. Therefore, viruses may be more likely to compete through cell lysis (Kerr et al. 2006), host mortality (Rohani et al. 2003), or induced immunity (Wen et al. 1991, Ferguson et al. 1999), and niche differences relevant to these processes are promising explanations for virus coexistence (e.g. Ojosnegros et al. 2012). Alternatively, competition between viruses may be so weak within the lifespan of a plant, that strong

niche differences are not needed for coinfection to be common (Chesson 2000, Adler et al. 2007).

While we found straightforward evidence for within-host coexistence between PAV and RPV, interference occurred between the viruses during transmission, reducing PAV's transmission rate. Interference was strongest with low nutrients supplied to the receiving host. In previous studies, RPV inhibited PAV transmission (Mordecai et al. 2016) and nutrient addition mediated PAV inhibition of RPV transmission (Lacroix et al. 2014). This interference was attributed to reductions in within-host virus density, but we did not see a negative effect of RPV presence on PAV's density in the source plants for the transmission experiment (Ch. 2) or during the invasion experiment. Therefore, interference may have occurred within aphids or during establishment of the new plant (Gildow and Rochow 1980, Wen et al. 1991). Dispersal interference can reduce the probability of coexistence between competing species (Klausmeier 2001), but we found that it was not intense enough to lead to PAV's exclusion. This combination of within-host niche differences and weak interference between PAV and RPV is consistent with model results based on prior experiments (Mordecai et al. 2016). We have rigorously confirmed the existence of within-host niche differences between the viruses, and demonstrated that these results are likely to remain consistent under different soil nutrient conditions.

While soil nutrients did not play a role in regulating virus coexistence, N addition did increase PAV density after it had established infections and PAV growth rate when data from only the invasion experiment was used. Plants that received N

addition were larger (Ch. 2), and the positive effect of N on PAV concentration has been attributed to increased plant growth in the past (Whitaker et al. 2015). Other factors that enhance plant growth and metabolism, including CO_2 and temperature, have also increased PAV concentration (Rúa et al. 2013, Nancarrow et al. 2014), which is consistent with theory linking host cell growth rate to viral replication (Smith et al. 2015). N addition also increased the transmission rates of RPV when it was supplied to the receiving plant, suggesting that positive effects of N on the virus density in the receiving plant may have enhanced detection, or N may have promoted aphid feeding on the receiving plant (Power et al. 1991, Nowak and Komor 2010). The positive effects of N addition on virus density and transmission contribute to an increasing understanding of how environmental nutrient supply affects disease prevalence across a variety of systems (Mitchell et al. 2003, Clasen and Elser 2007, Johnson et al. 2010, Civitello et al. 2013).

A positive relationship between within-host pathogen concentration and transmission rate has been found for some other plant and animal viruses (Doumayrou et al. 2012, Nguyen et al. 2013, Fraser et al. 2014). We did not find a significant relationship between PAV or RPV concentration and their respective transmission to new plants. The link between within-host concentration and transmission is important for applying theoretical predictions to systems. For example, regional coexistence automatically arises from local coexistence in a metacommunity when dispersal is proportional to local abundance, but exclusion can occur otherwise (Levins and Culver 1971, Klausmeier and Tilman 2002, Amarasekare 2003). In addition, a positive

relationship between within-host concentration and both transmission and virulence leads to the transmission-virulence trade-off, which is hypothesized to constrain the evolution of virulence (Alizon and van Baalen 2005). A weak connection between within-host concentration and transmission rate is not biologically implausible, particularly with insect vectors (Froissart et al. 2010), but requires modified theoretical predictions.

The coexistence of pathogens in host populations is becoming increasingly important to understand as we characterize the ubiquity of multi-pathogen infections (Roossinck 2012) and apply theory to our natural and managed systems. Coinfection is often assumed to be synonymous with stable coexistence (Sofonea et al. 2017), and coexistence is frequently built into coinfection models (Lipsitch et al. 2009), but transient coinfections may be common. Identifying when coexistence between coinfecting pathogens is stable sheds light on the consequences of coinfection for the host (Alizon et al. 2013), the maintenance of pathogen diversity (Poulin and Morand 2000, Malpica et al. 2006), and how pathogen interactions fit into the broader context of ecological interactions in a community (Pedersen and Fenton 2007, Johnson et al. 2015, Seabloom et al. 2015).

Acknowledgements

We are grateful to Christelle Lacroix for help with developing virus quantification methods and performing the experiments. We would also like to thank Melissa Rudeen, Anita Krause, and many undergraduate researchers, including Tashina

Picard, Alexis Rogers, Nicholas Cupery, Casey Easterday, and Kurra Renner, for assistance with the laboratory experiment. AEK was supported by an NSF IGERT graduate fellowship at the University of Minnesota (DGE-0653827) and an NSF Graduate Research Fellowship (base award number 0006595) and ETB and EWS received support from the NSF program in Ecology and Evolution of Infectious Diseases (grant DEB-1015805).

Conclusion

The three chapters of this dissertation contribute to a growing understanding of how environmental nutrients mediate interactions between pathogens, and how these interactions can impact host and pathogen communities. By investigating the relationships between plant viruses from the scale of a single host up to a grassland, we were able to bridge principles of individual medicine with disease epidemiology. Further, we designed each study with theory and empirical results from community ecology in mind. This approach allowed us to characterize ecological interactions occurring within a multi-pathogen disease system and evaluate drivers of pathogen diversity.

The first chapter demonstrated that co-occurrence between pathogen pairs is common and likely driven by insect vectors that co-transmit viruses or are attracted to the same plants (Kendig et al. 2017). These results suggested that plant-insect-virus interactions occurring at the scale of a single host are important for broader patterns of disease risk. We also found that co-occurrence of two B/CYDVs, PAV and RPV, was influenced by environmental factors, including P fertilization. This finding, as well as laboratory tests with PAV and RPV (Lacroix et al. 2014, 2017), inspired the investigation of how nutrients mediate PAV and RPV interactions for the second and third chapters.

From the second and third chapters, we learned that soil N concentration modified initial virus growth, concentration within the host, and transmission to new

hosts. N and P did not affect interactions between PAV and RPV within the host, but they did modify transmission interference of PAV. Resource-mediated pathogen interactions have been studied far less than immune-mediated interactions (Ferguson et al. 1999, Vasco et al. 2007, Ezenwa et al. 2010). To fill this gap in a meaningful way, future studies should first explore a range of resources that may mediate pathogen interactions before investigating the consequences.

We also found that nutrients and pathogen interactions independently affected host symptom severity and transmission, both of which can alter disease prevalence. The weak associations between within-host virus concentration and symptoms or transmission imply that these ecological effects are mediated by other pathways. For example, viruses may induce symptoms through the host immune system or developmental pathways (Culver and Padmanabhan 2007, Pallas and García 2011) and transmission may be more influenced by the amount of time an aphid feeds on the plant than virus concentration (Gray et al. 1991, Power et al. 1991). Identifying when within- and among-host processes are linked by pathogen concentration is crucial for understanding when and how ecological and evolutionary processes will alter disease dynamics (Mideo et al. 2008, Froissart et al. 2010, Handel and Rohani 2015).

Coexistence between PAV and RPV occurred regardless of nutrient supply rates in the experiment for the third chapter. The ease of mutual invasion, together with one-way facilitation of RPV and the high rate of co-occurrence in the field, suggests that interactions between PAV and RPV are not very intense. While we initiated this project expecting competition between viruses due to their similar structure and resource

requirements, our results suggest that the spatial and temporal scales of virus interactions may not be comparable to terrestrial and aquatic plants that have been the primary test subjects for resource competition theory (Tilman 1977, Miller et al. 2005, Harpole and Tilman 2007, Borer et al. 2014a). Specifically, plant virus interactions may not be intense because they do not grow to high enough concentrations to interfere with one another's resource use or elicit severe immune responses. This may be due to the small size of viruses relative to their host or the short lifespan of the infection or the host relative to the time needed for within-host virus populations to reach significant concentrations. Therefore, as we continue the application of ecological principles to disease systems (Johnson et al. 2015, Seabloom et al. 2015), we should explicitly consider the spatial and temporal scale of these organisms and their interactions before deciding what type of ecological theories are most relevant. For example, theories and empirical results from landscape ecology and invasion ecology are likely to be suitable complements to community ecology when formulating hypotheses about pathogen systems.

Bibliography

Adler, P. B., J. HilleRisLambers, and J. M. Levine. 2007. A niche for neutrality. Ecology Letters 10:95–104.

Ahlquist, P., A. O. Noueiry, W. Lee, B. David, and B. T. Dye. 2003. Host Factors in Positive-Strand RNA Virus Genome Replication. Journal of Virology 77:8181–8186.

Ali, M., S. Hameed, and M. Tahir. 2014. Luteovirus: insights into pathogenicity. Archives of Virology 159:2853–2860.

Alizon, S., and M. van Baalen. 2005. Emergence of a convex trade-off between transmission and virulence. The American Naturalist 165:E155–E167.

Alizon, S., A. Hurford, N. Mideo, and M. Van Baalen. 2009. Virulence evolution and the trade-off hypothesis: history, current state of affairs and the future. Journal of Evolutionary Biology 22:245–59.

Alizon, S., J. C. de Roode, and Y. Michalakis. 2013. Multiple infections and the evolution of virulence. Ecology Letters 16:556–567.

Allaire, J. J. 2014. manipulate: Interactive Plots for RStudio.

Almasi, R., W. A. Miller, and V. Ziegler-Graff. 2015. Mild and severe cereal yellow dwarf viruses differ in silencing suppressor efficiency of the P0 protein. Virus Research 208:199–206.

Amarasekare, P. 2003. Competitive coexistence in spatially structured environments: a synthesis. Ecology Letters 6:1109–1122.

Amarasekare, P., and R. M. Nisbet. 2001. Spatial heterogeneity, source-sink dynamics, and the local coexistence of competing species. The American Naturalist 158:572–84.

Anderson, R. M., and R. M. May. 1979. Population biology of infectious diseases: Part I. Nature 280:361–367.

Anderson, R. M., and R. M. May. 1982. Coevolution of hosts and parasites. Parasitology 85:411–426.

Arnott, S. A., I. Barber, and F. A. Huntingford. 2000. Parasite-associated growth enhancement in a fish-cestode system. Proceedings of the Royal Society B 267:657–63.

Astorga, A., J. Oksanen, M. Luoto, J. Soininen, R. Virtanen, and T. Muotka. 2012. Distance decay of similarity in freshwater communities: do macro- and micro-organisms follow the same rules? Global Ecology and Biogeography 21:365–75.

Balmer, O., and M. Tanner. 2011. Prevalence and implications of multiple-strain infections. The Lancet Infectious Diseases 11:868–878.

Barrett, L. G., J. M. Kniskern, N. Bodenhausen, W. Zhang, and J. Bergelson. 2009. Continua of specificity and virulence in plant host-pathogen interactions: Causes and consequences. New Phytologist 183:513–529.

Bashey, F. 2015. Within-host competitive interactions as a mechanism for the maintenance of parasite diversity. Philosophical Transactions of the Royal Society B 370:20140301.

Bates, D., M. Maechler, B. M. Bolker, and S. Walker. 2015. Fitting linear mixed-effects

models using lme4. Journal of Statistical Software 67:1–48.
Béchette, A., T. Stojsavljevic, M. Tessmer, J. A. Berges, G. A. Pinter, and E. B. Young. 2013. Mathematical modeling of bacteria-virus interactions in Lake Michigan incorporating phosphorus content. Journal of Great Lakes Research 39:646–654.
Bell, T. 2010. Experimental tests of the bacterial distance-decay relationship. The ISME Journal 4:1357–65.
Bellin, D., S. Asai, M. Delledonne, and H. Yoshioka. 2013. Nitric oxide as a mediator for defense responses. Molecular Plant-Microbe Interactions 26:271–7.
Benot, M.-L., A.-K. Bittebiere, A. Ernoult, B. Clément, and C. Mony. 2013. Fine-scale spatial patterns in grassland communities depend on species clonal dispersal ability and interactions with neighbours. Journal of Ecology 101:626–636.
Bertness, M. D., and R. Callaway. 1994. Positive interactions in communities. Trends in Ecology and Evolution 9:191–193.
Birch, E. W., N. a Ruggero, and M. W. Covert. 2012. Determining host metabolic limitations on viral replication via integrated modeling and experimental perturbation. PLoS computational biology 8:e1002746.
Bjørnstad, O. N. 2016. ncf: Spatial Nonparametric Covariance Functions. R package version 1.1-4.
Bjørnstad, O. N., and W. Falck. 2001. Nonparametric spatial covariance functions: Estimation and testing. Environmental and Ecological Statistics 8:53–70.
Bjørnstad, O. N., N. C. Stenseth, and T. Saitoh. 1999. Synchrony and scaling in dynamics of voles and mice in northern Japan. Ecology 80:622–637.
Bolker, B. M., and S. W. Pacala. 1999. Spatial moment equations for plant competition: Understanding spatial strategies and the advantages of short dispersal. The American Naturalist 153:575–602.
Borer, E., E. Seabloom, C. Michell, and A. Power. 2010a. Data from: Local context drives infection of grasses by vector-borne generalist viruses.
Borer, E. T., V. T. Adams, G. A. Engler, A. L. Adams, C. B. Schumann, and E. W. Seabloom. 2009. Aphid fecundity and grassland invasion: invader life history is the key. Ecological Applications 19:1187–96.
Borer, E. T., P. R. Hosseini, E. W. Seabloom, and A. P. Dobson. 2007. Pathogen-induced reversal of native dominance in a grassland community. Proceedings of the National Academy of Sciences of the United States of America 104:5473–8.
Borer, E. T., A.-L. Laine, and E. W. Seabloom. 2016. A multiscale approach to plant disease using the metacommunity concept. Annual Review of Phytopathology 54:397–418.
Borer, E. T., E. W. Seabloom, D. S. Gruner, W. S. Harpole, H. Hillebrand, E. M. Lind, P. B. Adler, J. Alberti, T. M. Anderson, J. D. Bakker, L. Biederman, D. Blumenthal, C. S. Brown, L. a Brudvig, Y. M. Buckley, M. Cadotte, C. Chu, E. E. Cleland, M. J. Crawley, P. Daleo, E. I. Damschen, K. F. Davies, N. M. DeCrappeo, G. Du, J. Firn, Y. Hautier, R. W. Heckman, A. Hector, J. HilleRisLambers, O. Iribarne, J. a Klein, J. M. H. Knops, K. J. La Pierre, A. D. B. Leakey, W. Li, A. S. MacDougall, R. L. McCulley, B. a Melbourne, C. E. Mitchell, J. L. Moore, B. Mortensen, L. R. O'Halloran, J. L. Orrock, J. Pascual, S. M. Prober, D. a Pyke, A.

C. Risch, M. Schuetz, M. D. Smith, C. J. Stevens, L. L. Sullivan, R. J. Williams, P. D. Wragg, J. P. Wright, and L. H. Yang. 2014a. Herbivores and nutrients control grassland plant diversity via light limitation. Nature 508:517–20.

Borer, E. T., E. W. Seabloom, C. E. Mitchell, and J. P. Cronin. 2014b. Multiple nutrients and herbivores interact to govern diversity, productivity, composition, and infection in a successional grassland. Oikos:EV 1-11.

Borer, E. T., E. W. Seabloom, C. E. Mitchell, and A. G. Power. 2010b. Local context drives infection of grasses by vector-borne generalist viruses. Ecology Letters 13:810–8.

Brisson, D., and D. E. Dykhuizen. 2004. ospC diversity in Borrelia burgdorferi: different hosts are different niches. Genetics 168:713–22.

Bustin, S., V. Benes, J. A. Garson, J. Hellemans, J. Huggett, M. Kubista, R. Mueller, T. Nolan, M. W. Pfaffl, G. L. Shipley, J. Vandesompele, and C. T. Wittwer. 2009. The MIQE guidelines: Minimum information for publication of quantitative real-time PCR experiments. Clinical Chemistry 55:611–622.

Byers, J. E., A. M. H. Blakeslee, E. Linder, A. B. Cooper, and T. J. Maguire. 2008. Controls of spatial variation in the prevalence of trematode parasites infecting a marine snail. Ecology 89:439–51.

Callaway, R. M. 1995. Positive interactions among plants. Botanical Review 61:306–349.

Caraco, T., M. C. Duryea, S. Glavanakov, W. Maniatty, and B. K. Szymanski. 2001. Host spatial heterogeneity and the spread of vector-borne infection. Theoretical Population Biology 59:185–206.

Chadwick, W., and T. J. Little. 2005. A parasite-mediated life-history shift in Daphnia magna. Proceedings of the Royal Society B 272:505–509.

Chesson, P. 2000. Mechanisms of maintenance of species diversity. Annu. Rev. Ecol. Syst. 31:343–66.

Chesson, P., and J. J. Kuang. 2008. The interaction between predation and competition. Nature 456:235–8.

Choudhury, S., H. Hu, H. Meinke, S. Shabala, G. Westmore, P. Larkin, and M. Zhou. 2017. Barley yellow dwarf viruses: infection mechanisms and breeding strategies. Euphytica 213.

Civitello, D. J., R. M. Penczykowski, J. L. Hite, M. A. Duffy, and S. R. Hall. 2013. Potassium stimulates fungal epidemics in Daphnia by increasing host and parasite reproduction. Ecology 94:380–388.

Clasen, J. L., and J. J. Elser. 2007. The effect of host Chlorella NC64A carbon:phosphorus ratio on the production of Paramecium bursaria Chlorella Virus-1. Freshwater Biology 52:112–122.

Cobey, S., and M. Lipsitch. 2012. Niche and neutral effects of acquired immunity permit coexistence of pneumococcal serotypes. Science 335:1376–80.

Cobey, S., and M. Lipsitch. 2013. Pathogen diversity and hidden regimes of apparent competition. The American naturalist 181:12–24.

Colijn, C., T. Cohen, C. Fraser, W. Hanage, E. Goldstein, N. Givon-Lavi, R. Dagan, and M. Lipsitch. 2010. What is the mechanism for persistent coexistence of drug-

susceptible and drug-resistant strains of Streptococcus pneumoniae? Journal of the Royal Society, Interface 7:905–19.
Coop, R. L., and I. Kyriazakis. 2001. Influence of host nutrition on the development and consequences of nematode parasitism in ruminants. Trends in Parasitology 17:325–330.
Cordell, D., J. O. Drangert, and S. White. 2009. The story of phosphorus: Global food security and food for thought. Global Environmental Change 19:292–305.
Cornet, S., C. Bichet, S. Larcombe, B. Faivre, and G. Sorci. 2014. Impact of host nutritional status on infection dynamics and parasite virulence in a bird-malaria system. Journal of Animal Ecology 83:256–265.
Cottenie, K., E. Michels, N. Nuytten, and L. De Meester. 2003. Zooplankton metacommunity structure: Regional vs. local processes in highly interconnected ponds. Ecology 84:991–1000.
Cotter, S. C., S. J. Simpson, D. Raubenheimer, and K. Wilson. 2011. Macronutrient balance mediates trade-offs between immune function and life history traits. Functional Ecology 25:186–198.
Crawley, M. 2007. The R Book. John Wiley & Sons, Ltd, West Sussex, England.
Creamer, R., and B. W. Falk. 1990. Direct detection of transcapsidated barley yellow dwarf luteoviruses in doubly infected plants. Journal of General Virology 71:211–217.
Cressler, C. E., W. A. Nelson, T. Day, and E. Mccauley. 2014. Disentangling the interaction among host resources, the immune system and pathogens. Ecology Letters 17:284–293.
Cribari-Neto, F., and A. Zeileis. 2010. Beta Regression in R. Journal Of Statistical Software 34.
Cronin, J. P., M. E. Welsh, M. G. Dekkers, S. T. Abercrombie, and C. E. Mitchell. 2010. Host physiological phenotype explains pathogen reservoir potential. Ecology Letters 13:1221–1232.
Culver, J. N., and M. S. Padmanabhan. 2007. Virus-induced disease: altering host physiology one interaction at a time. Annual Review of Phytopathology 45:221–243.
D'Arcy, C. J., and P. A. Burnett. 1995. Barley Yellow Dwarf: 40 Years of Progress. The American Phytopathological Society, St. Paul, MN, USA.
Dietrich, R., K. Ploss, and M. Heil. 2004. Constitutive and induced resistance to pathogens in Arabidopsis thaliana depend on nitrogen supply. Plant, Cell & Environment 27:896–906.
Dordas, C. 2009. Role of Nutrients in Controlling Plant Diseases in Sustainable Agriculture: A Review. Pages 443–460*in* E. Lichtfouse, M. Navarrete, P. Debaeke, S. Véronique, and C. Alberola, editors.Sustainable Agriculture. Springer, Dordrecht, Netherlands.
Doumayrou, J., A. Avellan, R. Froissart, and Y. Michalakis. 2012. An experimental test of the transmission-virulence trade-off hypothesis in a plant virus. Evolution 67:477–486.
Droop, M. R. 1974. The nutrient status of algal cells in continuous culture. Journal of

the Marine Biological Association of the United Kingdom 54:825–855.
Duffy, M. A., J. M. Housley, R. M. Penczykowski, C. E. Cáceres, and S. R. Hall. 2011. Unhealthy herds: Indirect effects of predators enhance two drivers of disease spread. Functional Ecology 25:945–953.
Dunn, J. M., P. J. Krause, S. Davis, E. G. Vannier, M. C. Fitzpatrick, L. Rollend, A. A. Belperron, S. L. States, A. Stacey, L. K. Bockenstedt, D. Fish, and M. A. Diuk-Wasser. 2014. Borrelia burgdorferi promotes the establishment of Babesia microti in the northeastern United States. PloS ONE 9:e115494.
Erion, G. G., and W. E. Riedell. 2012. Barley Yellow Dwarf Virus effects on cereal plant growth and transpiration. Crop Science 52:2794.
Ewald, P. W. 2004. Evolution of virulence. Infectious Disease Clinics of North America 18:1–15.
Ezenwa, V. O., R. S. Etienne, G. Luikart, A. Beja-Pereira, and A. E. Jolles. 2010. Hidden consequences of living in a wormy world: Nematode-induced immune suppression facilitates tuberculosis invasion in African buffalo. The American Naturalist 176:613–624.
Fabre, F., C. Kervarrec, L. Mieuzet, G. Riault, A. Vialatte, and E. Jacquot. 2003. Improvement of Barley yellow dwarf virus-PAV detection in single aphids using a fluorescent real time RT-PCR. Journal of Virological Methods 110:51–60.
Ferguson, N., R. Anderson, and S. Gupta. 1999. The effect of antibody-dependent enhancement on the transmission dynamics and persistence of multiple-strain pathogens. Proceedings of the National Academy of Sciences of the United States of America 96:790–4.
Ferrari, M. J., O. N. Bjørnstad, J. L. Partain, and J. Antonovics. 2006. A gravity model for the spread of a pollinator-borne plant pathogen. The American Naturalist 168:294–303.
Filipe, J. A. N., and M. M. Maule. 2004. Effects of dispersal mechanisms on spatio-temporal development of epidemics. Journal of Theoretical Biology 226:125–141.
Fine, P., K. Eames, and D. L. Heymann. 2011. “Herd immunity”: A rough guide. Clinical Infectious Diseases 52:911–916.
Fitt, B. D. L., Y. Huang, F. van den Bosch, and J. S. West. 2006. Coexistence of related pathogen species on arable crops in space and time. Annual Review of Phytopathology 44:163–82.
Fraser, C., K. Lythgoe, G. E. Leventhal, G. Shirreff, T. D. Hollingsworth, S. Alizon, and S. Bonhoeffer. 2014. Virulence and pathogenesis of HIV-1 infection: An evolutionary perspective. Science 343:1243727–1243727.
Froissart, R., J. Doumayrou, F. Vuillaume, S. Alizon, and Y. Michalakis. 2010. The virulence-transmission trade-off in vector-borne plant viruses: a review of (non-)existing studies. Philosophical Transactions of the Royal Society B 365:1907–18.
Frost, P. C., D. Ebert, and V. H. Smith. 2008. Responses of a bacterial pathogen to phosphorus limitation of its aquatic invertebrate host. Ecology 89:313–318.
Fuhrman, K. M., G. a. Pinter, and J. a. Berges. 2011. Dynamics of a virus-host model with an intrinsic quota. Mathematical and Computer Modelling 53:716–730.
Furlong, M. J., and E. Groden. 2003. Starvation induced stress and the susceptibility of

the Colorado potato beetle, Leptinotarsa decemlineata, to infection by Beauveria bassiana. Journal of Invertebrate Pathology 83:127–138.
Gaumann, E. 1950. The Nutrient Content of the Tissues as a Factor in Resistance and Spread. Page 267. Principles of Plant Infection. Crosby Lockwood & Sons, Ltd., London, England.
Gause, G. F. 1934. The Struggle for Existence. The Williams and Wilkins Company, New York, NY.
Gerla, D. J., A. S. Gsell, B. W. Kooi, B. W. Ibelings, E. Van Donk, and W. M. Mooij. 2013. Alternative states and population crashes in a resource-susceptible-infected model for planktonic parasites and hosts. Freshwater Biology 58:538–551.
Gibson, G. J. 1997. Investigating mechanisms of spatiotemporal epidemic spread using stochastic models. Phytopathology 87:139–146.
Gildow, F., and W. Rochow. 1980. Transmission interference between two isolates of barley yellow dwarf virus in Macrosiphum avenae. Phytopathology 70:122–126.
Gosme, M., and P. Lucas. 2011. Effect of host and inoculum patterns on take-all disease of wheat incidence, severity and disease gradient. European Journal of Plant Pathology 129:119–131.
Grace, J. B., and D. Tilman. 2003. Perpectives on Plant Competition. The Blackburn Press, Caldwell, NJ.
Graham, A. L., I. M. Cattadori, J. O. Lloyd-Smith, M. J. Ferrari, and O. N. Bjørnstad. 2007. Transmission consequences of coinfection: Cytokines writ large? Trends in Parasitology 23:284–91.
Gray, S., and F. E. Gildow. 2003. Luteovirus-aphid interactions. Annual review of phytopathology 41:539–66.
Gray, S., A. Power, D. Smith, A. J. Seaman, and N. S. Altman. 1991. Aphid transmission of barley yellow dwarf virus: Acquisition access periods and virus concentration requirements. Phytopathology 81:539–545.
Griesbach, J. a., B. J. Steffenson, M. P. Brown, B. W. Falk, and R. K. Webster. 1990. Infection of grasses by Barley yellow dwarf viruses in California. Crop Science 30:1173.
Griffiths, E. C., A. B. Pedersen, A. Fenton, and O. L. Petchey. 2011. The nature and consequences of coinfection in humans. The Journal of Infection 63:200–6.
Gross, K. 2008. Positive interactions among competitors can produce species-rich communities. Ecology Letters 11:929–936.
Hagan, W. A. 1943. Influence of Nutrition and Environmental Factors on Resistance to Disease. Page 27. The Infectious Diseases of Domestic Animals with Special Reference to Etiology, Diagnosis, and Biologic Therapy. Comstock Publishing Company, Inc., Ithaca, New York, USA.
Hall, S. R., J. L. Simonis, R. M. Nisbet, A. J. Tessier, and C. E. Cáceres. 2009. Resource ecology of virulence in a planktonic host-parasite system: An explanation using dynamic energy budgets. The American Naturalist 174253:149–162.
Handel, A., and P. Rohani. 2015. Crossing the scale from within-host infection dynamics to between-host transmission fitness: a discussion of current assumptions

and knowledge. Philosophical Transactions of the Royal Society B 370:20140302.
Hanson, C. A., J. A. Fuhrman, M. C. Horner-Devine, and J. B. H. Martiny. 2012. Beyond biogeographic patterns: processes shaping the microbial landscape. Nature Reviews Microbiology 10:497–506.
Harcombe, W. 2010. Novel cooperation experimentally evolved between species. Evolution; international journal of organic evolution 64:2166–72.
Hardin, G. 1960. The Competitive Exclusion Principle. Science 131:1292–1297.
Harpole, W. S., L. L. Sullivan, E. M. Lind, J. Firn, P. B. Adler, E. T. Borer, J. Chase, P. A. Fay, Y. Hautier, H. Hillebrand, A. S. MacDougall, E. W. Seabloom, R. Williams, J. D. Bakker, M. W. Cadotte, E. J. Chaneton, C. Chu, E. E. Cleland, C. D'Antonio, K. F. Davies, D. S. Gruner, N. Hagenah, K. Kirkman, J. M. H. Knops, K. J. La Pierre, R. L. McCulley, J. L. Moore, J. W. Morgan, S. M. Prober, A. C. Risch, M. Schuetz, C. J. Stevens, and P. D. Wragg. 2016. Addition of multiple limiting resources reduces grassland diversity. Nature 537:93–96.
Harpole, W. S., and D. Tilman. 2007. Grassland species loss resulting from reduced niche dimension. Nature 446:791–3.
Harvell, C., C. Mitchell, J. Ward, and S. Altizer. 2002. Climate warming and disease risks for terrestrial and marine biota. Science 296:2158–2162.
Heesterbeek, J. A. P., and K. Dietz. 1996. The concept of R0 in epidemic theory. Statistica Neerlandica 50:89–110.
Heffernan, J. M., R. J. Smith, and L. M. Wahl. 2005. Perspectives on the basic reproductive ratio. Journal of the Royal Society Interface 2:281–93.
Hersh, M. H., R. S. Ostfeld, D. J. McHenry, M. Tibbetts, J. L. Brunner, M. E. Killilea, K. LoGiudice, K. A. Schmidt, and F. Keesing. 2014. Co-infection of blacklegged ticks with Babesia microti and Borrelia burgdorferi is higher than expected and acquired from small mammal hosts. PLoS ONE 9:9–13.
Hethcote, H. W. 2000. The mathematics of infectious diseases. SIAM Review 42:599–653.
Hoagland, D. R., and D. I. Arnon. 1938. The water culture method for growing plants without soil. Circular/University of California, College of Agriculture, Agricultural Experiment Station.
Hodgson, D. J., R. B. Hitchman, a J. Vanbergen, R. S. Hails, R. D. Possee, and J. S. Cory. 2004. Host ecology determines the relative fitness of virus genotypes in mixed-genotype nucleopolyhedrovirus infections. Journal of Evolutionary Biology 17:1018–25.
Holt, R. D. 1977. Predation, apparent competition, and the structure of prey communities. Theoretical Population Biology 12:197–229.
Holt, R. D., and A. P. Dobson. 2006. Extending the principles of community ecology to address teh epidemiology of host-pathogen systems. Page *in* S. K. Collinge and C. Ray, editors. Disease Ecology: Community Structure and Pathogen Dynamics. Oxford University Press, New York, NY, USA.
Horbach, R., A. R. Navarro-Quesada, W. Knogge, and H. B. Deising. 2011. When and how to kill a plant cell: Infection strategies of plant pathogenic fungi. Journal of Plant Physiology 168:51–62.

Howick, V. M., and B. P. Lazzaro. 2014. Genotype and diet shape resistance and tolerance across distinct phases of bacterial infection. BMC Evolutionary Biology 14:1–13.
Hubbell, S. P. 2001. The Unified Theory of Biodiversity and Biogeography. Princeton University Press, Princeton, NJ, USA.
Hutchinson, G. 1959. Homage to Santa Rosalia or why are there so many kinds of animals? The American Naturalist 93:145–159.
Jarosz, A. M., and J. J. Burdon. 1988. The effect of small-scale environmental changes on disease incidence and severity in a natural plant-pathogen interaction. Oecologia 75:278–281.
Jin, X., N. Hao, F. Jiao, Y. Yang, D. Wang, C. Xu, and R. Zhai. 2014. The effect of nitrogen supply on potato yield, tuber size and pathogen resistance in Solanum tuberosum exposed to Phytophthora infestans. African Journal of Agricultural Research 9:2657–2663.
Johnson, P. T. J., and J. T. Hoverman. 2012. Parasite diversity and coinfection determine pathogen infection success and host fitness. Proceedings of the National Academy of Sciences of the United States of America 109:9006–11.
Johnson, P. T. J., J. C. de Roode, and A. Fenton. 2015. Why infectious disease research needs community ecology. Science 349:1259504-1-1259504–9.
Johnson, P. T. J., A. R. Townsend, C. C. Cleveland, P. M. Glibert, R. W. Howarth, V. J. McKenzie, E. Rejmankova, and M. H. Ward. 2010. Linking environmental nutrient enrichment and disease emergence in humans and wildlife. Ecological Applications 20:16–29.
Johnson, P. T. J., C. L. Wood, M. B. Joseph, D. L. Preston, S. E. Haas, and Y. P. Springer. 2016. Habitat heterogeneity drives the host-diversity-begets-parasite-diversity relationship: evidence from experimental and field studies. Ecology Letters 19:752–761.
Jokela, J., J. Taskinen, P. Mutikainen, and K. Kopp. 2005. Virulence of parasites in hosts under environmental stress: Experiments with anoxia and starvation. Oikos 108:156–164.
Jolles, A. E., P. Sullivan, A. P. Alker, and C. D. Harvell. 2002. Disease transmission of Aspergillosis in sea fans: Inferring process from spatial pattern. Ecology 83:2373–8.
Jover, L. F., T. C. Effler, A. Buchan, S. W. Wilhelm, and J. S. Weitz. 2014. The elemental composition of virus particles: implications for marine biogeochemical cycles. Nature Reviews Microbiology 12:519–28.
Kendig, A. E., E. T. Borer, C. E. Mitchell, A. G. Power, and E. W. Seabloom. 2017. Characteristics and drivers of plant virus community spatial patterns in US west coast grasslands. Oikos Accepted.
Kerr, B., C. Neuhauser, B. J. M. Bohannan, and A. M. Dean. 2006. Local migration promotes competitive restraint in a host-pathogen “tragedy of the commons”. Nature 442:75–8.
Kikuti, M., G. M. Cunha, I. A. D. Paploski, A. M. Kasper, M. M. O. Silva, A. S. Tavares, J. S. Cruz, T. L. Queiroz, M. S. Rodrigues, P. M. Santana, H. C. A. V.

Lima, J. Calcagno, D. Takahashi, A. H. O. Gonçalves, J. M. G. Araújo, K. Gauthier, M. A. Diuk-Wasser, U. Kitron, A. I. Ko, M. G. Reis, and G. S. Ribeiro. 2015. Spatial distribution of dengue in a Brazilian urban slum setting: Role of socioeconomic gradient in disease risk. PLoS Neglected Tropical Diseases 9:1–18.

King, A. J., K. R. Freeman, K. F. McCormick, R. C. Lynch, C. Lozupone, R. Knight, and S. K. Schmidt. 2010. Biogeography and habitat modelling of high-alpine bacteria. Nature communications 1:53.

Klausmeier, C. a. 2001. Habitat destruction and extinction in competitive and mutualistic metacommunities. Ecology Letters 4:57–63.

Klausmeier, C. A., E. Litchman, and S. A. Levin. 2004. Phytoplankton growth and stoichiometry under multiple nutrient limitation. Limnology and Oceanography 49:1463–1470.

Klausmeier, C. A., and D. Tilman. 2002. Spatial Models of Competition. Pages 43–78*in* U. Sommer and B. Worm, editors.Competition and Coexistence. Springer-Verlag Berlin Heidelberg, New York, NY, USA.

Lacroix, C., E. W. Seabloom, and E. T. Borer. 2014. Environmental nutrient supply alters prevalence and weakens competitive interactions among coinfecting viruses. The New Phytologist 204:424–433.

Lacroix, C., E. W. Seabloom, and E. T. Borer. 2017. Environmental nutrient supply directly alters plant traits but indirectly determines virus growth rate. Frontiers in Microbiology 8:1–16.

Ladha, J. K., A. Tirol-Padre, C. K. Reddy, K. G. Cassman, S. Verma, D. S. Powlson, C. van Kessel, D. de B. Richter, D. Chakraborty, and H. Pathak. 2016. Global nitrogen budgets in cereals: A 50-year assessment for maize, rice, and wheat production systems. Scientific Reports 6:19355.

Lafferty, K. D., and R. D. Holt. 2003. How should environmental stress affect the population dynamics of diseases. Ecology Letters 6:654–664.

Lafferty, K. D., and A. M. Kuris. 1999. How environmental stress affects the impacts of parasites. Limnology and Oceanography 44:925–931.

Laine, A.-L. 2006. Evolution of host resistance: looking for coevolutionary hotspots at small spatial scales. Proceedings of the Royal Society B: Biological Sciences 273:267–273.

Lange, B., M. Reuter, D. Ebert, K. Muylaert, and E. Decaestecker. 2014. Diet quality determines interspecific parasite interactions in host populations. Ecology and Evolution 4:3093–3102.

Leclercq-Le Quillec, F., M. Plantegenest, G. Riault, and C. A. Dedryver. 2000. Analyzing and modeling temporal disease progress of Barley yellow dwarf virus serotypes in barley fields. Phytopathology 90:860–6.

Leibold, M. A., M. Holyoak, N. Mouquet, P. Amarasekare, J. M. Chase, M. F. Hoopes, R. D. Holt, J. B. Shurin, R. Law, D. Tilman, M. Loreau, and A. Gonzalez. 2004. The metacommunity concept: A framework for multi-scale community ecology. Ecology Letters 7:601–613.

Leon, J. A., and D. B. Tumpson. 1975. Competition between two species for two complementary or substitutuable resources. Journal of Theoretical Biology

50:185–201.
Levins, R., and D. Culver. 1971. Regional coexistence of species and competition between rare species. Proceedings of the National Academy of Sciences of the United States of America 68:1246–1248.
von Liebig, J. 1840. Die Chemie in irher Anwendung auf Agricultur und Physiologie. Friedrich Vieweg, Braunschwieg.
Lipsitch, M., C. Colijn, T. Cohen, W. Hanage, and C. Fraser. 2009. No coexistence for free: neutral null models for multistrain pathogens. Epidemics 1:2–13.
Liu, Y., H. Zhai, K. Zhao, B. Wu, and X. Wang. 2012. Two suppressors of RNA silencing encoded by cereal-infecting members of the family Luteoviridae. Journal of General Virology 93:1825–1830.
Lloyd-Smith, J. O. 2013. Vacated niches, competitive release and the community ecology of pathogen eradication. Philosophical Transactions of the Royal Society B 368.
Loreau, M. 2004. Does functional redundancy exist? Oikos 104:606–611.
Maestre, F. T., R. M. Callaway, F. Valladares, and C. J. Lortie. 2009. Refining the stress-gradient hypothesis for competition and facilitation in plant communities. Journal of Ecology 97:199–205.
Malmstrom, C. M., C. C. Hughes, L. A. Newton, and C. J. Stoner. 2005a. Virus infection in remnant native bunchgrasses from invaded California grasslands. The New Phytologist 168:217–30.
Malmstrom, C. M., A. J. McCullough, H. A. Johnson, L. A. Newton, and E. T. Borer. 2005b. Invasive annual grasses indirectly increase virus incidence in California native perennial bunchgrasses. Oecologia 145:153–64.
Malpica, J. M., S. Sacristán, A. Fraile, and F. García-Arenal. 2006. Association and host selectivity in multi-host pathogens. PLoS ONE 1:e41.
Mancio-Silva, L., K. Slavic, M. T. Grilo Ruivo, A. R. Grosso, K. K. Modrzynska, I. M. Vera, J. Sales-Dias, A. R. Gomes, C. R. Macpherson, P. Crozet, M. Adamo, E. Baena-Gonzalez, R. Tewari, M. Llinás, O. Billker, and M. M. Mota. 2017. Nutrient sensing modulates malaria parasite virulence. Nature 547:213–216.
Mandadi, K. K., and K.-B. G. Scholthof. 2013. Plant immune responses against viruses: How does a virus cause disease? The Plant cell 25:1489–505.
Manguin, S., M. J. Bangs, J. Pothikasikorn, and T. Chareonviriyaphap. 2010. Review on global co-transmission of human Plasmodium species and Wuchereria bancrofti by Anopheles mosquitoes. Infection, Genetics and Evolution 10:159–177.
Mattsson, M., E. Johansson, T. Lundborg, M. Larsson, and C. M. Larsson. 1991. Nitrogen utilization in n-limited barley during vegetative and generative growth: I. Growth and nitrate uptake kinetics in vegetative cultures grown at different relative addition rates of nitrate-n. Journal of Experimental Botany 42:197–205.
McElhany, P., L. Real, and A. Power. 1995. Vector preference and disease dynamics: a study of barley yellow dwarf virus. Ecology 76:444–457.
Mckirdy, S. J., and R. A. C. Jones. 1993. Occurrence of Barley Yellow Dwarf Virus serotypes MAV and RMV in over-summering grasses. Australian Journal of Agricultural Research 44:1195–1209.

Medel, R., E. Vergara, A. Silva, and M. Kalin-Arroyo. 2004. Effects of vector behavior and host resistance on mistletoe aggregation. Ecology 85:120–126.
Mellado, A., and R. Zamora. 2016. Spatial heterogeneity of a parasitic plant drives the seed-dispersal pattern of a zoochorous plant community in a generalist dispersal system. Functional Ecology 30:459–467.
Mengiste, T. 2012. Plant immunity to necrotrophs. Annual Review of Phytopathology 50:267–294.
Mideo, N., S. Alizon, and T. Day. 2008. Linking within- and between-host dynamics in the evolutionary epidemiology of infectious diseases. Trends in Ecology & Evolution 23:511–7.
Mihaljevic, J. R. 2012. Linking metacommunity theory and symbiont evolutionary ecology. Trends in Ecology & Evolution 27:323–9.
Miller, T. E., J. H. Burns, P. Munguia, E. L. Walters, J. M. Kneitel, P. M. Richards, N. Mouquet, and H. L. Buckley. 2005. A critical review of twenty years' use of the resource-ratio theory. The American Naturalist 165:439–48.
Miller, W. A., and L. Rasochova. 1997. Barley yellow dwarf viruses. Annual Review of Phytopathology.
Mitchell, C. E., P. B. Reich, D. Tilman, and J. V. Groth. 2003. Effects of elevated CO2, nitrogen deposition, and decreased species diversity on foliar fungal plant disease. Global Change Biology 9:438–451.
Monod, J. 1949. The growth of bacterial cultures. Annual Reviews in Microbiology 3:371–394.
Mordecai, E. a., K. Gross, and C. E. Mitchell. 2016. Within-host niche differences and fitness trade-offs promote coexistence of plant viruses. The American Naturalist 187:E13–E26.
Muller, E. M., and R. van Woesik. 2012. Caribbean coral diseases: Primary transmission or secondary infection? Global Change Biology 18:3529–3535.
Murall, C. L., K. S. McCann, and C. T. Bauch. 2012. Food webs in the human body: linking ecological theory to viral dynamics. PloS ONE 7:e48812.
Nancarrow, N., F. E. Constable, K. J. Finlay, A. J. Freeman, B. C. Rodoni, P. Trebicki, S. Vassiliadis, A. L. Yen, and J. E. Luck. 2014. The effect of elevated temperature on barley yellow dwarf virus-PAV in wheat. Virus Research 186:97–103.
Neema, C., J. P. Laulhere, and D. Expert. 1993. Iron deficiency induced by chrysobactin in Saintpaulia leaves inoculated with Erwinia chrysanthemi. Plant Physiology 102:967–973.
Nega, A. 2014. Review on Barely yellow dwarf viruses. Journal of Biology, Agriculture and Healthcare 4:64–91.
Nekola, J. C., and P. S. White. 1999. The distance decay of similarity in biogeography and ecology. Journal of Biogeography 26:867–878.
Nessa, B., M. U. Salam, A. H. M. M. Haque, J. K. Biswas, M. S. Kabir, W. J. Macleod, M. D. Antuono, H. N. Barman, M. A. Latif, and J. Galloway. 2015. Spatial pattern of natural spread of rice false smut (Ustilaginoidea virens) disease in fields. American Journal of Agriculture and Biological Sciences 10:63–73.
Nguyen, N. M., D. Thi Hue Kien, T. V. Tuan, N. T. H. Quyen, C. N. B. Tran, L. Vo

Thi, D. L. Thi, H. L. Nguyen, J. J. Farrar, E. C. Holmes, M. A. Rabaa, J. E. Bryant, T. T. Nguyen, H. T. C. Nguyen, L. T. H. Nguyen, M. P. Pham, H. T. Nguyen, T. T. H. Luong, B. Wills, C. V. V. Nguyen, M. Wolbers, and C. P. Simmons. 2013. Host and viral features of human dengue cases shape the population of infected and infectious Aedes aegypti mosquitoes. Proceedings of the National Academy of Sciences 110:9072–9077.

Nowak, H., and E. Komor. 2010. How aphids decide what is good for them: experiments to test aphid feeding behaviour on Tanacetum vulgare (L.) using different nitrogen regimes. Oecologia 163:973–84.

Ojosnegros, S., N. Beerenwinkel, T. Antal, M. a Nowak, C. Escarmís, and E. Domingo. 2010. Competition-colonization dynamics in an RNA virus. Proceedings of the National Academy of Sciences of the United States of America 107:2108–12.

Ojosnegros, S., E. Delgado-Eckert, and N. Beerenwinkel. 2012. Competition-colonization trade-off promotes coexistence of low-virulence viral strains. Journal of the Royal Society, Interface / the Royal Society:2244–2254.

Ostfeld, R. S., and F. Keesing. 2012. Effects of host diversity on infectious disease. Annual Review of Ecology, Evolution, and Systematics 43:157–182.

Pallas, V., and J. A. García. 2011. How do plant viruses induce disease? Interactions and interference with host components. The Journal of General Virology 92:2691–2705.

Parry, H. R. 2013. Cereal aphid movement: general principles and simulation modelling. Movement Ecology 1:14.

Paull, S. H., B. E. Lafonte, and P. T. J. Johnson. 2012a. Temperature-driven shifts in a host-parasite interaction drive nonlinear changes in disease risk. Global Change Biology 18:3558–3567.

Paull, S. H., S. Song, K. M. McClure, L. C. Sackett, A. M. Kilpatrick, and P. T. J. Johnson. 2012b. From superspreaders to disease hotspots: Linking transmission across hosts and space. Frontiers in Ecology and the Environment 10:75–82.

Pedersen, A. B., and A. Fenton. 2007. Emphasizing the ecology in parasite community ecology. Trends in Ecology & Evolution 22:133–9.

Petney, T. N., and R. H. Andrews. 1998. Multiparasite communities in animals and humans: frequency, structure and pathogenic significance. International Journal for Parasitology 28:377–93.

Poulin, R., and S. Morand. 2000. The diversity of parasites. The Quarterly Review of Biology 75:277–293.

Power, A. G. 1991. Virus spread and vector dynamics in genetically diverse plant populations. Ecology 72:232–241.

Power, A. G., E. T. Borer, P. Hosseini, C. E. Mitchell, and E. W. Seabloom. 2011. The community ecology of barley/cereal yellow dwarf viruses in Western US grasslands. Virus Research 159:95–100.

Power, A. G., and C. E. Mitchell. 2004. Pathogen spillover in disease epidemics. The American Naturalist 164:S79–S89.

Power, A., A. Seaman, and S. Gray. 1991. Aphid transmission of barley yellow dwarf virus: Inoculation access periods and epidemiological implications.

Phytopathology 81:545–548.
Pulliam, H. R. 1988. Sources, sinks, and population regulation. The American Naturalist 132:652–661.
R Core Team. 2016. R: A language and environment for statistical computing. R Foundation for Statistical Computing, Vienna, Austria.
Ramiro, R. S., L. C. Pollitt, N. Mideo, and S. E. Reece. 2016. Facilitation through altered resource availability in a mixed-species rodent malaria infection. Ecology Letters.
Ramsay, J., and G. Hooker. 2017. Dynamic Data Analysis: Modeling Data with Differential Equations. Springer Science+Business Media, New York, NY, USA.
Rappussi, M. C. C., B. Eckstein, D. Flôres, I. C. R. Haas, L. Amorim, and I. P. Bedendo. 2012. Cauliflower stunt associated with a phytoplasma of subgroup 16SrIII-J and the spatial pattern of disease. European Journal of Plant Pathology 133:829–840.
Rasband, W. S. 2014. ImageJ. National Institutes of Health, Bethesda, Maryland, USA.
Raso, G., P. Vounatsou, B. H. Singer, E. K. N'Goran, M. Tanner, and J. Utzinger. 2006. An integrated approach for risk profiling and spatial prediction of Schistosoma mansoni-hookworm coinfection. Proceedings of the National Academy of Sciences of the United States of America 103:6934–9.
Raybould, A. F., L. C. Maskell, M. L. Edwards, J. I. Cooper, and A. J. Gray. 1999. The prevalence and spatial distribution of viruses in natural populations of Brassica oleracea. New Phytologist 141:265–275.
Read, A. F. 1994. The evolution of virulence. Trends in Microbiology 2:73–76.
Ridzon, R., K. Gallagher, C. Ciesielski, E. E. Mast, M. B. Ginsberg, B. Roberston, C. Luo, and A. DeMaria. 1997. Simultaneous transmission of human immunodeficiency virus and hepatitise C virus from a needle-stick injury. The New England Journal of Medicine 336:919–922.
Rigaud, T., M.-J. Perrot-Minnot, and M. J. F. Brown. 2010. Parasite and host assemblages: embracing the reality will improve our knowledge of parasite transmission and virulence. Proceedings of the Royal Society B 277:3693–702.
Rohani, P., C. J. Green, N. B. Mantilla-Beniers, and B. T. Grenfell. 2003. Ecological interference between fatal diseases. Nature 422:885–888.
de Roode, J. C., R. Culleton, S. J. Cheesman, R. Carter, and A. F. Read. 2004. Host heterogeneity is a determinant of competitive exclusion or coexistence in genetically diverse malaria infections. Proceedings of the Royal Society B 271:1073–1080.
Roossinck, M. J. 2012. Plant virus metagenomics: Biodiversity and ecology. Annual Review of Genetics 46:359–69.
Rúa, M. A., J. Umbanhowar, S. Hu, K. O. Burkey, and C. E. Mitchell. 2013. Elevated CO2 spurs reciprocal positive effects between a plant virus and an arbuscular mycorrhizal fungus. New Phytologist 199:541–549.
Seabloom, E. W., C. D. Benfield, E. T. Borer, A. G. Stanley, T. N. Kaye, and P. W. Dunwiddie. 2011. Provenance, life span, and phylogeny do not affect grass species' responses to nitrogen and phosphorus. Ecological Applications 21:2129–

2142.
Seabloom, E. W., O. N. Bjørnstad, B. M. Bolker, and O. J. Reichman. 2005. Spatial signature of environmental heterogeneity, dispersal, and competition in successional grasslands. Ecological monographs 75:199–214.
Seabloom, E. W., E. T. Borer, K. Gross, A. E. Kendig, C. E. Mitchell, E. A. Mordecai, and A. G. Power. 2015. The community ecology of pathogens: coinfection, coexistence and community composition. Ecology Letters 18:401–415.
Seabloom, E. W., E. T. Borer, C. Lacroix, C. E. Mitchell, and A. G. Power. 2013. Richness and composition of niche-assembled viral pathogen communities. PLoS ONE 8:e55675.
Seabloom, E. W., E. T. Borer, C. E. Mitchell, and A. G. Power. 2010. Viral diversity and prevalence gradients in North American Pacific Coast grasslands. Ecology 91:721–32.
Seabloom, E. W., P. R. Hosseini, A. G. Power, and E. T. Borer. 2009. Diversity and composition of viral communities: Coinfection of barley and cereal yellow dwarf viruses in California grasslands. The American Naturalist 173:E79-98.
Siepielski, A. M., and M. A. McPeek. 2010. On the evidence for species coexistence: a critique of the coexistence program. Ecology 91:3153–3164.
Silvertown, J. 2004. Plant coexistence and the niche. Trends in Ecology & Evolution 19:605–611.
Smith, V. 2007. Host resource supplies influence the dynamics and outcome of infectious disease. Integrative and Comparative Biology 47:310–316.
Smith, V. H., and R. D. Holt. 1996. Resource competition and within-host disease dynamics. Trends in Ecology & Evolution 11:386–389.
Smith, V. H., R. D. Holt, M. S. Smith, Y. Niu, and M. Barfield. 2015. Resources, mortality, and disease ecology: importance of positive feedbacks between host growth rate and pathogen dynamics. Israel Journal of Ecology & Evolution 9801:1–13.
Smith, V., T. Jones, and M. Smith. 2005. Host nutrition and infectious disease: an ecological view. Frontiers in Ecology and the Environment 3:268–274.
Soetaert, K., and T. Petzoldt. 2010. Inverse modelling, sensitivity and Monte Carlo analysis in R using package FME. Journal of Statistical Software 33:1–28.
Sofonea, M. T., S. Alizon, and Y. Michalakis. 2017. Exposing the diversity of multiple infection patterns. Journal of Theoretical Biology 419:278–289.
Solomon, P. S., and R. P. Oliver. 2002. Evidence that γ-aminobutyric acid is a major nitrogen source during Cladosporium fulvum infection of tomato. Planta 214:414–420.
Sone, K., K. Ohkubo, T. Matsuo, and K. Hata. 2012. Spatial distribution pattern of pine trees killed by pine wilt disease in a sparsely growing, young pine stand. Journal of Plant Studies 2:1–6.
Steffen, W., K. Richardson, J. Rockstrom, S. E. Cornell, I. Fetzer, E. M. Bennett, R. Biggs, S. R. Carpenter, W. de Vries, C. A. de Wit, C. Folke, D. Gerten, J. Heinke, G. M. Mace, L. M. Persson, V. Ramanathan, B. Reyers, and S. Sorlin. 2015. Planetary boundaries: Guiding human development on a changing planet. Science

347:1259855-1-1259855–10.
Sterner, R. W., and J. J. Elser. 2002. Ecological Stoichiometry: The Biology of Elements from Molecules to the Biosphere. Princeton University Press, Princeton, NJ, USA.
Stevens, C. J., E. M. Lind, Y. Hautier, W. S. Harpole, E. T. Borer, S. Hobbie, E. W. Seabloom, L. Ladwig, J. D. Bakker, C. Chu, S. Collins, K. F. Davies, J. Firn, H. Hillebrand, K. J. La Pierre, A. MacDougall, B. Melbourne, R. L. McCulley, J. Morgan, J. L. Orrock, S. M. Prober, A. C. Risch, M. Schuetz, and P. D. Wragg. 2015. Anthropogenic nitrogen deposition predicts local grassland primary production worldwide. Ecology 96:1459–1465.
Strobeck, C. 1973. N species competition. Ecology 54:650–654.
Syller, J. 2012. Facilitative and antagonistic interactions between plant viruses in mixed infections. Molecular Plant Pathology 13:204–216.
Thompson, S., P. Alvarez-Loayza, J. Terborgh, and G. Katul. 2010. The effects of plant pathogens on tree recruitment in the Western Amazon under a projected future climate: A dynamical systems analysis. Journal of Ecology 98:1434–1446.
Tilman, D. 1977. Resource competition between plankton algae: An experimental and theoretical approach. Ecology 58:338–348.
Tilman, D. 1981. Tests of resource competition theory using Four species of Lake Michigan algae. Ecology 62:802–815.
Tilman, D. 1982. Resource Competition and Community Structure. Princeton University Press, Princeton, NJ, USA.
Tilman, D. 1994. Competition and biodiversity in spatially structured habitats. Ecology 75:2–16.
Tollenaere, C., H. Susi, and A. L. Laine. 2016. Evolutionary and epidemiological implications of multiple infection in plants. Trends in Plant Science 21:80–90.
Turechek, W. W., and L. V Madden. 2000. Analysis of the association between the incidence of two spatially aggregated foliar diseases of strawberry. Phytopathology 90:157–70.
Turelli, M. 1978. Does environmental variability limit niche overlap? Proceedings of the National Academy of Sciences of the United States of America 75:5085–9.
Valladares, F., C. C. Bastias, O. Godoy, E. Granda, and A. Escudero. 2015. Species coexistence in a changing world. Frontiers in Plant Science 6:1–16.
Vasco, D. A., H. J. Wearing, and P. Rohani. 2007. Tracking the dynamics of pathogen interactions: modeling ecological and immune-mediated processes in a two-pathogen single-host system. Journal of Theoretical Biology 245:9–25.
Vasconcelos, S. D., J. S. Cory, K. R. Wilson, S. M. Sait, and R. S. Hails. 1996. Modified behavior in baculovirus-infected lepidopteran larvae and its impact on the spatial distribution of inoculum. Biological Control 7:299–306.
Vellend, M. 2010. Conceptual synthesis in community ecology. The Quarterly Review of Biology 85:183–206.
Vitousek, P. M., J. D. Aber, R. W. Howarth, G. E. Likens, P. A. Matson, D. W. Schindler, W. H. Schlesinger, and D. G. Tilman. 1997. Human alteration of the global nitrogen cycle: sources and consequences. Ecological Applications 7:737–

750.
Voss, J. D., and L. L. Richardson. 2006. Nutrient enrichment enhances black band disease progression in corals. Coral Reefs 25:569–576.
Wale, N., D. G. Sim, and A. F. Read. 2017. A nutrient mediates intraspecific competition between rodent malaria parasites in vivo. Proceedings of the Royal Society B 284.
Walsh, J. F., D. H. Molyneux, and M. H. Birley. 1993. Deforestation: effect on vector-borne disease. Parasitology 106:S55–S75.
Walters, G. R., and J. A. Plumb. 1980. Environmental stress and bacterial infection in channel catfish, Ictalurus punctatus Rafinesque. Journal of Fish Biology 17:177–185.
Wen, F., and R. M. Lister. 1991. Heterologous encapsidation in mixed infections among four isolates of barley yellow dwarf virus. Journal of General Virology 72:2217–23.
Wen, F., R. M. Lister, and F. A. Fattouh. 1991. Cross-protection among strains of barley yellow dwarf virus. Journal of General Virology 72:791–9.
Whitaker, B. K., M. A. Rúa, and C. E. Mitchell. 2015. Viral pathogen production in a wild grass host driven by host growth and soil nitrogen. New Phytologist 207:760–768.
Whitham, S. A., and Y. Wang. 2004. Roles for host factors in plant viral pathogenicity. Current Opinion in Plant Biology 7:365–371.
Wiewiora, B., G. Zurek, and M. Zurek. 2015. Endophyte-mediated disease resistance in wild populations of perennial ryegrass (Lolium perenne). Fungal Ecology 15:1–8.
Wright, J. 2002. Plant diversity in tropical forests: a review of mechanisms of species coexistence. Oecologia:1–14.
Wright, S. J., O. Calderón, A. Hernandéz, M. Detto, and P. A. Jansen. 2016. Interspecific associations in seed arrival and seedling recruitment in a Neotropical forest. Ecology 97:2780–2790.
Zeier, J., B. Pink, M. Mueller, and S. Berger. 2004. Light conditions influence specific defence responses in incompatible plant-pathogen interactions: uncoupling systemic resistance from salicylic acid and PR-1 accumulation. Planta 219:673–683.
Zeller, M., and J. C. Koella. 2017. The role of the environment in the evolution of tolerance and resistance to a pathogen. The American Naturalist 190:389–397.
Zuur, A., E. Ieno, N. Walker, A. Saveliev, and G. Smith. 2009. Mixed Effects Models and Extensions in Ecology with R. Page (W. Gail, M., Krickeberg, K., Samet, J. M., Tsiatis, A., Wong, Ed.). Springer, New York, NY, USA.
Zvereva, A. S., and M. M. Pooggin. 2012. Silencing and innate immunity in plant defense against viral and non-viral pathogens. Viruses 4:2578–2597.

Appendices

Appendix 1: Supplementary Methods

Methods S1. Effects of correlogram df settings

The df setting for the spline correlogram function (Bjørnstad 2016), which we used to analyze spatial variation in host quality and the spatial patterns of infection, can change the outcome of our analyses. Results presented in the main text use df=15. When df = 20, the x-intercepts of cross-correlations are generally smaller and there are slightly fewer significant cross-correlations (compare Table S1 to Table 2, main text). In addition, the effect of vector-sharing on aggregation (Fig. 2, Table S2) and the effects of perennial grass cover and spatial variation in aphid preference on the frequency of PAV and RPV aggregation (Fig. 3a, Table S3) were found to be significant in models with df = 20 while the effect of P addition (Fig. 3c, Table S3) on PAV and RPV aggregation was not.

Methods S2. Methods for quantifying virus concentration with qPCR

To estimate the density of each virus species within the plants, we used RNA extraction and one-step reverse transcription-quantitative polymerase chain reaction (RT-qPCR). The aboveground tissue for each plant was cut into small pieces with a sterilized blade, and 50 mg of randomly selected segments were used for RNA extraction following the manufacturer's instructions for TRIzol™ Reagent (Invitrogen™). We designed forward and reverse qPCR primers and TaqMan® probes for each virus that target regions coding for the coat protein (Table S5, Lacroix et al. 2017). To prepare RT-qPCR standards for each virus, we extracted RNA from *A. sativa* tissue with known infections, performed a reverse transcription-PCR (RT-PCR; see Lacroix et al. 2014 for further details), and converted the RT-PCR product to RNA (MEGAscript® T7 Kit, Applied Biosystems®), which was diluted to a series of 10^7 to 10^3 copies of viral RNA.

For RT-qPCR of the Ch. 2 plants and the transmission experiment source plants in Ch. 3, 7 µL of RNA (or water, for the negative controls) were combined with 0.25 µM TaqMan® probes, 0.3 µM of forward and reverse primers for PAV or RPV (Table S5), 1X buffer, and 1X enzyme mixture (RNA-to-C_T™ 1-Step Kit, Applied Biosystems®). The reaction was kept at 48°C for 30 minutes for the reverse transcription, 95°C for 10 minutes for activation of Taq polymerase, and 50 cycles of 95°C for 25 seconds and 60°C for one minute were repeated for denaturation, annealing, and extension. Coinfection source plants and many of the RPV source plants from Chapters 2 and 3 were analyzed twice – once for PAV and once for RPV. Most PAV source plants were only analyzed for PAV, and RT-PCR was used to check for the presence of RPV. For qPCR of the invasion experiment plants in Ch. 3, 7 µL of RNA (or water, for the negative controls) were combined with 0.12 µM TaqMan® probes, 0.3 µM of forward and reverse primers for RPV and 0.4 µM of forward and reverse primers for PAV (Table S5), 1X buffer, and 2.5 µL enzyme mixture (Path-ID™ Multiplex One-Step RT-PCR Kit, Applied Biosystems®). The reaction was kept at 48°C for 10 minutes

for the reverse transcription, 95°C for 10 minutes for activation of Taq polymerase, and 50 cycles of 95°C for 15 seconds and 52.5°C for 45 seconds were repeated for denaturation, annealing, and extension.

For both experiments, each sample was replicated three times in a 96-well plate, which was analyzed with the Applied Biosystems® StepOnePlus™ Real-time PCR System. The detection threshold was set automatically by the system. Standard curves were used to calculate efficiency, with a 100% efficiency indicating that DNA strands approximately doubled in quantity with each PCR cycle (Bustin et al. 2009). We excluded standards from analysis if they had a lower concentration than any detected negative controls (indicating a potential false positive), the detection cycle number largely deviated from surrounding standards (indicating a pipetting error), or there was only one replicate and removing the replicate caused the efficiency to meet the target range of 85-115%. Samples in runs with standard curves outside the target efficiency range or with negative controls detected within the standard curve were re-analyzed when possible, but included in analyses otherwise. We estimated the quantity of RNA within a well using the detection threshold and standard curve. To estimate the density of PAV or RPV in a sample (number virions per mg plant tissue), we took the mean of the technical replicates (wells), scaled it from the volume of RNA used for qPCR analysis to the 50 ul RNA extract, and then divided it by the mass of plant tissue used for the RNA extraction. We also multiplied the virus density by the estimated mass of a virion to get the virus concentration (pg virus per g plant tissue, Table S6).

Some of the samples were quantified by RT-qPCR, but fell below the lowest concentration on the standard curve (10^3 copies/well), and we were not able to consistently detect standards with 10^2 copies/well. We removed replicates with these low values or no values at all from the mean when higher valued replicates were available to prevent them from skewing the estimate. Samples with all low or undetected replicates were assigned a value of zero. Because standard curves were modified to only include samples with concentrations higher than unexpected detections in controls, all samples with concentrations lower than unexpected detections were assigned a value of zero. Thirty-six percent of PAV infections in Ch. 2 had quantities below the lower threshold of the standard curve. Therefore, we re-analyzed this dataset, including these values rather than replacing them with zero, and present those results in addition to our main results.

Methods S3. Methods for estimating model parameters

We estimated parameters that describe the interaction between the plant and environmental resources using results from a published study in which *Hordeum vulgare L.* cv. Golf (barley) was supplied with 0.11 g N g^{-1} N day^{-1} in the form of nitrate in a liquid solution (Mattsson et al. 1991). UV absorption was used to measure N loss in the beaker in which the plants and nutrient solutions were placed. We estimated the value for the maximum uptake rate (u) from a figure and rounded down to the nearest marked increment (Fig. 4A in Mattsson et al. 1991). To convert the units to full mass, we multiplied the value by the average root:full mass ratio across all of our healthy mock-inoculated experimental plants (0.07). We estimated the half-saturation constant

(c) as 25 mmol nitrate m^{-3} (Fig. 4B in Mattsson et al. 1991). Nitrogen has an atomic mass of 14.0067 g mol^{-1} and a cubic meter of water is 1000 kg, which were used to convert the value to g N kg^{-1} substrate. The mass of water-saturated soil in one pot from our experiment was 0.1233 kg. This value was used to convert the half-saturation constant to g N pot^{-1}. The minimum tissue N concentration required for growth (y) of *H. vulgare L.* in this same experiment was approximately 0.01 g N g^{-1} root (Fig. 5A in Mattsson et al. 1991), which we multiplied by our average experimental value of root:full mass (0.07).

To estimate the supply rate (s) and initial mass of N in the environment (E_0) we multiplied the atomic mass of N in ammonium nitrate (28.0134 g mol^{-1}) by the concentration of ammonium nitrate in the modified Hoagland solution (375 μM, Table S4) to get the g N L^{-1} in the N addition treatments. We watered the plants with 30 mL of modified Hoagland solution seven times during the experiment and the plants were grown under these conditions for 40 days. Through this calculation, we estimated that the high N treatments received $5.5e^{-5}$ g N day^{-1}. We multiplied these values by six to get the initial environmental nutrient values of $3.3e^{-4}$ g N.

Because most of the plant tissue from our experiment was used to quantify virus density and transmission to new plants (results not presented here), we did not measure tissue nutrient content them and performed a small experiment to determine how N addition affected plant tissue nutrient content. We grew *A. sativa* plants in the conditions described in the main experiment and applied the four nutrient treatments and four inoculation treatments described for the main experiment. However, mortality led to three plants in each nutrient treatment that had three different inoculation treatments, and the same inoculation treatments were not consistent across nutrient treatments. The plants grew under the nutrient treatments for approximately 43 days. We oven dried the tissue at 65ºC for 48 hours, ground it using a bead beater, and put it into tin capsules. We used a CHN analyzer to measure particulate carbon, hydrogen, and nitrogen in the leaf tissue. Then, we fit a beta regression model using the "betareg" package in R to determine how the nutrient treatments affected the proportion of tissue weight attributed to N (Cribari-Neto and Zeileis 2010). We ignored the inoculation treatment because there were not enough replicates, and results from an experiment using the same nutrient and inoculation treatments found no effect of single infection on tissue N concentration (Lacroix et al. 2017). N addition, but not P addition significantly affected N concentration. The model prediction for the high N treatments was 0.0266, which became the initial tissue nutrient concentration (R_0).

To estimate the initial host mass (H_0) we grew plants under the same conditions that were used for the experiment with 13 plants watered with the low nutrients solution, 14 plants watered with high N, 17 plants watered with high P, and 14 plants watered with high N and P (Table S4). We measured the height of plants from the soil on days six, seven, nine, and ten post planting. We then used ImageJ software to estimate the height of healthy mock-inoculated plants from the main experiment using aboveground plant scans (Rasband 2014). We used a linear regression to determine the relationship between height and full mass for the experimental mock-inoculated plants and applied this relationship to the height data from plants measured on day six, when

most had just emerged from the soil, to estimate their full mass. We found that the average initial mass of plants grown in the N treatment was 0.0132 g.

With these parameters from the literature and experiments, we were then left with the plant intrinsic growth rate (r) and mortality rate (b) to estimate for the plant-resource model (Eq. 1-3). We used the "manipulate" package to form initial estimates for r and b based on visual assessments of model predictions compared to the healthy plant time series data from the N treatment of the experiment (Allaire 2014). Then, we used the "modCost" and "modFit" functions from the "FME" package (Soetaert and Petzoldt 2010) to fit Eq. 1-3 with one resource to these data (Table S13). We used the parameterized model to estimate E, R, and H at 10.5 days post planting, when inoculations occurred, which became the initial values for the model that included the pathogen (Eq. 1-4, Table 3, Fig. S4B).

To estimate the initial pathogen concentration, we multiplied the virion mass (Table S6) by published estimates of the number of PAV virions found in an aphid ($6.4e^6$) (Fabre et al. 2003) or in wheat 96 hours after inoculation of PAV ($1.6e^6$) (Nancarrow et al. 2014), but both of these estimates were much larger than our observed minimum RPV concentration (0.007 pg/g), so we set the initial concentration to 0.001 pg/g.

We used subsets of our data to estimate the remaining model parameters using the same R functions described for fitting the plant-resource model. First, we assumed that the pathogen, like the host, depended on N for growth, and we made assumptions to represent virulence as a function of pathogen presence ($q = 0$, $w = 1e^{-100}$). We used the RPV concentration time series and corresponding host mass from the coinfection N treatment, which is consistent with these assumptions, to estimate the pathogen's intrinsic growth rate (k), mortality rate (m), deviation from the host in minimum tissue nutrient concentration needed for growth (z) and maximum mass loss rate (v, Table S14, Fig. S4A). Next, we estimated w for the case when virulence is related to pathogen concentration using the host mass series from the coinfection N treatment. Finally, we assumed that virulence was caused by pathogen resource use. We chose not to estimate separate values for z_1 and z_2 because it would have been difficult to tease apart the effects of different z_1 and z_2 values and pathogen dependence on resource 1 or 2 on the relationship between resource supply and the proportion of mass lost. To estimate the concentration of N or the secondary resource required for virus replication (q_1 and q_2), we set v equal to zero and used the host mass series from the coinfection N treatment and RPV infection N treatment to fit the model. Because host growth depended on N and not the secondary treatment, changing q_2 had no effect on host mass, so we assume q_2 is equal to q_1.

Appendix 2: Supplementary Tables

Table S1. Summary of cross-correlations by experimental plot for virus pairs when df=20 for the spline correlogram settings. Prop. sig. is the proportion of experimental plots with significant cross-correlations.

Virus Pair	Expt. year	Prop. sig.	Mean ± std. error of sig. x-int. (m)	Mean ± std. error of sig. y-int. (m)
MAV-PAV	1	6/24	0.684 ± 0.025	0.1898 ± 0.0088
MAV-PAV	2	18/34	2.20 ± 0.17	0.2382 ± 0.0044
MAV-RPV	1	15/24	2.37 ± 0.18	0.1944 ± 0.0033
MAV-RPV	2	13/34	2.47 ± 0.27	0.2125 ± 0.0048
PAV-RPV	1	7/24	2.05 ± 0.46	0.1438 ± 0.0025
PAV-RPV	2	15/35	2.30 ± 0.22	0.2326 ± 0.0052
MAV-RMV	2	2/34	0.86 ± 0.16	0.141 ± 0.020
PAV-RMV	2	2/35	1.90 ± 0.29	0.175 ± 0.029
RPV-RMV	2	4/35	2.28 ± 0.57	0.1334 ± 0.0084

Table S2. Linear coefficients, standard error, and P-values for fixed effects and variance of random effects for model testing the effect of vector sharing on the frequency of aggregation between virus pairs in the second experimental year (generalized linear mixed-effects model, logit-link). P-value for "Vector sharing" was obtained from a likelihood ratio test comparing this model with the intercept-only model. Data included 207 observations.

	Estimate (fixed) or Variance (random)	Standard Error	P-value
Fixed effects			
Intercept	-3.6	1.2	0.003
Vector sharing	2.84	0.90	0.003
Random effects			
Viruses:site	2.14		
Site	4.38		

Table S3. Linear coefficients, standard error, and P-values for model testing the effects of nutrient addition, spatial variation in aphid preference, spatial variation in experimental plant weight, and perennial grass percent cover on the frequency of aggregation between PAV and RPV in the second experimental year (generalized linear model, logit-link). Only the significant predictor variables following backwards stepwise selection are included in the table. P-values for predictor variables were obtained from a likelihood ratio test comparing this model with one lacking the focal variable. Model df = 34.

	Estimate	Standard Error	P-value
Intercept	-4.6	1.7	0.006
P addition	2.4	1.0	0.007
Heterogeneity in aphid preference	2.8	1.4	0.02
Perennial grass percent cover	0.056	0.023	0.005

Table S4. Modified Hoagland solution recipe used to create nutrient treatments

Compound	Molar Mass	Concentration (μM)
K_2SO_4	174.25	1250

$MgSO_4 \cdot 7H_2O$	246.48	1000
KH_2PO_4	136.09	1 (50 for elevated P)
$CaSO_4 \cdot 2H_2O$	172.17	2000
NH_4NO_3	80.04	7.5 (375 for elevated N)
KCl	74.56	25
H_3BO_3	61.83	12.5
$MnSO_4 \cdot H_2O$	169.02	1
$ZnSO_4 \cdot 7H_2O$	278.56	1
$CuSO_4 \cdot 5H_2O$	249.69	0.25
$H_2MoO_4 \cdot (H_2O)$	161.95	0.25
NaFeEDDHA (6% Fe)	434.8	10

The low and high concentrations of KH_2PO_4 and NH_4NO_3 are 0.2% and 10% of half-strength Hoagland solution, respectively (Hoagland and Arnon 1938, Seabloom et al. 2011, Lacroix et al. 2014, 2017).

Table S5. Sequences for qPCR primers and probes

Type	Virus	Sequence (5' to 3')
Forward primer	RPV	GAGGTTAGCGAGGAGTTAGAATTC
Reverse primer	RPV	AACTACCTCAGAGTTGCCACATTC
Probe	RPV	VICACATCTTCAAGACTCCTAACCTCGCCATMGBNFQ
Forward primer	PAV	TGGTCGCCCAAAAATCTAAAAC
Reverse primer	PAV	GGAGTAAGGCTCGCAGTAAATTGCCGCATAAACAC
Probe	PAV	FAMGGTGACCGAGGCTTGGACCGACTTCTTTMGBNFQ

Note: We added a T7 promoter to the 5' end of the reverse primers (5′-TAATACGACTCACTATAGGGAGA-3′) for producing standards with RT-PCR prior to transcription (Lacroix et al. 2017).

Table S6. Estimation of virion mass and intermediate values used in the calculation

Description	PAV	RPV
Bases per genome[1,2]	5677	5600
Mass of genome (g)[3]	$4.71e^{-18}$	$4.65e^{-18}$
Number of coat proteins per virion[4]	180	180
Ratio of fusion protein:major coat protein[5]	1:1000 to 1:4	1:1000 to 1:4
Number of major coat proteins per virion	144 to 179.82	144 to 179.82
Number of fusion proteins per virion	0.18 to 36	0.18 to 36
Mass of major coat protein (kDa)[6,7]	22	24.5
Mass of fusion protein (kDa)[6]	72	72
Mass of major coat proteins per virion (g)	$5.26e^{-18}$-$6.57e^{-18}$	$5.86e^{-18}$-$7.31e^{-18}$
Mass of fusion proteins per virion (g)	$2.15e^{-20}$-$430e^{-20}$	$2.15e^{-20}$-$430e^{-20}$
Total virion mass (g)	$1.13e^{-17}$-$1.43e^{-17}$	$1.20e^{-17}$-$1.48e^{-17}$

Average mass (pg; used for analyses)	$1.28e^{-5}$	$1.34e^{-5}$

Table S6 References:

1. Miller, W. A., P. M. Waterhouse, and W. L. Gerlach. 1988. Sequence and organization of barley yellow dwarf virus genomic RNA. Nucleic Acids Research. 16: 6097-6111.
2. Vincent, J. R., R. M. Lister, and B. A. Larkins. 1991. Nucleotide sequence analysis and genomic organization of the NY-RPV isolate of barley yellow dwarf virus. The Journal of General Virology 72:2347–2355.
3. Assuming an average molecular weight of 499.5 g/mol
4. D'Arcy, C. J., and P. A. Burnett. 1995. Barley Yellow Dwarf: 40 Years of Progress. The American Phytopathological Society, St. Paul, MN, USA.
5. Brown, C. M., S. P. Dinesh-Kumar, and W. A. Miller. 1996. Local and distant sequences are required for efficient readthrough of the barley yellow dwarf virus PAV coat protein gene stop codon. Journal of virology 70:5884–92.
6. Cheng, S. L., L. L. Domier, and C. J. D'Arcy. 1994. Detection of the readthrough protein of barley yellow dwarf virus. Virology 202:1003–6.
7. Scalla, R., and W. F. Rochow. 1977. Protein component of two isolates of barley yellow dwarf virus. Virology 78:576–580.

Table S7. Statistical models for the effects of coinfection, nutrient addition, days post inoculation (dpi), and their interactions on log-transformed RPV concentration over the first three harvesting days. The first model has N:P (NP Ratio) representing nutrient addition and the second model has categorical variables (N addition is "high N", P addition is "high P").

Model	Fixed effects	Estimate	Std. error	df	χ^2	p-value
1	(Intercept)	3.009	1.193	--	--	--
1	dpi	0.583	0.127	--	--	--
1	NP ratio	-1.853	1.151	--	--	--
1	coinfection	3.771	1.742	1	2.802	0.094
1	**dpi:NP ratio**	**0.154**	**0.133**	**1**	**5.719**	**0.017**
1	dpi:coinfection	-0.359	0.193	1	2.830	0.093
1	NP ratio:coinfection	-1.339	1.757	1	0.073	0.787
1	dpi:NP ratio:coinfection	0.177	0.198	1	0.846	0.358
2	(Intercept)	2.761	2.005	--	--	--
2	dpi	0.591	0.223	--	--	--
2	high N	-3.480	2.818	--	--	--
2	high P	0.933	2.756	--	--	--
2	coinfection	3.456	2.993	1	2.741	0.098
2	dpi:high N	0.304	0.324	--	--	--
2	dpi:high P	-0.003	0.310	--	--	--
2	high N:high P	2.286	3.942	--	--	--
2	dpi:coinfection	-0.287	0.332	1	2.893	0.089
2	high N:coinfection	-2.426	4.289	1	0.108	0.742
2	high P:coinfection	-1.825	4.207	1	0.262	0.609

2	**dpi:high N:high P**	**-0.326**	**0.448**	**1**	**4.088**	**0.043**
2	dpi:high N:coinfection	0.287	0.481	1	0.095	0.758
2	dpi:high P:coinfection	0.123	0.464	1	0.554	0.457
2	high N:high P:coinfection	7.024	6.035	1	0.109	0.741
2	dpi:high N:high P:coinfection	-0.755	0.673	1	1.425	0.233

Note: Chi-squared tests were used to assess both linear mixed-effects models (n=132 for each), which had experimental block as the random effect (s.d. = 0.835, s.d. = 0.860 for models 1 and 2, respectively). Effects and interactions with $p<0.05$ are bolded. Model 1 is shown in Fig. 2C-D.

Table S8. Statistical models for the effects of coinfection, nutrient addition, days post inoculation (dpi), and their interactions on log-transformed PAV concentration over the first three harvesting days. The first model has N:P (NP ratio) representing nutrient addition and the second model has categorical variables (N addition is "high N", P addition is "high P"). Values below the lower standard curve threshold are included.

Model	Fixed effects	Estimate	Std. error	df	F	p-value
1	(Intercept)	3.680	0.937	--	--	--
1	dpi	0.222	0.106	--	--	--
1	NP ratio	-2.283	0.921	--	--	--
1	coinfection	-0.699	1.432	1	2.134	0.147
1	**dpi:NP ratio**	**0.223**	**0.103**	**1**	**6.209**	**0.014**
1	dpi:coinfection	-0.008	0.159	1	0.118	0.732
1	NP ratio:coinfection	1.041	1.433	1	0.807	0.371
1	dpi:NP ratio:coinfection	-0.074	0.159	1	0.218	0.641
2	(Intercept)	3.323	1.620	--	--	--
2	dpi	0.289	0.184	--	--	--
2	high N	-4.239	2.270	--	--	--
2	high P	-0.601	2.270	--	--	--
2	coinfection	-0.066	2.460	1	2.095	0.150
2	dpi:high N	0.382	0.255	--	--	--
2	dpi:high P	0.062	0.255	--	--	--
2	high N:high P	6.635	3.231	--	--	--
2	dpi:coinfection	-0.112	0.273	1	0.087	0.769
2	high N:coinfection	1.467	3.498	1	0.149	0.700
2	high P:coinfection	0.149	3.465	1	0.019	0.890
2	**dpi:high N:high P**	**-0.739**	**0.365**	**1**	**5.688**	**0.019**
2	dpi:high N:coinfection	-0.045	0.388	1	0.099	0.754
2	dpi:high P:coinfection	0.058	0.382	1	0.459	0.499
2	high N:high P:coinfection	-3.816	4.960	1	0.983	0.324
2	dpi:high N:high P:coinfection	0.266	0.552	1	0.232	0.631

Note: F-tests were used to assess both linear models (n=133 for each). Effects and interactions with $p<0.05$ are bolded.

Table S9. Statistical model for the effects of coinfection, N:P (NP Ratio), and their interaction on RPV concentration over the last five harvesting days

Fixed effects	Estimate	Std. error	df	F	p-value
(Intercept)	64621.175	18417.770	--	--	--
NP ratio	-15076.338	18288.384	1	0.715	0.399
coinfection	**68895.735**	**26935.947**	**1**	**10.208**	**0.002**
NP ratio:coinfection	8189.679	26614.722	1	0.095	0.759

Note: The linear model was assessed with F-tests (n=226). Effects and interactions with $p<0.05$ are bolded. This model is shown in Fig. 2C-D.

Table S10. Statistical models for the effects of infection (PAV, RPV, or coinfection represented by PAV:RPV), nutrient addition, days post inoculation (dpi), and their interactions on plant shoot mass (g). The first model has categorical variables (N addition is "high N", P addition is "high P") representing nutrient addition and the second model has N:P (NP Ratio).

Model	Fixed effects	Estimate	Std. error	df	χ^2	p-value
1	(Intercept)	0.058	0.051	--	--	--
1	dpi	0.015	0.002	--	--	--
1	high N	-0.012	0.061	--	--	--
1	high P	0.074	0.063	1	0.891	0.345
1	PAV	0.131	0.076	--	--	--
1	RPV	0.095	0.057	--	--	--
1	**dpi:high N**	**0.003**	**0.003**	**1**	**18.107**	**$2.088e^{-5}$**
1	dpi:high P	-0.005	0.003	1	0.154	0.695
1	high N:high P	-0.049	0.087	1	1.053	0.305
1	dpi:PAV	-0.012	0.004	--	--	--
1	high N:PAV	-0.054	0.103	1	0.098	0.754
1	high P:PAV	-0.105	0.101	1	0.275	0.600
1	dpi:RPV	-0.010	0.003	--	--	--
1	high N:RPV	0.025	0.083	1	0.002	0.969
1	high P:RPV	-0.060	0.081	1	2.984	0.084
1	PAV:RPV	-0.073	0.109	--	--	--
1	dpi:high N:high P	0.006	0.005	1	0.956	0.328
1	dpi:high N:PAV	0.004	0.005	1	0.458	0.499
1	dpi:high P:PAV	0.006	0.005	1	0.398	0.528
1	high N:high P:PAV	0.152	0.147	1	0.799	0.371
1	dpi:high N:RPV	$3.28e^{-4}$	0.004	1	0.101	0.750
1	dpi:high P:RPV	0.003	0.004	1	0.964	0.326
1	high N:high P:RPV	-0.025	0.116	1	1.746	0.186
1	**dpi:PAV:RPV**	**0.007**	**0.006**	**1**	**6.300**	**0.012**
1	high N:PAV:RPV	0.026	0.151	1	0.313	0.576
1	high P:PAV:RPV	0.012	0.143	1	0.002	0.963
1	dpi:high N:high P:PAV	-0.010	0.008	1	2.953	0.086
1	dpi:high N:high P:RPV	-0.001	0.006	1	0.009	0.923

1	dpi:high N:PAV:RPV	-0.002	0.008	1	0.061	0.804
1	dpi:high P:PAV:RPV	$3.70e^{-4}$	0.008	1	0.055	0.815
1	high N:high P:PAV:RPV	-0.055	0.206	1	0.123	0.725
1	dpi:high N:high P:PAV:RPV	0.002	0.011	1	0.024	0.878
2	(Intercept)	0.089	0.038	--	--	--
2	dpi	0.014	0.001	--	--	--
2	NP ratio	-0.022	0.027	1	17.232	$3.31e^{-5}$
2	PAV	0.082	0.045	--	--	--
2	RPV	0.047	0.035	--	--	--
2	**dpi:NP ratio**	**0.002**	**0.001**	**1**	**5.489**	**0.019**
2	dpi:PAV	-0.009	0.002	--	--	--
2	NP ratio:PAV	-0.002	0.043	1	0.289	0.591
2	dpi:RPV	-0.007	0.002	--	--	--
2	NP ratio:RPV	0.036	0.036	1	2.231	0.135
2	PAV:RPV	-0.072	0.061	--	--	--
2	dpi:NP ratio:PAV	0.001	0.002	1	0.0034	0.9534
2	dpi:NP ratio:RPV	-0.001	0.002	1	0.7078	0.4002
2	**dpi:PAV:RPV**	**0.007**	**0.003**	**1**	**6.141**	**0.013**
2	NP ratio:PAV:RPV	0.012	0.063	1	0.1143	0.7353
2	dpi:NP ratio:PAV:RPV	-0.001	0.003	1	0.123	0.725

Note: Chi-squared tests were used to assess both linear mixed-effects models (n=662 for each), which had experimental block as the random effect (s.d. = 0.0601, s.d. = 0.0604) for models 1 and 2, respectively). Effects and interactions with $p<0.05$ are bolded. Model 1 is shown in Fig. 3A-B.

Table S11. Statistical models for the effects of infection (PAV, RPV, or coinfection represented by PAV:RPV), nutrient addition, days post inoculation (dpi), and their interactions on plant chlorophyll (SPAD). The first model has categorical variables (N addition is "high N", P addition is "high P") representing nutrient addition and the second model has N:P (NP Ratio).

Model	Fixed effects	Estimate	Std. error	df	χ^2	p-value
1	(Intercept)	26.858	1.861	--	--	--
1	dpi	-0.157	0.096	--	--	--
1	high N	-1.025	2.537	--	--	--
1	high P	-1.665	2.591	1	0.566	0.452
1	PAV	0.028	3.690	--	--	--
1	RPV	3.863	2.463	--	--	--
1	dpi:high N	0.182	0.139	--	--	--
1	dpi:high P	0.069	0.138	1	0.085	0.771
1	high N:high P	3.253	3.590	1	1.105	0.293
1	dpi:PAV	-0.022	0.191	--	--	--
1	high N:PAV	0.738	4.880	--	--	--
1	high P:PAV	1.553	4.950	1	0.497	0.481
1	dpi:RPV	-0.246	0.130	--	--	--

1	high N:RPV	-4.006	3.648	--	--	--
1	high P:RPV	0.472	3.564	1	0.469	0.493
1	PAV:RPV	-2.224	4.975	--	--	--
1	dpi:high N:high P	-0.201	0.195	1	3.552	0.059
1	dpi:high N:PAV	-0.017	0.255	--	--	--
1	dpi:high P:PAV	-0.070	0.253	1	0.538	0.463
1	high N:high P:PAV	-8.001	7.057	1	1.169	0.280
1	dpi:high N:RPV	0.252	0.191	--	--	--
1	dpi:high P:RPV	-0.023	0.188	1	0.076	0.783
1	high N:high P:RPV	-0.303	5.107	1	0.177	0.674
1	dpi:PAV:RPV	0.078	0.257	--	--	--
1	high N:PAV:RPV	2.794	6.846	--	--	--
1	high P:PAV:RPV	-3.571	6.598	1	0.866	0.352
1	dpi:high N:high P:PAV	0.391	0.361	1	0.0393	0.8428
1	dpi:high N:high P:RPV	0.026	0.269	1	1.0289	0.3104
1	**dpi:high N:PAV:RPV**	**-0.105**	**0.348**	**1**	**4.160**	**0.041**
1	dpi:high P:PAV:RPV	0.350	0.344	1	0.0400	0.8415
1	high N:high P:PAV:RPV	12.280	9.449	1	0.3403	0.5596
1	dpi:high N:high P:PAV:RPV	-0.784	0.482	1	2.864	0.091
2	(Intercept)	26.609	1.178	--	--	--
2	dpi	-0.125	0.058	--	--	--
2	NP ratio	-0.376	1.073	--	--	--
2	PAV	-1.174	2.132	1	0.046	0.831
2	RPV	2.630	1.498	1	0.001	0.980
2	**dpi:NP ratio**	**0.074**	**0.059**	**1**	**9.592**	**0.002**
2	dpi:PAV	0.046	0.108	1	0.297	0.586
2	NP ratio:PAV	0.957	1.961	1	0.000	0.998
2	dpi:RPV	-0.161	0.079	1	3.819	0.051
2	NP ratio:RPV	-1.400	1.577	1	0.000	0.991
2	PAV:RPV	0.055	2.771	1	0.246	0.620
2	dpi:NP ratio:PAV	-0.041	0.102	1	0.752	0.386
2	dpi:NP ratio:RPV	0.085	0.082	1	1.237	0.266
2	dpi:PAV:RPV	0.035	0.143	1	0.017	0.897
2	NP ratio:PAV:RPV	0.296	2.796	1	0.111	0.739
2	dpi:NP ratio:PAV:RPV	-0.034	0.141	1	0.060	0.807

Note: Chi-squared tests were used to assess both linear mixed-effects models (n=553 for each), which had experimental block as the random effect (s.d. = 1.25, s.d. = 1.24) for models 1 and 2, respectively). Effects and interactions with $p<0.05$ are bolded. Model 1 is shown in Fig. 3D-E.

Table S12. Statistical model for the effects of coinfection and log-transformed RPV density on residual shoot mass, after it has been fit with a model accounting for the interaction between dpi and N addition.

Fixed effects	Estimate	Std. error	df	F	p-value

(Intercept)	0.071	0.035	--	--	--
log(concentration)	**-0.006**	**0.004**	**1**	**4.71**	**0.031**
coinfection	-0.038	0.049	1	3.54	0.061
log(concentration):coinfection	0.002	0.005	1	0.208	0.649

Note: The linear model was assessed with F-tests (n=329). Effects and interactions with $p<0.05$ are bolded. This model is shown in Fig. 3C.

Table S13. Parameter fits for non-infected plant (Eq. 1-3, Table 3)

Parameter	Fitted values	Std. error	Initial predictions	Fitted range	t value	p-value
r	0.281	0.025	0.3	0, 10	11.038	$2.61e^{-11}$
b	0.095	0.011	0.1	0, 1	8.349	$7.87e^{-9}$

Note: Model was fit to healthy, mock-inoculated plant data from the N treatment (deviance = 0.399). Fitted range is the range of values the fitting function was restricted to searching within.

Table S14. Parameter fits for plant and pathogen model (Eq. 1-4, Table 3)

Model	Parameter	Fitted values	Std. error	Initial predictions	Fitted range	t value	p-value
1	*k*	1.147	1.59	1.14	0, 10	0.719	0.474
1	*m*	0.088	1.54	0.08	0, 1	0.057	0.955
1	*v*	0.015	0.129	1.16	0, 1	0.119	0.906
1	z_1	$5.079e^{-4}$	$7.332e^{-4}$	0.0005	$-6.9e^{-4}$, 0.999	0.693	0.491
2	*w*	0.299	1.979	0.3	0, 1	0.151	0.881
3	*q*	$8.702e^{-6}$	$6.700e^{-6}$	$4e^{-5}$	0, 1	1.299	0.201

Note: Model was fit to RPV-infected plant data (deviance = $8.71e^{7}$, 0.667, and ZZ for models 1, 2, and 3, respectively). Fitted range is the range of values the fitting function was restricted to searching within.

Table S15. Statistical model of PAV inoculation rates for the invader in response to the nutrient treatment (N, P), DPI, and their interactions.

Factor	Estimate	Std. Error	df	χ^2	p-value
(Intercept)	-4.271	2.013	--	--	--
N	-1.925	2.344	1	0.182	0.670
P	-1.517	2.233	1	0.024	0.878
DPI	**0.286**	**0.121**	**1**	**43.427**	**$4.401e^{-11}$**
N:P	1.232	3.387	1	0.028	0.868
N:DPI	0.180	0.186	1	1.083	0.298
P:DPI	0.132	0.178	1	0.497	0.481
N:P:DPI	-0.088	0.271	1	0.107	0.744

Note: The generalized linear mixed effects model (n=98) was fit with a logit-link function and experimental block as the random effect (s.d. = 2.159). The model was

also fit with nutrients represented by the ratio between N and P, and there were no significant effects of the nutrient treatment. Main effects and interactions with $p<0.05$ according to Chi-squared tests are bolded.

Table S16. Statistical model of PAV growth rate for the invader (baseline) compared to single inoculations at high density and low density. The effects of nutrient treatment (N, P), virus role, DPI, and their interactions are included. Estimates of DPI and its interactions indicate virus growth rate.

Factor	Estimate	Std. Error	df	χ^2	p-value
(Intercept)	-2.415	1.734	--	--	--
N	-0.717	2.389	1	0.024	0.877
P	2.048	2.476	1	0.079	0.779
DPI	0.493	0.191	--	--	--
High Density	9.151	2.398	--	--	--
Low Density	-1.282	2.346	--	--	--
N:P	-2.654	3.441	1	0.951	0.330
N:DPI	0.114	0.270	1	0.396	0.529
P:DPI	-0.269	0.277	1	0.001	0.979
N:High Density	0.029	3.377	2	2.171	0.338
N:Low Density	2.132	3.217			
P:High Density	-2.825	3.438	2	0.355	0.838
P:Low Density	-0.816	3.282			
DPI:High Density	**-0.544**	**0.271**	**2**	**21.524**	**$2.119e^{-5}$**
DPI:Low Density	**0.295**	**0.259**			
N:P:DPI	0.330	0.387	1	0.213	0.644
N:P:High Density	2.810	4.819	2	1.234	0.539
N:P:Low Density	0.820	4.609			
N:DPI:High Density	0.027	0.382	2	2.553	0.279
N:DPI:Low Density	-0.272	0.363			
P:DPI:High Density	0.418	0.388	2	0.681	0.712
P:DPI:Low Density	0.219	0.368			
N:P:DPI:High Density	-0.389	0.545	2	0.551	0.759
N:P:DPI:Low Density	-0.288	0.520			

Note: The linear mixed effects model (n=191) was fit with experimental block as the random effect (s.d. = 0.925). The model was also fit with nutrients represented by the ratio between N and P, and there were no significant effects of the nutrient treatment. Main effects and interactions with $p<0.05$ according to Chi-squared tests are bolded.

Table S17. Statistical model of RPV growth rate for the invader (baseline) compared to single inoculations at high density and low density. The effects of nutrient treatment (N, P), virus role, DPI, and their interactions are included. Estimates of DPI and its interactions indicate virus growth rate.

Factor	Estimate	Std. Error	df	F	p-value
(Intercept)	9.028	1.865	--	--	--
N	1.543	2.597	1	1.932	0.166
P	0.043	2.503	1	0.881	0.349
DPI	0.379	0.212	--	--	--
High Density	5.320	2.537	--	--	--
Low Density	-6.169	2.408	--	--	--
N:P	-0.717	3.514	1	0.171	0.680
N:DPI	-0.114	0.305	1	0.160	0.690
P:DPI	0.012	0.284	1	0.510	0.476
N:High Density	-2.423	3.559	2	2.428	0.091
N:Low Density	-4.937	3.391			
P:High Density	0.332	3.564	2	0.670	0.513
P:Low Density	0.993	3.289			
DPI:High Density	**-0.253**	**0.292**	**2**	**8.562**	**$2.845e^{-4}$**
DPI:Low Density	**0.212**	**0.273**			
N:P:DPI	0.045	0.406	1	0.325	0.570
N:P:High Density	1.228	4.953	2	0.030	0.970
N:P:Low Density	2.815	4.654			
N:DPI:High Density	0.194	0.417	2	0.345	0.709
N:DPI:Low Density	0.404	0.395			
P:DPI:High Density	-0.053	0.407	2	0.274	0.760
P:DPI:Low Density	-0.032	0.371			
N:P:DPI:High Density	-0.108	0.571	2	0.219	0.804
N:P:DPI:Low Density	-0.339	0.534			

Note: The linear model (n=179) was also fit with nutrients represented by the ratio between N and P, and there were no significant effects of the nutrient treatment. Main effects and interactions with $p<0.05$ according to F-tests are bolded.

Table S18. Statistical model of PAV density in established infections from the invasion experiment. The effects of nutrient treatment (N, P), virus role (baseline = single inoculation, compared to resident), and their interactions are included.

Factor	Estimate	Std. Error	df	χ^2	p-value
(Intercept)	929.562	231.702	--	--	--

N	**446.912**	**249.399**	**1**	**4.239**	**0.040**
P	353.335	249.509	1	0.820	0.365
Resident	195.651	249.519	1	0.166	0.683
N:P	-149.414	354.380	1	0.663	0.415
N:Resident	-167.687	354.562	1	0.787	0.375
P:Resident	-275.058	354.715	1	1.718	0.190
N:P:Resident	-111.376	502.559	1	0.049	0.825

Note: The linear mixed effects model (n=201) was fit with crossed random effects of experimental block (s.d. = 185.0) and DPI (s.d. = 245.3). The model was also fit with nutrients represented by N:P, and there were no significant effects of the nutrient treatment. Effects and interactions with $p<0.05$ according to the likelihood ratio test are bolded.

Table S19. Statistical model of RPV density in established infections from the invasion experiment. The effects of nutrient treatment (N, P), virus role (baseline = single inoculation, compared to resident), and their interactions are included.

Factor	Estimate	Std. Error	df	χ^2	p-value
(Intercept)	$5.522e^6$	$1.680e^6$	--	--	--
N	$-9.743e^4$	$9.185e^5$	1	0.006	0.939
P	$1.933e^5$	$9.532e^5$	1	1.255	0.263
Resident	$-2.068e^5$	$9.084e^5$	1	0.172	0.678
N:P	$-1.231e^6$	$1.330e^6$	1	0.646	0.422
N:Resident	$9.929e^5$	$1.316e^6$	1	2.380	0.123
P:Resident	$-6.716e^5$	$1.324e^6$	1	0.046	0.830
N:P:Resident	$9.485e^5$	$1.882e^6$	1	0.254	0.614

Note: The linear mixed effects model (n=180) was fit with crossed random effects of experimental block (s.d. = $1.99e^6$) and DPI (s.d. = $2.34e^6$). The model was also fit with nutrients represented by N:P, and there were no significant effects of the nutrient treatment.

Table S20. Statistical model of PAV transmission. The log-transformed virus density in the source plant, source plant nutrient treatments (N, P), and their interactions were added to whether the source plant was coinfected (Co), the receiving plant nutrient treatment (RecN, RecP), and their interactions.

Factor	Estimate	Std. Error	df	χ^2	p-value
(Intercept)	-2.451	1.893	--	--	--
log(PAV density)	0.429	0.254	1	2.205	0.138
N	3.319	2.416	1	0.002	0.969
P	2.028	2.721	1	0.636	0.425
RecN	-0.313	0.421	--	--	--
RecP	-1.203	0.420	--	--	--

Co	-1.158	0.421	--	--	--
log(PAV density):N	-0.399	0.325	1	1.392	0.238
log(PAV density):P	-0.199	0.368	1	0.099	0.753
N:P	-2.549	3.875	1	3.400	0.065
RecN:RecP	1.427	0.594	--	--	--
RecN:Co	0.784	0.562	--	--	--
RecP:Co	1.257	0.561	--	--	--
log(PAV density):N:P	0.242	0.533	1	0.204	0.652
RecN:RecP:Co	**-1.590**	**0.789**	**1**	**3.986**	**0.046**

Note: The generalized linear mixed effects model (n=509) was fit with a logit-link function and source plant identity (s.d. = 0.388) crossed with DPI (s.d. = 0.604) as the random effects. The model was also fit with nutrients represented by N:P, and there were no significant effects of the nutrient treatment. Effects and interactions with $p<0.05$ according to Chi-squared tests are bolded.

Table S21. Statistical model of RPV transmission. The log-transformed virus density in the source plant, source plant nutrient treatments (N, P), and their interactions were added to whether the source plant was coinfected (Co), the receiving plant nutrient treatment (RecN, RecP), and their interactions.

Factor	Estimate	Std. Error	df	χ^2	p-value
(Intercept)	-0.961	1.556	--	--	--
log(RPV density)	0.144	0.148	1	2.704	0.100
N	-0.252	2.224	1	0.346	0.557
P	-0.633	2.177	1	0.017	0.897
RecN	**1.406**	**0.357**	1	**28.768**	**$8.161e^{-8}$**
RecP	0.151	0.319	1	0.046	0.830
Co	0.280	0.407	1	0.705	0.401
log(RPV density):N	-0.004	0.213	1	0.292	0.589
log(RPV density):P	0.045	0.211	1	0.046	0.829
N:P	2.076	3.215	1	0.568	0.451
RecN:RecP	-0.313	0.486	1	0.228	0.633
RecN:Co	-0.770	0.539	1	2.519	0.112
RecP:Co	-0.274	0.507	1	0.108	0.742
log(RPV density):N:P	-0.164	0.307	1	0.280	0.596
RecN:RecP:Co	0.324	0.747	1	0.183	0.668

Note: The generalized linear mixed effects model (n=683) was fit with a logit-link function and source plant identity (s.d. = 0.971) nested in experimental block (s.d. = 0.443) as the random effects. The model was also fit with nutrients represented by N:P, and there was a significant main effect of N:P (see main text). Effects and interactions with $p<0.05$ according to the likelihood ratio test are bolded.

Appendix 3: Supplementary Figures

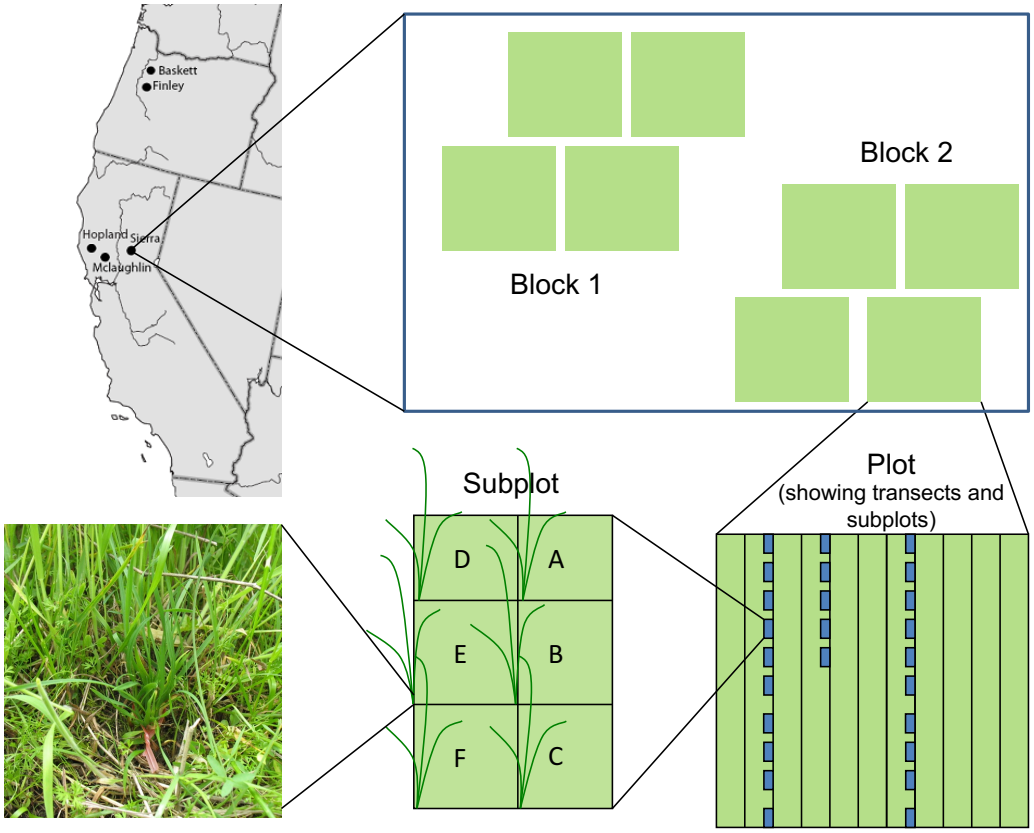

Figure S1. The spatially nested experimental design. Individual grasses were planted into locations A-E of subplots, which were arranged along transects across a plot. Four plots were in each block, with each plot receiving a different nutrient addition treatment. Each site had two blocks. Three sites ae located in California and two are in Oregon. Figure re-published with permission from Borer et al. 2010, Ecology Letters (doi: 10.1111/j.1461-0248.2010.01475.x).

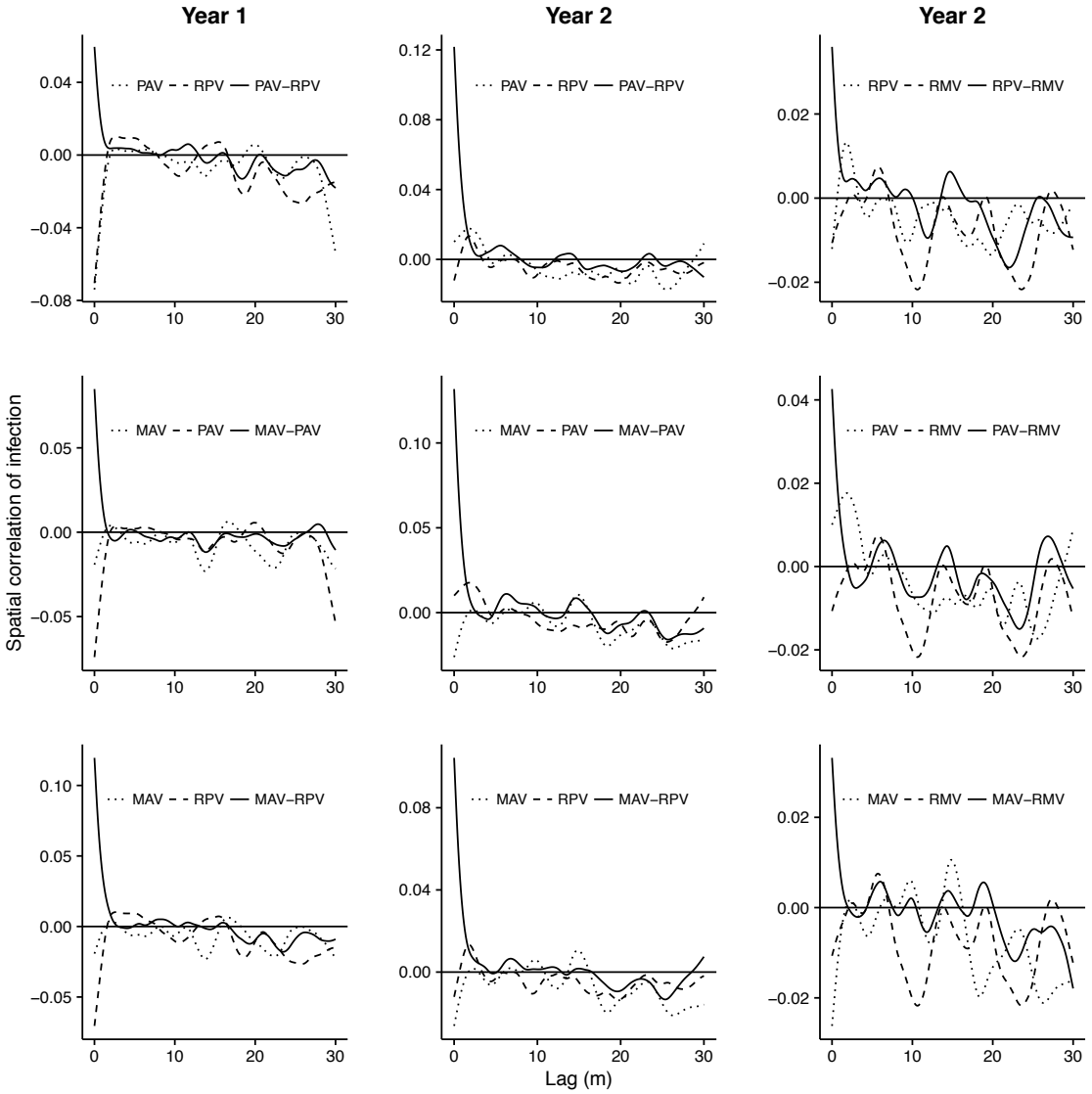

Figure S2. Cross-correlograms for each virus pair in 2007 (first column) and 2008 (second and third columns) along with correlograms for each virus involved in the pair. Mean correlation values across experimental plots are shown. 95% CI are not presented for clarity. Please see Table 2 for information about significance of cross-correlograms. Significant single virus correlograms are shown in Fig. S3 and discussed in the main text.

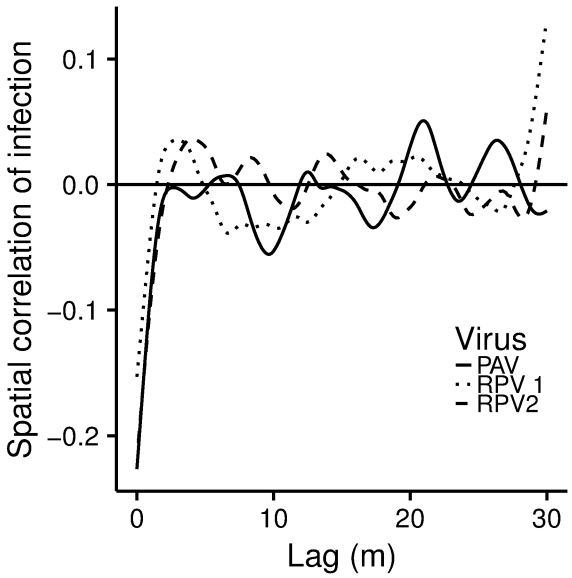

Figure S3. The three autocorrelations from the first experimental year that had non-random spatial patterns. 95% CI are excluded for clarity. Numbers following "RPV" indicate different experimental plots.

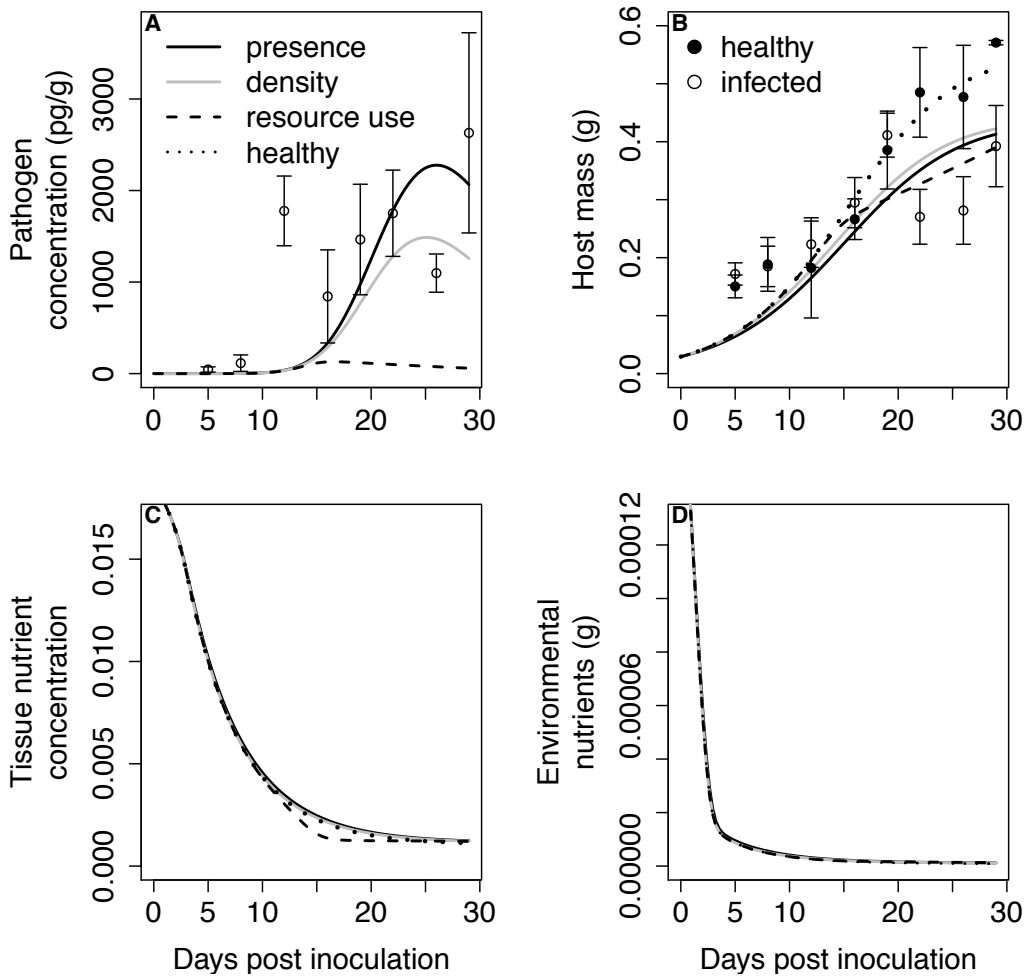

Figure S4. Model fits to (A) virus and (B) host data and predicted changes in (C) tissue nutrient concentration and (D) environmental nutrients. Only the "presence" model was fit to pathogen data (A), while all models were fit to host data (B).

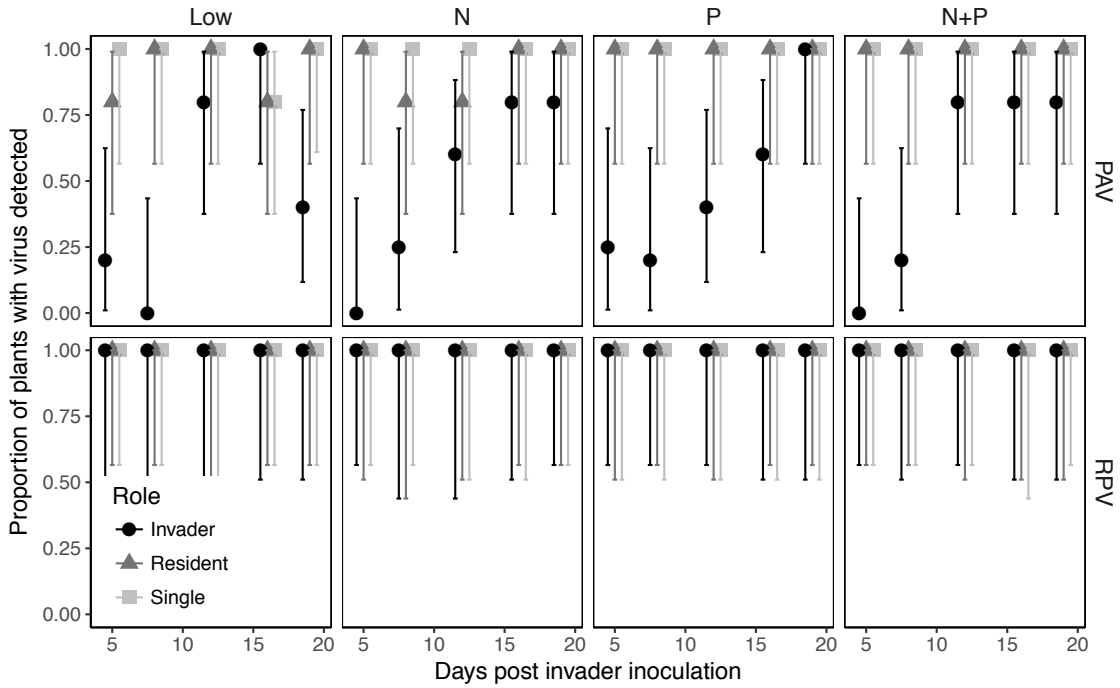

Figure S5. The proportion of plants from the invasion experiment successfully inoculated with PAV and RPV as invaders, residents, and single viruses over time (mean ± 95% CI). PAV detection increased over time when it was an invader.